Selection of an artificial binding protein against the ectodomain of PTH1R

Dissertation

Zur Erlangung des akademischen Grades

doctor rerum naturalium (Dr. rer. nat.)

vorgelegt bei der Naturwissenschaftlichen Fakultät I

Biowissenschaften

der Martin-Luther-Universität Halle-Wittenberg

von

Qi Zhang

geboren am 21.09.1983 in Shaanxi, China

Gutachter /in

1. PD. Dr. Hauke Lilie

2. Prof. Dr. Jochen Balbach

3. Prof. Dr. Annette G. Beck-Sickinger

Verteidigungsdatum: 14.03.2013

Zusammenfassung

In den vergangenen Jahrzehnten fanden mehr als 30 Immunglobuline (IgGs) und deren Derivate Anwendung in der klinischen Praxis. Trotz des großen Erfolgs solcher Antikörper-basierter Medikamente traten auch einige Limitationen auf. Gerüstproteine stellen eine Alternative zu herkömmlichen Antikörpern dar. Sie weisen meist eine hohe thermodynamische Stabilität auf und bestehen aus einer einzelnen Polypeptidkette ohne Disulfidbrücken. Universelle Bindestellen können wie beim humanen Fibronectin III und bei Anticalinen in flexiblen *Loop*-Regionen erzeugt werden oder auf rigiden Sekundärstrukturelementen, wie im Fall der Affibodies, DARPine und Affiline. In der vorliegenden Arbeit wurde eine Protein-Bibliothek auf Basis des humanen γB-Kristallins, unter Randomisierung von 8 oberflächenexponierten Aminosäuren auf einem β-Faltblatt der N-terminalen Domäne des Proteins, hergestellt. Ein kürzlich entwickeltes *Screening*-System, das T7-basierte Phagen-Display, wurde zur Durchmusterung der Bibliothek auf potentielle Binder angewandt. Dabei erfolgt die Assemblierung der Protein-präsentierenden Phagenpartikel ohne einen Transportschritt über die Zellmembran hinweg bereits im Cytoplasma von *E. coli*.

G-Protein gekoppelte Rezeptoren (GPCRs) bilden nur schwerlich für Strukturuntersuchungen geeignete, geordnete Kristallstrukturen aus. Kleine, gut lösliche Bindeproteine könnten sie in einer bestimmten Konformation fixieren und so den Anteil an hydrophilen Resten auf der Proteinoberfläche erhöhen. Als Zielmolekül wurde in dieser Arbeit der Parathormon-Rezeptor Typ 1 (PTH1R), ein Vertreter der Klasse–B-GPCRs, ausgewählt. Nach vier Selektionsrunden konnte eine bindende hγBC-Variante (namentlich 2G4) wiederholt isoliert werden. Sie bindet die N-terminale extrazelluläre Domäne des PTH1R (nPTH1R) mit niedriger mikromolarer Affinität in einem stöchiometrischen Verhältnis von 1:1. Es konnte gezeigt werden, dass zwei Phenylalanine an den randomisierten Positionen 2 und 17

den größten Anteil an der Bindung zum Zielmolekül aufweisen, wobei auch die sieben angrenzenden Positionen I3, C18, E36, A38, G40, E61 und Y62 zur Bindung beitragen. Die Bindung von 2G4 an nPTH1R kann zudem nicht durch PTH kompetiert werden, was für unterschiedliche, nicht überlappende Bindungstellen beider Bindungspartner spricht. Es konnte auch keine nPTH1R-Konformationsänderung durch die Bindung von 2G4 beobachtet werden, welche sich positiv oder negativ auf die PTH/nPTH1R-Interaktion auswirken würde.

Mögliche Anwendungen dieses vielversprechenden Binders liegen zum einen im Einsatz für Ko-Kristallisationsexperimente, zum anderen in der Affinitätschromatographie zur Gewinnung homogener, funktionaler Rezeptorpräparationen.

Summary

In the past decades, more than 30 immunoglobulins (IgGs) and their derivatives have been applied for clinical treatment of various indications. Despite of the great success on antibody drug development, certain limitations have appeared. Scaffolds, as alternatives to antibodies, are mostly single-chain proteins with high thermodynamic stability and devoid of disulfide bonds. A universal binding site can be generated in flexible loops, as for human fibronectin III and anticalins, or on a rigid secondary structure, as in the cases of Affibodies, DARPins, and Affilins. In this thesis, a naïve scaffold library, based on human γB crystallin (hγBC), was constructed with eight randomized positions on the surface-exposed β-sheet of the N-terminal domain. A recently developed screening method, T7 phage display technique, was chosen for the so-called biopanning process, allowing the assembly of phage-scaffold complexes directly in the cytoplasm of *E. coli* cells without transportation across the cell membrane.

G-protein-coupled receptors (GPCRs) are quite difficult to crystallize in a highly ordered state for structural studies. Small and highly soluble binding proteins could help to lock them in a specific conformation and increase the hydrophilic percentage of the protein surface. Within this work the parathyroid hormone 1 receptor (PTH1R), a class B GPCR, was chosen as a target molecule. Four rounds of a biopanning process were performed and one hγBC binding variant, called 2G4, was repeatedly isolated. It binds the N-terminal extracellular domain of PTH1R (nPTH1R) with low micromolar affinity in a 1:1 stochiometry. Two phenylalanines on randomization positions 2 and 17 were found to contribute the most to the binding interaction and the surrounding seven substitution sites I3, C18, E36, A38, G40, E61 and Y62 also participate in the binding event. There is no competition binding of 2G4 and PTH to nPTH1R via identical or overlapping binding sites, nor does 2G4 binding induce a conformational switch in nPTH1R that would interfere either positively or negatively

with PTH binding.

The promising binder could have several potential applications, such as in co-crystallization experiments or in affinity chromatography to increase the homogeneity of functional receptor.

Abbreviations:

aa	amino acid
ADCC	antibody-dependent cell-mediated cytotoxicity
ATP	adenosine triphosphate
AU	absorbance units
Axxx	absorbance at wavelength xxx
BCIP	5-bromo-4-chloro-3'-indolyphosphate p-toluidine salt
bp	base pair
BSA	bovine serum albumin
CD	circular dichroism
cDNA	complementary DNA
CDR	complementary determining region
C_H	constant domain of antibody heavy chain
C_L	constant domain of antibody light chain
DARPIN	designed ankyrin-repeat protein
CV	column volume
CIAP	calf intestine alkaline phosphatase
Da	dalton
DNA	deoxyribonucleic acid
DSF	differential scanning fluorimetry
DTT	dithiothreitol
E. coli	*Escherichia coli*
EDTA	ethylenediamine tetraacetic acid
ELISA	enzyme-linked immunosorbent assay
ESI	electrospray ionization
EtOH	ethonal
Fab	fragment antigen-binding
Fc	fragment crystallisable

Fv	fragment variable
g	earth's gravitational acceleration
GdmCl	guanidine hydrochloride
GSH	reduced glutathione
GSSG	oxidized glutathione
h	hour
hγBC	human γB crystallin
HIC	hydrophobic interaction chromatography
HRP	horseradish peroxidase
HSQC	heteronuclear single quantum correlation
Ig	immunoglobulin
IMAC	immobilized metal-ion affinity chromatography
IPTG	isopropyl β-D-1-thiogalactopyranoside
ITC	isothermal titration calorimetry
kbp	kilo base pair
LB	lysogeny broth
M	molar
MALDI	matrix-assisted laser desorption/ionization
MES	2- (N-morpholino) ethane sulfonic acid
MWCO	molecular weight cut-off
min	minute
NBT	nitro-blue tetrazolium chloride
NMR	nuclear magnetic resonance
nPTH1R	N-terminal parathyroid hormone 1 receptor
Ni-NTA	nickel-nitrilotriacetic acid
OD	optical density
o/n	overnight
PAGE	polyacrylamide gel electrophoresis
PBS	phosphate buffered saline
PBST	PBS containing 0.1% (v/v) tween-20

PCR	polymerase chain reaction
PDB	protein data bank
PEG	polyethylene glycol
pfu	plaque forming unit for phages
PMSF	phenylmethylsulfonyl fluoride
POD	peroxidase
PVDF	polyvinylidene difluoride
RP-HPLC	reverse phase high-performance liquid chromatography
rpm	rotational speed per minute
RT	room temperature
SDS	sodium dodecyl sulfate
sec	second
SEC	size exclusion chromatography
scFv	single chain fragment variable
sIB	solubilized inclusion body
SPR	surface plasmon resonance
TEV	tobacco etch virus
Tm	melting temperature of primer
TMB	3, 3', 5, 5'- tetramethylbenzidine
TROSY	transverse relaxation optimized spectroscopy
UV	ultraviolet
V_H	variable domain of antibody heavy chain
V_L	variable domain of antibody light chain
v/v	volume/volume
w/v	weight/volume

Table of Contents

1 Introduction

1.1 Antibodies

Antibodies, also termed as immunoglobulins, are Y-shaped glycoproteins produced by B lymphocytes of vertebrates. Their function is to recognize foreign targets, called antigens, and to initiate the immune response in several ways, such as by the prevention of pathogens from damaging cells, by the stimulation of macrophages and by the activation of complement pathway or effector cells.

Initially, antibodies were identified by their electrical charge in the electrophoresis experiments to compare serum of hyperimmunized and unimmunized rabbits, by Tiselius and Kabat in 1939. Later on, Edelman and Porter elucidated the chemical structure of antibodies by chemical solvents and protein-degrading enzymes, respectively, and shared the 1972 Nobel Prize in Medicine. Specific antibodies were further successfully produced by injection of antigen into a mammal, such as mouse, rat, rabbit and so on. Such antibodies produced by different B lymphocytes and then isolated from the mammal serum, are termed as polyclonal antibodies. By contrast, monoclonal antibodies (mABs) were derived from a single cell line by hybridoma technique and bind to the same epitope in monovalent affinity. When antibodies were developed for therapeutic administration in humans, heterogeneity of antibodies between different mammalian species may trigger immune response. In 1986, humanized antiobodies were reported about inserting the CDR coding segments from a mouse into a human antibody construct (Jones *et al.*, 1986). Later in 1991, phage display technology was firstly described for selection of human antibody Fab fragment against tetanus toxin (Barbas *et al.*, 1991).

Structurally, antibodies consist of two identical heavy chains and two identical light chains, linked by disulfide bonds (Fig. 1.1). The types of heavy chain determine the class

of antibody: IgA, IgD, IgE, IgM and IgG, for mammalian and another major serum antibody IgY found in birds and yolk. All isotypes of antibodies can be produced by mature B cells in a secreted form. Structurally, light chain contains two domains, the variable domain (V_L) and constant domain (C_L), while heavy chain comprises one variable domain (V_H) and three constant domains (C_H1- C_H3) with a hinge region for subtype IgA, IgD, IgG or four constant domains (C_H1- C_H4) for IgE and IgM. With proteolysis by papain in the presence of the reducing agent cysteine, antibodies can be digested into F_{ab}- and F_c-fragment. F_{ab}-fragment consists of the whole light chain, the variable domain and the first constant domain of the heavy chain. Rest parts of the heavy chain make the F_c-fragment, which mediates different physiological effects including lysis of cells and so on by binding to F_c receptor and other immune molecules. The variable domain (F_v), is responsible for antigen binding, especially three variable loops of β-sheets on each chain, referred as complementarity determining regions (CDR). These six CDRs upbuild the antigen binding site, termed as paratope. The amino acid residues of the CDRs determine the shape and ionic properties of the antigen-binding site, therefore, the binding affinity and target specificity is defined by the CDRs.

In the past decades, more than 30 recombinant or humanized immunoglobulins (IgGs) and their derivatives have been approved for clinic uses (Beck *et al.*, 2008; Reichert, 2010), to treat diseases suffered by large numbers of patients, like cancer and inflammatory diseases, but also for more specialized indications owing to special regulatory procedures required for rare medical therapies (orphan diseases, Beck, 2010). First-generation approved antibodies came to the market for clinically validated targets in the late 1990s. These antibodies include rituximab (Genentech/Roche/Biogen Idec) against CD20, infliximab (Remicade; Centocor/Merck) against tumour necrosis factor α (TNFα), trastuzumab (Herceptin; Genentech/Roche) against human epidermal growth factor receptor 2 (HER2, also known as ERBB2) and cetuximab (Erbitux; ImClone Systems) against epidermal growth factor receptor (EGFR, Aggarwal, 2009). The following second- and third- generation antibodies were designed with improved variable domains to decrease immunogenicity, and/or targeting different epitopes,

and/or triggering other mechanisms of action, and/or in alternative antibody formats (such as conjugating the Fab domain to polyethylene glycol and Fc-fusion proteins, Storey, 2010; Strohl, 2009; Oflazoglu and Audoly, 2010). Beside medical applications, antibodies were also commonly used to identify proteins in enzyme-linked immunosorbent assay (ELISA), western blot, and immunofluorescence techniques.

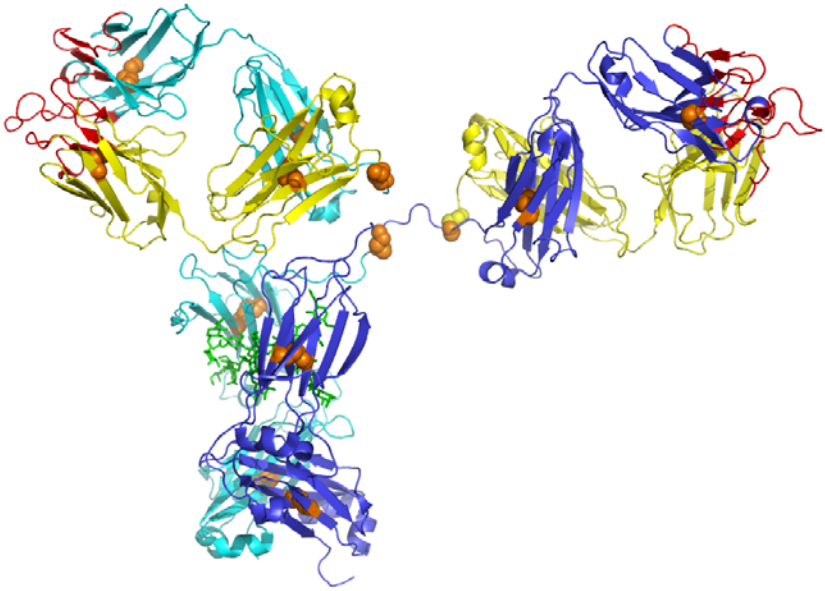

Fig. 1.1: 3D structure of IgG-molecule. Antibodies comprise two heavy chains (shown in blue) and two light chains (shown in yellow). They are linked by disulfide bonds (shown in orange atoms). The glycosylation (shown in green) locates in the heavy chain. The figure was built by Pymol software (PDB entry 1hzh).

Although antibodies have made so many successful stories, certain limitations are also quite apparent, such as, their large size, complicated composition by four polypeptide chains, glycosylation of the heavy chains, and disulphide bonds. Hence, full size antibodies need to be produced in eukaryotic cell lines, whose optimization and fermentation is relative cost-intensive. During clinical treatment, the large size of intact antibody is also not suitable for the deeper tumor penetration. Besides, inappropriate activation of Fc receptor could cause massive cytokine release and related toxic effects. In imaging applications, a long serum half-life of intact antibody often results in poor contrast (Holliger and Hudson, 2005). Furthermore, application of antibodies often leads to a complicated patent situation.

Small versions of antibodies can be obtained through proteolysis (with enzymes papain and pepsin) and later genetically engineered into either monovalent (Fab, scFv, single variable V_H and V_L domains) or bivalent fragments (diabodies, minibodies, etc., Holliger and Hudson, 2005). They can be produced in microbial hosts, but their stability still depend on intradomain disulfide bonds (Wörn and Plückthun, 2001), which form only in periplasm with oxidizing environment. In addition, some antibody fragments are easily aggregated, especially when fused to added domains in the aim of higher therapeutic efficacy, detection or immobilization.

1.2 Artificial binding proteins

The demand to improve on all these drawbacks and maintain binders with high affinity and specificity to target encourages the development of scaffolds for alternative binding protein, with a universal binding surface. These scaffold proteins usually smaller than 20 kDa, compared with the sizes of monoclonal antibodies 150 kDa, or antibody fragments of 25-50 kDa.

The term “scaffold” describes a stable polypeptidic framework with a high tolerance for modifications such as multiple insertions, deletions or substitutions. So far, approximately 50 proteins have been designed for scaffolds (Skerra, 2007). These proteins demonstrate benefits, like single chain, small size, high stability without disulfide bonds, allowing cost-efficient production in bacteria cells and ease of modification.

Artificial binding proteins have been applied in therapy, diagnostics and research. Due to their small size, most scaffolds will probably exhibit good tissue penetration but short serum half-lives. In December 2009, the first scaffold-derived drug was approved by the FDA (Beck, 2010). Ecallantide, a Kunitz domain-based scaffold, targets human plasma kallikrein, was applied for the treatment of attacks of hereditary angioedema (Hughes,

2009; Zuraw *et al.*, 2010). Ecallantide can compensate the shortage of the natural kallikrein inhibitor C1 and the traditional therapy with C1 extracted from human plasma maybe later substituted. To date, more than 10 scaffolds have already entered clinical trials, of which 6 are in Phase II trials, such as TRU-015, based on a small modular immunopharmaceutical (SMIP) scaffold, against target CD20 for treatment of non-Hodgkin lymphoma (NHL), and Dom-0200/Art621, based on antibody domain, targeting TNF for rheumatoid arthritis and psoriasis disease and so on (Beck, 2010).

In diagnostics, the high specificity and affinity of scaffold-antigen interactions have led to applications in sandwich enzyme-linked immosorbent assay, flow cytometry, and immunohistochemistry. Non-Ig binding proteins are particularly suitable for *in vivo* imaging since their smaller size benefits in better tissue penetration, lack of Fc-mediated non-specific adhesion and, most importantly, much faster excretion via the kidney, which leads to increased target/blood ratios and thus better contrast of tumor staining. For example, the Affibody ABY-025, which specifically binds to human epidermal growth factor receptor 2 (HER2), has already been utilized for *in vivo* diagnostics (Gebauer and Skerra, 2009).

Scaffolds can also facilitate to co-crystallize with proteins, which *per se* do not yield crystals that diffract well due to the high intrinsic flexibility, often seen in kinases or only a small portion of hydrophilic segment for crystal contacts, like membrane proteins. Specific binders could help to restrict the protein in a homogeneous conformation or increase the hydrophilic area of protein surface for crystal contacts. Full-size antibodies are not suitable for such functions, since their large structures comprise multi domains connected by flexible hinges. In contrast, both Fab and Fv fragments, have been successfully applied in membrane protein crystallography (Iwata *et al.*, 1995; Dutzler *et al.*, 2003), however, fermentation are required to produce sufficient amount for crystallization. Alternative scaffolds Protein Z (Affibody) and DARPins have already been co-crystallized with macromolecular targets (Högbom *et al*, 2003; Binz *et al.*, 2004; Kohl *et al.*, 2005).

Scaffolds can also serve in immunoaffinity chromatography, since they can be easily produced in a large quantity at low cost and their robust structure can accommodate simple elution of the purified protein by pH-shift, and followed by harsh cleaning in place (e.g., 1M NaOH for several hours).

Until now, numerous scaffolds were designed according to diverse potential applications. They differ in size, topology, mode of interaction and applicability. For example, human fibronectin III has an antibody-like β-sandwich structure (94 residues, Fig 2A) with CDR-like exposed loops as binding site, but in contrast to antibodies, it doesn't rely on disulfide bonds (Koide and Koide, 2007). Another example demonstrating flexible loop-mediated interaction is anticalin, which is derived from the lipocalin, an eight-stranded β-barrel proteins (ca. 180 residues). The binding area was generated on four variable loops at the open end (Skerra, 2008).

The mechanism of protein interaction through flexible loops has been described by the induced-fit model (Jimenez *et al.*, 2003). In this enthalpically driven process, the fixation of variable loops leads to an unfavorable entropic effect. In contrast, binding sites based on a rigid secondary structure have the advantage in decreasing entropic loss. Affibodies (58 residues, Fig 2B), based on the Z-domain of *staphylococcal* protein A, consist of three α-helices. A binding site was generated by 13 substitutions on two of its α-helices (Nygren, 2008). Designed ankyrin repeat domains (DARPins, 166 residues) provide a rigid interface on repeated β-turns and α-helices structure (Binz *et al.*, 2004). In the case of Affilins, based on the human ubiquitin, amino acid residues on the β-sheet were randomized to construct a *de novo* binding area (Fiedler *et al.*, 2004; Hoffmann 2012, Fig 2C).

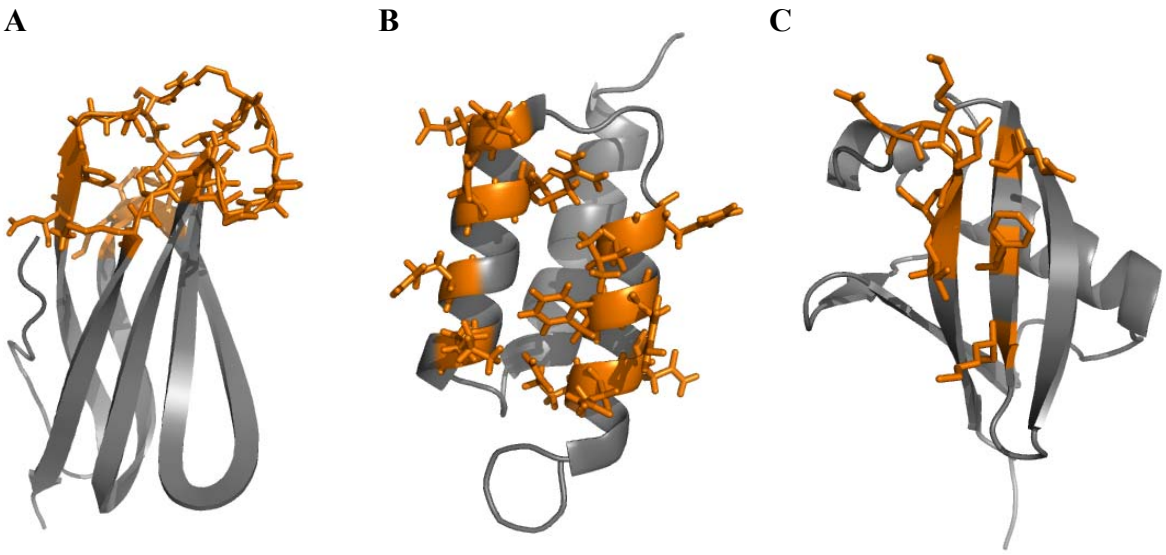

Fig. 1.2: Artificial paratopes designed on the scaffold structures. A. 26 amino acid positions randomized on the loop region of human fibronectin III to form a CDR-like binding site. **B.** 13 random mutagenesis on the surface of an α-helical bundle protein, Affibody. **C.** 8 randomization sites on the surface-exposed β-sheet of ubiquitin (Hoffmann *et al.*, 2012). The figures were built by Pymol software (PDB entry 1fna, 1q2n, 1ubi).

1.3 Human γB crystallin as scaffold

In our studies, human γB crystallin (Fig. 1.3) was utilized as alternative binding molecule. It consists of 176 amino acid residues, ca 21 kDa. γB crystallin is a best-known member of βγ-crystallin family, with a role in preserving lens transparency. γ-crystallins are specifically expressed in eye lens fibre cells of vertebrates and mainly found in relative dehydrated core regions, where the refractive index is high (Kumaraswamy *et al.*, 1996). They are the last crystallins to be synthesized during fibre cell differentiation, following first the α-crystallins and then the β-crystallins (Bloemendal *et al.*, 2004). Point mutations to surface residues of γ-crystallin can cause human congenital cataracts, probably by way of reducing the protein solubility. Deamidation of human γ-crystallins is also related to increasing aggregation of crystallins and aging (Kumaraswamy *et al.*, 1996).

There are seven subtypes of γ-crystallin in mammalian lenses, A-F and S. γB crystallin is composed of two highly symmetrical domains, each comprising two anti-parallel

β-sheets (Fig 3, Jaenicke and Slingsby, 2001). The orientation of both domains is constricted by interaction of hydrophobic residues in the interface between two domains. It has no turn over in the whole life time, due to its stability in tertiary structure and interaction with other cell components. It remains in native state between pH 1-10. In 0.1 M phosphate buffer pH 7, the thermal stability is up to 75 °C (Mayr *et al.*, 1997). 8 M urea alone is not able to denature the protein. The unfolded state can be reached only by the combination of urea with either high temperature or low pH (Jaenicke, 1994). With the high interior stability, γB crystallin is able to tolerate amino acid substitutions for further applications, some even in harsh conditions. Besides, wild type γB crystallin has demonstrated neither binding affinity to any other molecules nor detectable enzymatic activity of its own (Ebersbach *et al.*, 2007). γB crystallin contains seven cysteines, but no disulfide bonds, so it could be conveniently prouduced in cytoplasm of *E. coli* cells.

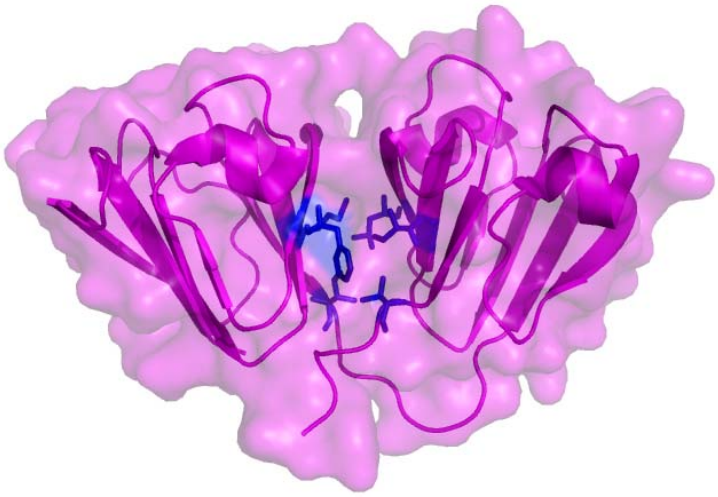

Fig. 1.3: Overall X-ray structure of human γB crystallin. The molecule comprises two highly symmetrical domains and linked by a connecting loop. The two domains interact with each other by hydrophobic amino acid residues, M43, F56, I81, I132, L145 and V170, high lighted in blue. The figure was built by Pymol software (PDB entry 2jdf).

The high level of solubility and stability, ease of production and modification makes γB-crystallin a promising scaffold for the design of a universal binding site. Randomization positions were selected via computer simulation. Variable amino acid positions were found by comparing 84 βγ crystallin sequences for homology with the ENTREZ database. Then surface accessibilities of the selected residues were analyzed

with the Swiss PDB viewer. Finally, eight solvent-accessible amino acid residues on the first β-sheet of N-terminal domain were chosen for generation of a *de novo* binding site (Fig. 1.4): Lys2, Thr4, Tyr6, Ser15, Glu17, Thr19, Arg36, Glu38. The interface area was calculated to be approximately 560 $Å^2$ (Ebersbach *et al.*, 2007).

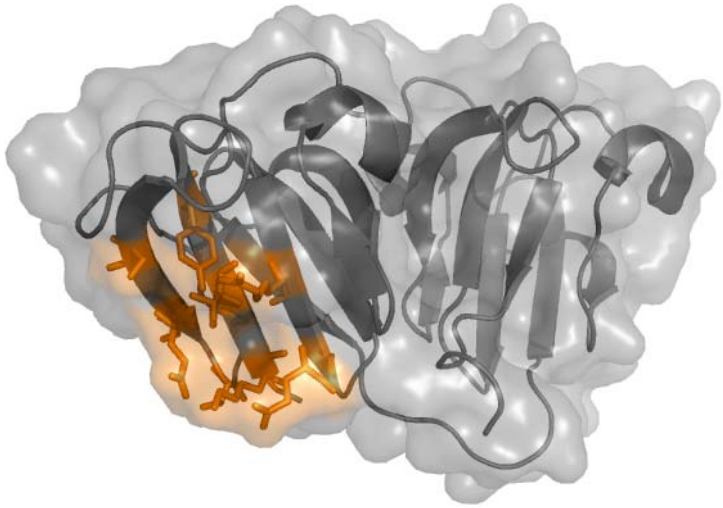

Fig. 1.4: *de novo* binding site on the human γB crystallin molecule. Eight amino acid positions (K2, T4, Y6, S15, E17, T19, R36, E38) were selected to generate a binding area on the surface-exposed β-sheet of N-terminal human γB crystallin, shown in orange. The figure was built by Pymol software (PDB entry 2jdf).

Complementary DNA library was constructed by introducing randomized mutations at the codons of the identified residues in primers and followed by ligation of each PCR fragment. With different mutation strategies, the distribution of amino acid type at the randomization sites varies. In traditional NNK-motif based method for the first generation of hγBC library (Ebersbach *et al.*, 2007), 32 codons ending with guanine or thymidine were utilized for all amino acids. This strategy leads to an unequal distribution of amino acids, especially an over representation of Arg, Ser and Leu, as well as to the presence of one stop codon and one cysteine codon. For eight randomization sites, the theoretical library diversity should be $32^8=1.1\times10^{12}$ on DNA level, and $21^8=3.8\times10^{10}$ on protein level. In the trinucleotide based method (Virnekäs *et al.*, 1994) trinuleotide phosphoramidities which represent directly the amino acids needed at randomization positions are used in oligonucleotide synthesis and these condons could be mixed at a desired ratio. The diversity of library on DNA level is

identical to that on protein level. Another advantage of this method is that all stop condons could be successfully excluded, which occupies 1/32 possibilities in NNK-based method. In this particular thesis, trinucleotide synthons of all 20 amino acids except unwanted cysteine were equally mixed and utilized during DNA synthesis. The theoretical diversity of this cDNA library could reach $19^8=1.7\times10^{10}$ individual variants. Compared to the diversity of NNK-based method ($32^8=1.1\times10^{12}$), this trinucleotide based library is easier to be covered during the selection procedure. The previously constructed hγBC library has already been used for selection against various target molecules, e.g. the steroid hormones (estradiol with BSA conjugated), Fc fragment of human immunoglobulin G (IgG-Fc), proform of human nerve growth factor (proNGF), and human papillomavirus E7 protein (Ebersbach *et al.*, 2007, Mirecka *et al.*, 2009). Low micro molar binding variants were obtained without great structural changes and high thermal stability was preserved (Ebersbach *et al.*, 2007).

1.4 T7 phage display

Using the established cDNA library, high affinity binding variants could be isolated with the help of screening methodology, such as phage display (Smith, 1985), ribosome display (He and Taussig, 2002), microbial or yeast cell surface display (Lee *et al.*, 2003; Kondo and Ueda, 2004), mRNA display (Xu *et al.*, 2002). Each has its own advantages and limitations. Proper display technique could be chosen according to biophysical characteristics of the target molecule, scaffold properties, library diversity, and potential applications of selected variants.

In this work, T7 phage display technique was used for selection of hγBC binding variants against target molecule. T7 is a lytic phage, consisting of a capsid shell, a head-tail connector, a tail and tail fibers (Fig. 1.5). The capsid shell is composed of 415 copies of capsid protein (gene 10), which forms 60 hexamers on the face and 11 pentamers at the vertices (Rosenberg *et al*., 1996). Usually there are two forms of capsid

protein, 10A (344 aa) and 10B (397 aa). 10B is expressed due to a translational frameshift of 10A at amino acid position 341. This finding initiated the concept that T7 phage capsid could accommodate variation and might display foreign protein on the surface. Nowadays, utilizing the Novagen's T7Select® Phage Display System, peptides or proteins can be displayed on the phage surface by fusion to phage capside protein 10B. Three types of T7Select phage display vectors are provided: high-copy, mid-copy, and low-copy, with copy number 415, 5-15, 0.1-1 displayed peptides or proteins on each phage, respectively. Constructed cDNA library is cloned into the T7Select vector, and assembled into phage by incubation with T7 Packaging Extracts. The phage library is then amplified in *E. coli* cells for biopanning. The target molecule is incubated with the phage library and unbound or weak binding complex could be removed by multiple washing steps. The binding variants with high affinity are eluted and then analyzed by sequencing across the cloning region of the phage DNA (Fig. 1.6). The limitation of T7 phage display technique lies on the library diversity directly correlating to the applied quantity of T7 Packaging Extracts.

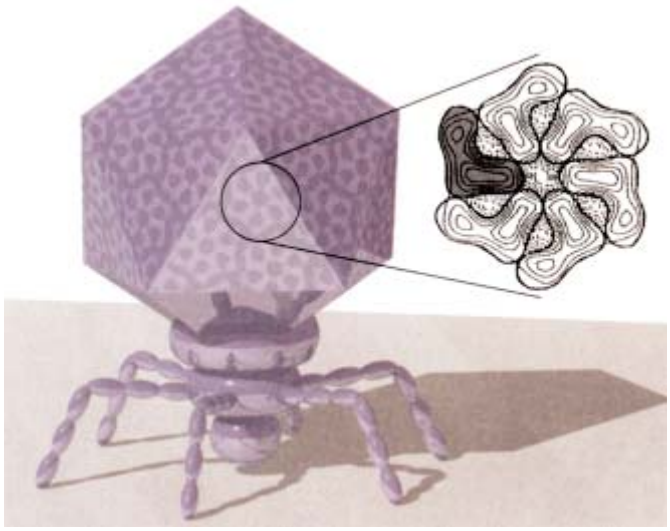

Fig. 1.5: Structure of the T7 phage. T7 phage is composed of a capsid shell, a head-tail connector, a tail and 6 tail fibers. One hexamer capsid unit on the surface of the icosahedral particle (diameter about 55 nm) is shown by the diffraction pattern from polyheads (Steven *et al.*, 1983). The monomer is colored in gray. The figure is adapted from Rosenberg *et al.*, 1996.

Compared to filamentous phages, T7 phages assemble in the cytoplasm of *E. coli* cells and are released by cell lysis. Therefore, fast-folding scaffold variants don't need to be

transported across cell membrane to the periplasm for packaging, which is, on the contrary, indispensable for filamentous phage display (Russel, 1991). Scaffolds are more directly and efficiently displayed on the phage surface. Besides, T7 phages grow and replicate faster than filamentous phages, with culture lysis in 2-3 hours after infection. During the selection procedure, time and effort could be greatly saved. Furthermore, the T7 phage particle is extremely robust, and very stable to harsh conditions if required in the biopanning process, which might inactivate other kinds of phages (Rosenberg *et al.*, 1996). T7 DNA can be easily extracted in a large amount for either sequence analysis of promising candidates or efficient *in vitro* packaging (Son *et al.*, 1988). Unlike classical immunization technology, here described selection *in vitro* could be conducted in conditions as the target molecules or further applications require, e.g. different pH, detergents, reduced or oxidized environment.

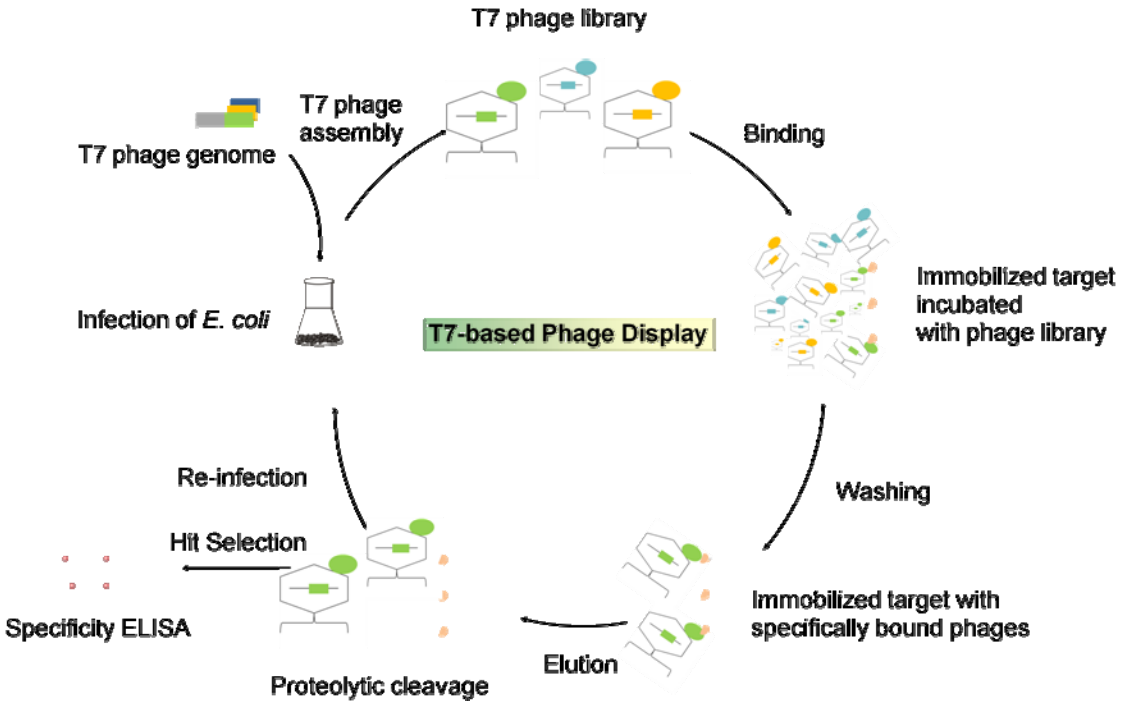

Fig. 1.6: Principle of T7-based phage display. T7 phage library is firstly constructed by incubation of T7 genome inserted with DNA library and phage packaging extracts. The phage library is then incubated with immobilized target molecule. Unbound phages are removed by washing steps and bound phages were eluted by proteolytic cleavage. The output phages are further analyzed by hit ELISA and amplified by re-infection of freshly prepared *E. coli* cells for the next round of selection.

1.5 N-terminal domain of parathyroid hormone 1 receptor as target protein

G-protein-coupled receptors (GPCRs) locate in plasma membrane and play an essential role in signal transduction across membranes. They can be activated by different ligands: photons, ions, odorants, amino acids, fatty acids, neurotransmitters, peptides, proteolytic enzymes. Phylogenetically, GPCRs can be classified as six major classes, of which class A is represented by rhodopsin family, the largest group (about 700 members), and class B receptors, termed as secretin receptor family, activated by endogenous peptide hormones (Parthier *et al.*, 2009; Attwood and Findlay, 1994). The natural ligands of class B GPCRs include secretin, parathyroid hormone (PTH), glucagon, the incretins glucagon-like peptide 1 (GLP-1) and glucose-dependent insulinotropic polypeptide (GIP), corticotropin-releasing factor (CRF), growth-hormone releasing factor (GRF), pituitary adenylate cyclase activating polypeptide (PACAP), vasoactive intestinal peptide (VIP), and calcitonin. Conformational change in the receptor is induced by ligand binding, activating either cAMP signal pathway or phosphatidylinositol signal pathway.

More than one third of all current therapeutics are directed at GPCRs (Millar and Newton, 2010). Although they are highly druggable, only a little was known about their structure in atomic level. GPCRs contain an extracellular domain, seven transmembrane helices and an intracellular segment. So far, crystal structures of class A GPCRs in different conformation state have contributed greatly on understanding activation of GPCRs. In contrast, no full-length class B GPCRs have been determined to date. Only the structures of extracellular domain in the presence or absence of ligands have been solved by X-ray crystallography or nuclear magnetic resonance (NMR) spectroscopy (Parthier *et al.*, 2009).

Parathyroid hormone 1 receptor (PTH1R) belongs to class B G-protein-coupled receptor (GPCRs), found highly expressed in bone and kidney (Mannstadt *et al.*, 1999, Fig. 1.7).

Parathyroid hormone (PTH) is synthesized in parathyroid glands and secreted into the bloodstream in response to low extracellular calcium or elevated extracellular phosphate. The major biological function of PTH acts by N-terminal domain direct interaction with PTH1R. In kidney, PTH enhances calcium reabsorption in the distal convoluted tubule and reduces phosphate reabsorption primarily by inhibiting the expression amounts of two sodium-phosphate co-transporters, NPT-2a and NPT-2c, located in the brush border membrane of the proximal tubules (Murer *et al.*, 2004; Pfister *et al.*, 1998; Segawa *et al.*, 2002). In bone, PTH can stimulate both osteoblasts for bone formation and also osteoclasts resulting in greater bone resorption. Continuous exposure to high concentration of PTH will lead to bone loss, like in hyperparathyroidism, while intermittent administration of PTH can enhance bone formation and increase bone mass (Moen and Scott, 2006). The activated PTH1R initiates intracellular signal pathway primarily through the α-subunit of the stimulatory G-protein to activate protein kinase A and augment synthesis of cAMP (Abou-Samra *et al.*, 1992). Other signal processes can also be triggered, such as through Gqα to activate phospholipase C (Offermanns et al., 1996) and increase intracellular concentration of inositol trisphosphate and calcium (Abou-Samra *et al.*, 1992).

Synthetic or recombinant N-terminal fragment PTH 1-34 and full length PTH 1-84 have already been used for osteoporosis patients for many years to enhance the bone formation, only by administration of daily injections, but not oral, same as other short bioactive peptides (Gensure *et al.*, 2005). Due to its peptide character, PTH could be quickly cleared in the blood (Orwoll *et al.*, 2003). Structure-based design of non-peptide-analogue will be further investigated in the aim of more efficient therapy with a longer half-life time, less side effects or conveniently oral administration. Although PTH1R is of great interest in therapeutic use, their structure in atomic level still remains unclear, like other family members from class B GPCRs. Structures of N-terminal extracellular domain of PTH1R with and without ligand PTH have been already published (Pioszak and Xu, 2008; Pioszak *et al.*, 2010, Fig 1.8). In order to develop PTH-mimetic drug, structure of full length receptor without ligand and

conformation changes induced by PTH binding should be further explored.

GPCRs, like other membrane proteins, are quite difficult to crystallize. They have no bacterial homologs and are difficult to be isolated in a large amount for structure studies. GPCRs are very flexible since they are required to change conformations during activation process. Therefore, without bound ligand, they could be either inactive or fully active, coupled to G proteins (Kenakin, 2001). The well-diffracting crystal formation has been hindered by this conformation heterogeneity. Besides, different varieties of detergents are required to maintain and stabilize GPCRs in native structure. The condition for crystallization must be compatible with the membrane environment for functional protein (Wiener, 2004). These limitations restrict the development of research on GPCRs.

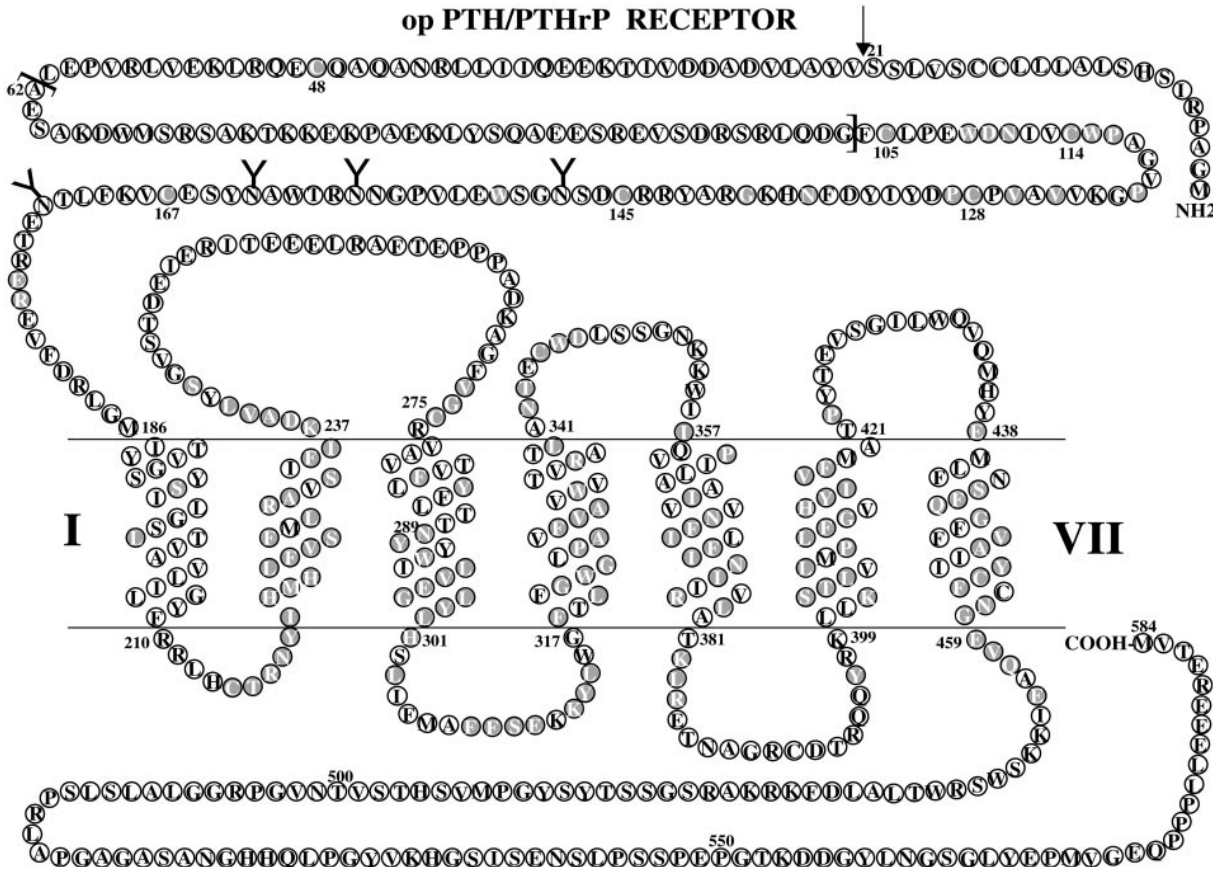

Fig. 1.7: Primary amino acid sequence and predicted structure model of opossum PTH1R. The arrow pointed out the cleavage site of the signal peptide. Gray circles stand for the conserved residues with the rat secretin receptor. "Y" points out the oretical sites of N-glycosylation. [ ] shows boundaries of exon 2. The figure is adapted from Vilardaga *et al*., 2001.

Different studies have been explored to overcome these problems by locking the receptor in a specific conformation and increase the structural rigidity. In the case of the β1 adrenergic receptors (AR), point mutations were introduced to receptor itself and a stabilized mutant was successfully crystallized (Serrano-Vega *et al.*, 2008; Warne *et al.*, 2008). The structure of β2 AR was solved by co-crystallized with an antibody fragment (Rasmussen *et al.*, 2007) or fused with protein T4 lysozyme (Cherezov *et al.*, 2007). The co-crystallized antibody fragment and T4 lysozyme were used to fix the third intracellular loop (IC3), which is coupled to G proteins during the activation. The antibody fragment fixes the β2 AR conformation by binding to the third intracellular loop, which is coupled to G proteins during the activation, and the T4 lysozyme is fused to the truncated cytoplasmic ends of helices V and VI. The bound soluble protein partners could help to reduce the flexibility and increase the homogeneity of GPCRs. Besides, the class A GPCRs don't contain a large hydrophilic extracellular domain, only small loops that connect the large hydrophobic segments inserted in detergents. Therefore, the crystal contacts of β2 AR structure are totally mediated by the antibody fragment and T4 lysozyme. Some other membrane proteins have also been successfully co-crystallized with antibody fragments, such as cytochrome c oxidase (Harrenga *et al.*, 1999), potassium channel KcsA (Zhou *et al.*, 2001), the ClC chloride channel (Dutzler *et al.*, 2003).

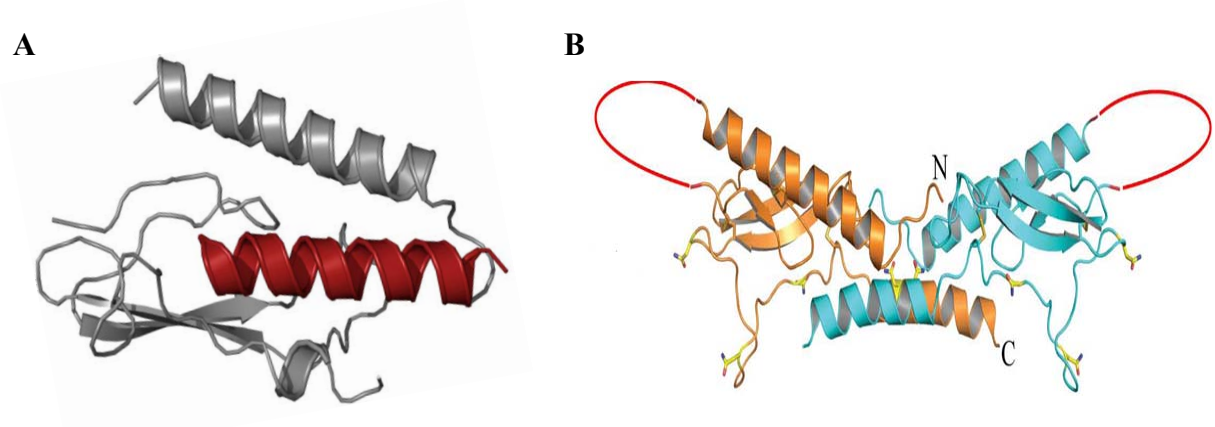

Fig. 1.8: 3D structure of N-terminal extracellular domain of PTH1R in the presence (A) and absence (B) of PTH ligand. A. PTH ligand was shown in red and nPTH1R in grey. The figure was built by Pymol software (PDB entry 3c4m). **B.** Without PTH ligand, nPTH1R exists as dimer form. The figure was adapted from Pioszak *et al.*, 2010.

In all these studies, antibody fragments have been selected by classical hybridoma technology. After injection of detergent-solubilized membrane proteins to animals, it was difficult to monitor their conformation state in a certain time. Hence, binders towards the epitopes of membrane proteins in native conformation are not easy to be obtained (Huber *et al.*, 2007). Antibody fragments themselves also have certain limitations in association with their multi-chain structure and stability based on disulfide bonds, which lead to difficult and expensive manufacture.

In this thesis, these problems would be overcome by combination of *in vitro* selection methodology and conveniently prepared artificial binding proteins. Different from class A GPCRs, class B family members contain a relative larger extracellular domain, which has an important role in ligand binding. Besides locking the transmembrane helices, extrinsic stabilization of the class B GPCR ectodomains is likewise required for crystallization and structure determination. Therefore, extracellular domain of parathyroid hormone 1 receptor was chosen as a target molecule to select binding proteins for fixation and stabilization.

1.6 Aim of the thesis

The limitations of antibodies and their derivatives encourage the development of alternative protein scaffolds with universal binding surface and subsequent *in vitro* selection technologies. The isolated binders with high affinity and stability could be applied in therapeutic, diagnostic or research fields. Membrane proteins are highly druggable, but not easy to crystallize, especially like GPCRs. Structurally, they are very flexible because they are required to change conformations during activation process. Articificial binding proteins could serve to fix and stabilize the GPCRs in a specific conformation for structure determination. Therefore, in this thesis, artificial binding proteins, based on hγBC, would be selected against a target molecule from class B GPCR, parathyroid hormone 1 receptor (PTH1R). For this purpose, hγBC binding

variants would be isolated by T7 phage display technique. Binding affinity, as well as enthalpy, entropy and stochiometry would be further estimated by ELISA, isothermal titration calorimetry (ITC) and NMR titration. The secondary structure and thermal stability of isolated variant would be analyzed by CD spectroscopy and Differential Scanning Fluorimetry (DSF). The structural information on the nature of the physical interaction of binder and nPTH1R would be analyzed by alanine scanning experiments and NMR studies, revealing the specific amino acid residues involved in the binding event. The hereby obtained result could help to establish a new library with perspective to isolate binders with higher affinity and specificity, which could be utilized in a variety of fields according to their own properties.

2 Materials and methods

2.1 Materials

2.1.1 Chemicals

Adenosine 5'-triphosphoric acid (ATP)	AppliChem (Darmstadt)
Agarose LE	Biozym (Hess. Oldendorf)
Agarose Sieve 3:1	Biozym (Hess. Oldendorf)
Ammonium sulfate	AppliChem (Darmstadt)
L-Arginine	AppliChem (Darmstadt)
Bacto Agar	BD Diagnositics (Heidelberg)
Bacto Soytone	BD Diagnositics (Heidelberg)
Bacto Tryptone	BD Diagnositics (Heidelberg)
Bacto Yeast extract	BD Diagnositics (Heidelberg)
Boric acid	Carl Roth GmbH & Co. (Karlsruhe)
Bovine serum albumin	Sigma (Steinheim)
10 × Bovine serum albumin in PBS	Pierce (Rockford)
Bromphenol blue	AppliChem (Darmstadt)
BugBuster	Novagen (Darmstadt)
Carbenicillin	Carl Roth GmbH & Co. (Karlsruhe)
10 × Casein blocking buffer	Sigma (Steinheim)
Chloramphenicol	Carl Roth GmbH & Co. (Karlsruhe)
Cobalt(II) chloride hexahydrate	AppliChem (Darmstadt)
Coomassie R250	AppliChem (Darmstadt)
Copper(II) dichloride dihydrate	AppliChem (Darmstadt)
Copper (II) sulfate pentahydrate	AppliChem (Darmstadt)
Difco Select Soytone	BD Diagnositics (Heidelberg)
DL-Dithiothreitol	AppliChem (Darmstadt)

dNTP-Mixture (10 mM every nucleotide)	Fermentas (St. Leon-Rot)
Ethanol purest and technical	Carl Roth GmbH & Co. (Karlsruhe)
Ethidium bromide	Carl Roth GmbH & Co. (Karlsruhe)
Ethylenediamine tetraacetic acid (EDTA)	Carl Roth GmbH & Co. (Karlsruhe)
EZ-Link® Sulfo-NHS-LC-Biotin	Thermo (Waltham, USA)
Glycerol 99.5 %	AppliChem (Darmstadt)
L-Glutathione oxidized	Carl Roth GmbH & Co. (Karlsruhe)
L-Glutathione reduced	AppliChem (Darmstadt)
Guanidine hydrochloride	Carl Roth GmbH & Co. (Karlsruhe)
Hydrochloric acid (37%)	Carl Roth GmbH & Co. (Karlsruhe)
Imidazole	E. Merck KGaA (Darmstadt)
Fe(III)-citrate	Carl Roth GmbH & Co. (Karlsruhe)
Isopropyl β-D-1-thiogalactopyranoside (IPTG)	Fermentas (St. Leon-Rot)
Isopropanol	Carl Roth GmbH & Co. (Karlsruhe)
Kanamycin, monosulfate	Carl Roth GmbH & Co. (Karlsruhe)
Lysozyme	AppliChem (Darmstadt)
Magnesium sulfate heptahydrate	AppliChem (Darmstadt)
Manganese(II) chloride tetrahydrate	AppliChem (Darmstadt)
β-Mercaptoethanol	AppliChem (Darmstadt)
2- Morpholinoethanesulfonic acid (MES)	AppliChem (Darmstadt)
Nickel(II) chloride hexahydrate	AppliChem (Darmstadt)
pepton	Carl Roth GmbH & Co. (Karlsruhe)
Phenylmethylsulfonyl fluoride (PMSF)	AppliChem (Darmstadt)
Polyethylene glycol 8000	Carl Roth GmbH & Co. (Karlsruhe)
Silver nitrate	Carl Roth GmbH & Co. (Karlsruhe)
Sodium chloride	AppliChem (Darmstadt) & E. Merck KGaA (Darmstadt)
Sodium dihydrogen phosphate monohydrate	Carl Roth GmbH & Co. (Karlsruhe)
Sodium dodecyl sulfate (SDS)	AppliChem (Darmstadt)
Di- Sodium hydrogen phosphate	AppliChem (Darmstadt)

Sodium hydroxide	Carl Roth GmbH & Co. (Karlsruhe)
Sodium molybdate dehydrate	AppliChem (Darmstadt)
Sodium selenite	AppliChem (Darmstadt)
Tetracycline, hydrochloride	Carl Roth GmbH & Co. (Karlsruhe)
3,3',5,5'- Tetramethylbenzidine (TMB-xtra)	Kem-En-Tec Diagnostics A/S (Denmark)
Tris	AppliChem (Darmstadt)
Triton X-100	AppliChem (Darmstadt)
Tween 20	AppliChem (Darmstadt)
Urea	Carl Roth GmbH & Co. (Karlsruhe)
BME Vitamin complex	Sigma (Steinheim)
Zinc sulfate heptahydrate	AppliChem (Darmstadt)

2.1.2 Oligonucleotides

The oligonucleotides (primers, Tab. 2.1) were synthesized in Thermo Fisher Scientific (Ulm).

Tab. 2.1: Primer list

Primer	Sequence (5' to 3')
QZp01	GATAAAACCCATGGAGCCTCCGCC
QZp02	GGCGGAGGCTCCATGGGTTTTATC
QZp03	CCCAAGCTTTTATTAATGGTGATGGTGG
QZp04	GATCGAACCCATGGAGCCTCCGCC
QZp05	GGCGGAGGCTCCATGGGTTCGATCAAG
QZp06	CCCAAGCTTTTATTAATGGTGATGGTGGTGATGGTACAAATCCATGACTC
QZp07	TGGCGGAGGCTCCATGGG
LYP013	CCGGAATTCTGAACAAAAACTCATCTCAG
LYP016	ACGCCAGAATGTCGTTCACAG

pgBTG_FWBsa	CGTTAGGTCTCCCATGGGCAAAATCACCTTTTATGAAG
ChγBC_i-SF_fwd	ACGACCACCGGTCTCGCGTATCGTATGAAAATCTATG
Ci_RV	CGTTAGGTCTCCTCGAGGGATCCATACAGGTC
Co_FW	ACGACCACCGGTCTCGCGTATCGTTATTTCATGAAAATCC
Co_RV	CGTTAGGTCTCCTCGAGGGATCCATACAGATC

2.1.3 DNA vectors

DNA vectors used for cloning and expression are described in Table 2.2.

Tab. 2.2: DNA vector list

DNA vector	Characterization	Source
pET23dK^{R}	Expression vector for hγBC variants, modified with kanamycin resistent	Innoprofile NWG artificial binding proteins
T7Select10-3b	Mid-copy phage vector for hγBC library, with carbenicillin resistent	Novagen (United States)

2.1.4 Microorganisms

The *Escherichia coli* strains are described in Table 2.3.

Tab. 2.3: **Overview of *E. coli* strains**

E. coli strain	Genotype	Reference
DH5α	*SupE44,ΔlacU169,hsdR17,recA1, gyrA96,thi-1,relA1, lacI^{q}*	Biodynamic
BL21 (DE3)	*F^{-} ompT hsdSB($r_B^{-}m_B^{-}$)gal dcm (λcIst857ind1 Sam7 nin5 lacUV5-T7 gene1)*	Studier and Moffatt, 1986
Novablue (DE3)	*endA1 hsdR17(rK12– mK12+) supE44 thi-1 recA1 gyrA96 relA1 lac (DE3)F'[proA+B+ lacI qZΔM15::Tn10] (TetR)*	Novagen
BLT5403/ BLT5615		T7Select® System

2.1.5 Culture media and antibiotics

Components of each culture media are described in Table 2.4. The minimal medium I was used to express ^{15}N and $^{13}C/^{15}N$ labeled proteins and the minimal medium II for nPTH1R. ^{13}C-glucose, thiamine, antibiotics and other minirals were sterile filtered with 0.22 µm filter and added prior to the inoculation. All the other media were autoclaved at 121 °C for 15 min. For plating, corresponding antibiotic was added when media were cooled down to about 50 °C (Tab. 2.5).

Tab. 2.4: **Culture media components**

Media	Components
LB-medium (1l)	10 g Bacto Trypton, 5 g Bacto Yeast Extract, 10 g NaCl
LB-agar (1l)	LB-media with 15 g agar
2YT-medium (1l)	16 g Bacto Trypton, 10 g Bacto Yeast Extract, 5 g NaCl
1× ZY-medium (1l)	10 g Trypton, 5 g Hefeextract
50×M-solution	1.25 M Na_2HPO_4, 1.25 M KH_2PO_4, 2.5 M NH_4Cl, 0.25 M Na_2SO_4
50×5052-solution (1l)	25 % glycerin, 25 g glucose, 100 g alpha lactose monohydrat
1000×trace-solution	60 mM HCl, 50 mM $FeCl_3$, 20 mM $CaCl_2$, 10 mM $MnCl_2$, 10 mM $ZnSO_4$, 2 mM $CoCl_2$, 2 mM $CuCl_2$, 2 mM $NiCl_2$, 2 mM Na_2MoO_4, 2 mM Na_2SeO_3, 2 mM H_3BO_3
autoinduction-medium	1× ZY-media, 1×M-solution, 1×5052-solution, 0.2×trace-solution, 2 mM
ZYM-5052	MgSO4
MS medium	
dYT medium (1l)	16 g pepton, 10 g yeast extract, 5 g NaCl
5 x M9-solution (1l)	85 g $Na_2HPO_4 \cdot 12H_2O$, 15 g KH_2PO_4, 2.5 g NaCl, 5 g $^{15}NH_4Cl$
TS2-solution	100 mg $ZnSO_4 \cdot 7H_2O$, 30 mg $MnCl_2 \cdot 4H_2O$, 300 mg H_3BO_3, 200 mg $CoCl_2 \cdot 6H_2O$, 20 mg $NiCl_2 \cdot 6H_2O$, 10 mg $CuCl_2.2H_2O$, 900 mg $Na_2MoO_4 \cdot 2H_2O$, 20 mg Na_2SeO_3
minimal medium I (1l)	200 ml 5xM9, 2 ml TS_2-solution, 1 ml of 1M $MgSO_4$, 1 ml of 100 mM $CaCl_2$, 1 ml of 10 mM Fe(III)-citrate, 20 ml of 10 % ^{13}C-glucose, 5 ml BME Vitmin complex

minimal medium II (1l)	2 g Na_2MoO_4, 2.46 g $(NH_4)_2SO_4$, 0.5 g NH_4Cl, 14.6 g K_2HPO_4, 3.6 g NaH_2PO_4, 1 g ammonium hydrogencitrate, 1.2 g $MgSO_4 \cdot 7H_2O$, 5 g glucose, 100 mg thiamine, 0.74 g $CaCl_2 \cdot 2H_2O$, 0.18 g $ZnSO_4 \cdot 7H_2O$, 0.1 g $MnSO_4 \cdot H_2O$, 20.1 g Na_2-EDTA, 16.7 g $FeCl_3 \cdot 6H_2O$, 0.1 g $CuSO_4 \cdot 5H_2O$, 0.21 g $CoCl_2 \cdot 6H_2O$

Tab. 2.5: **Overview of antibiotics' concentration**

Antibiotic	Stock solution	Concentration in stock solution mg/ml	Concentration in media µg/ml
Carbenicillin	ethanol	100	100
Chloramphenicol	ethanol	30	30
Kanamycin	H_2O	50	50
Tetracycline	ethanol	12.5	12.5

2.1.6 Enzymes

Restriction enzymes

BamHI (10 u/µl)	Fermentas (St. Leon-Rot)
Eco31I (10 u/µl)	Fermentas (St. Leon-Rot)
EcoRI (10 u/µl)	Fermentas (St. Leon-Rot)
HindIII (10 u/µl)	Fermentas (St. Leon-Rot)
NcoI FastDigest®	Fermentas (St. Leon-Rot)
XhoI FastDigest®	Fermentas (St. Leon-Rot)

Polymerases

Taq polymerase (5 u/µl)	Fermentas (St. Leon-Rot)
Pfu polymerase (2.5 u/µl)	Fermentas (St. Leon-Rot)
Phusion polymerase (2 u/µl)	Finnzymes (Espoo, Finland)

Ligase

T4-DNA-Ligase (5 u/µl)	NEB (Ipswich, USA)

Nuclease	
Benzonase (25 U/µl)	E. Merck KGaA (Darmstadt)
DNaseI	AppliChem (Darmstadt)
Immunoconjugates	
anti-hγBC-antibody-peroxidase-conjugated	Scil proteins (Halle)
anti-his_6tag-antibody-peroxidase-conjugated	Roche (Mannheim)
anti-mouse-antibody-peroxidase-conjugated	Scil proteins (Halle)
Protease	
SUMO protease	Eva Bosse-Doenecke (Martin-Luther university of Halle-Witternberg)
Tobacco etch virus (TEV) protease	Invitrogen (Carlsbad, USA)
Phosphatase	
calf intestine alkaline phosphatase (CIAP)	Fermentas (St. Leon-Rot)

2.1.7 Standards and Kits

Standards

Gene Ruler™ 1kb DNA Ladder	Fermentas (St. Leon-Rot)
Gene Ruler™ 100bp DNA Ladder	Fermentas (St. Leon-Rot)
PageRuler™ Unstained Protein Ladder	Fermentas (St. Leon-Rot)
PageRuler™ Prestained Protein Ladder	Fermentas (St. Leon-Rot)

Kits

SV Mini Preps DNA Purification System	Promega (USA)
SV Gel and PCR Clean-up System	Promega (USA)
T7Select® System	Novagen (USA)

2.1.8 Buffers and solutions

All the buffers and solutions were produced with ultra pure filtrated water. Buffers for the chromatography were sterile filtrated, degassed and precooled at 4°C.

MES-buffer	50 mM MES, 50 mM Tris/HCl, 2 % SDS (w/v), 2 mM EDTA, pH 7.3
TAE-buffer	40 mM Tris/HAc, 2 mM EDTA, pH 8.5
PBS	50 mM NaH_2PO_4, 150 mM NaCl, pH 7.4
PBST (0.1%)	PBS, 0.1% Tween (v/v)
5 x SDS-Sample buffer	pH 6.8, 250 mM Tris/HCl, 5% (w/v) SDS, 50% Glycerol , 0.005% (w/v) Bromphenol blue

Buffers for the chromatography

Immobilized metal ion affinity chromatography (IMAC)

NPI-20	50 mM NaH2PO4, 150 mM NaCl, 20 mM Imidazol pH 7.4
NPI-35	50 mM NaH2PO4, 500 mM NaCl, 35 mM Imidazol pH 7.4
NPI-500	50 mM NaH2PO4, 150 mM NaCl, 500 mM Imidazol pH 7.4

Size exclusion chromatography (SEC)

PBS-EDTA	50 mM NaH2PO4, 150 mM NaCl, 1 mM EDTA, pH 7.8

Hydrophobic interaction chromatography (HIC)

buffer A	50 mM tris/HCl pH 8.0, 0.8 M L-Arginine, 1 M ammonium sulfate
buffer B	50 mM tris/HCl pH 8.0, 0.8 M L-Arginine

2.1.9 Other materials

1.5 ml reaction tube Protein LowBind	Eppendorf (Hamburg)
96-well microtiter plate (Medisorp, Maxisorp, Multisorp)	Nunc (Wiesbaden)
96-well microtiter plate (Highbinding, Lowbinding)	Greiner Bio-One (Frickenhausen)
96-well microtiter plate streptavidin coated	Thermo (Waltham, USA)
Cellulose nitrate filter (0.45µm)	Sartorius stedim (Göttingen)
Dialysis Cassette 3,500 MWCO Slide-A-Lyzer	Thermo (Waltham, USA)

Dialysis Units Mini 7,000 MWCO Slide-A-Lyzer	Thermo (Waltham, USA)
Dialysis Membrane 1,000 MWCO	Carl Roth GmbH & Co. (Karlsruhe)
DNA-ExitusPlus	AppliChem (Darmstadt)
Dynabeads® M-280 Streptavidin	Invitrogen (Norway)
Disposal hypodermic needle	Carl Roth GmbH & Co. (Karlsruhe)
Electroporation cuvette (1 mm)	BTX Harvard Apparatus (Holliston, USA)
Luer-Lok™-Syringe 1/3/5/20 ml	BD Plastipak™ (Heidelberg)
Membranfilter (PES, 0.22 µm and 0.45 µm)	Sartorius (Göttingen)
Membranfilter (0.2 µm)	PALL corperation (Michigan, USA)
NuPAGE. 4-12% Bis-Tris Gel 1,0mm	Invitrogen (Carlsbad, USA)
Parafilm	Pechiney Plastic Packaging (Chicago,USA)
pH indicator sticks	Carl Roth GmbH & Co. (Karlsruhe)
Quartz glass cuvette	Hellma (Jena)
Syringe driven filter units 4 mm, 0.2 µm	Millipore (Darmstadt)
Syringe filter (0.22 µm and 0.45 µm)	TPP (Trasadingen, Switzerland)
Vivaflow 200	Sartorius (Göttingen)
Vivaspin 20 centrifugal concentrator MWCO 3 kDa	Sartorius (Göttingen)
Vivaspin 4 centrifugal concentrator MWCO 5 kDa	Sartorius (Göttingen)
Vivaspin 500 centrifugal concentrator MWCO 3.5 kDa	Sartorius (Göttingen)
Ziptip Pipette Tips	Millipore (Darmstadt)

2.1.10 Devices and accessories

Absorption spectrophotometer

DU 730 UV-Vis-Spectrometer	Beckman coulter (Krefeld)

Autoclave

Systec V75	Systec (Wettenberg)

Balances

Analytical balance SI-234	Denver Instrument (Bohemia, USA)
Balance SI-2002	Denver Instrument (Bohemia, USA)

Biacore

Biacore T100	GE Healthcare Life Sciences (Freiburg)

CD-Spectrophotometers

Jasco J-815 Spectropolarimeter	Jasco (Groß-Umstadt)
Jasco J-810 Spectropolarimeter	Jasco (Groß-Umstadt)

Centrifuges and rotors

Heraeus Pico 17 centrifuge	Thermo (Waltham, USA)
Allergra X-15R centrifuge	Beckman Coulter GmbH (Krefeld)
Avanti J-26XP	Beckman Coulter (Krefeld)
Rotors: FX 6100	Beckman Coulter GmbH (Krefeld)
SX4750A	Beckman Coulter GmbH (Krefeld)
JA-25.50	Beckman Coulter GmbH (Krefeld)

Chromatography devices

ÄKTAxpress	GE Healthcare Life Sciences (Freiburg)
ÄKTAexplorer	GE Healthcare Life Sciences (Freiburg)

Chromatography columns

Immobilized metal ion affinity chromatography (IMAC)

HisTrap HP 1 ml column	GE Healthcare Life Sciences (Freiburg)
HisTrap HP 5 ml column	GE Healthcare Life Sciences (Freiburg)

Hydrophobic interaction chromatography (HIC)

HiTrap phenyl FF 1 ml column	GE Healthcare Life Sciences (Freiburg)

Size exclusion chromatography (SEC)	
PD-10 Desalting	GE Healthcare Life Sciences (Freiburg)
HiPrep 26/10 Desalting	GE Healthcare Life Sciences (Freiburg)
HiLoad 16/60 Superdex 75 *prep grade*	GE Healthcare Life Sciences (Freiburg)
Electroporation	
Electro Cell Manipulator 630	BTX, Havard Apparatus (USA)
Electroporation cuvetten 1 mm	BTX, Havard Apparatus (USA)
Fermentation	
Biostat C-DCU3	B. Braun (Melsungen)
Fluorescence spectrophotometer	
Fluorescence spectrophotometer FP-6500	Jasco (Groß-Umstadt)
Gel documentation instrument	
Bio-Vision 3000 Vilber	Lourmat (Eberhardzell)
Gelelectrophoresis	
EV 261 Electrophoresis	Camlab (Cambridge, UK)
Power Supply Consort	
agarose gelelectrophoresis	
Owl B1A EasyCast Mini Gel	Thermo Scientific (Langenselbold)
SDS-PAGE gelelectrophoresis	
XCell SureLock. Electrophoresis Cell	Invitrogen (Carlsbad, CA)
Homogenizer Gaulin APV	
High pressure homogeniser gaulin	APV Homogeniser GmbH (Lübeck)
Incubaters	
Heraeus BK 5060 E-S	Heraeus (Hanau)
Shaking incubator *Innova* 44R	New Brunswick Scientific (Nürtingen)
Isothermal Titration Calorimeter	
VP-ITC Isothermal Titration Calorimeter	Microcal LLC (Northampton, USA)
pH meter	
inoLab pH720	WTW (Weilheim)
Electrode SenTix 81	

Plate readers	
Multimode Detector DTX880	Beckman Coulter (Krefeld)
Multimode Detektor Biomek Paradigm	Beckman Coulter (Krefeld)
Roller	
Stuart SRT9	Bibby Scientific (Staffordshire, UK)
Vortex	
Vortex Genie 2	Scientific Industries (Bohemia, USA)
Thermocycler und Thermomixer	
Tpersonal	Biometra (Göttingen)
LabCycler gradient 96	Sensoquest (Göttingen)
Thermomixer comfort	Eppendorf (Hamburg)
Ultrasonication	
VC 750 Vibra Cell	Sonics & Materials (Newton, USA)
6 mm Sonotrode	Zinsser Analytic (Frankfurt/M.)

2.1.11 Softwares

Biacore Control & Evaluation software	GE Healthcare Life Sciences (Freiburg)
BIO-1D 5.1.26	Vilber Lourmat (Eberhardzell)
Clone Manager 9	Scientific & Educational Software (Cary, USA)
DSF analysis software	Dominik Schneider (Halle)
Origin 7.0	MicroCal (Northampton, USA)
ProtParam	http://www.expasy.org
PyMOL	DeLano Scientific (South San Francicso, USA)
UNICORN 4.11 Control-Software	GE Healthcare Life Sciences (Freiburg)

2.2 Methods

2.2.1 Molecular biological methods

2.2.1.1 Plasmid preparation

The plasmid-DNA from *E.coli* was prepared with SV Mini Preps DNA Purification Kit (Promega), according to the provided centrifuge protocol. To elute the DNA on the column 30-50 µl nuclease free water was used.

2.2.1.2 Agarose gel electrophoresis

For separation of nucleotide fragments less than 1 kb, 2% (w/v) Sieve 3:1 agarose gel was used. For separation of nucleotide fragments more than 1 kb, 1% (w/v) LE agarose gel was utilized. The separation was conducted at 80 V/14 cm, 80 min with TAE buffer. Then the gel was stained in fresh 2 µg/ml EtBr solution for 20-30 min.

2.2.1.3 Recovery of DNA from agarose gel

The separated DNA fragment was recovered with SV Gel and PCR clean-up system kit (Promega) according to the provided centrifuge protocol. The DNA was eluted by 30-50 µl nuclease free water from the binding column.

2.2.1.4 DNA digestion and dephosphorylation

Digestion of DNA fragment and plasmid was performed in a 20 µl system, which consists of 1 µg plasmid or 100 ng DNA fragment, 2 µl digestion buffer (10 ×), and 1 µl restriction enzyme. For large scale preparation in the aim of further ligation, the volume of each component increases proportionately. The reaction was at 37 °C for 1 h and the

enzymes were inactivated according to the manual. In order to minimize the re-ligation of digested plasmid, dephosphorylation was performed with 0.2 µl alkaline phosphatase and 2 µl buffer in a 20 µl reaction system at 37°C for 1 h.

The digested DNA was purified by agarose gelelectrophoresis, followed by SV Gel and PCR clean-up system kit.

2.2.1.5 Ligation

Digested and purified DNA fragments were ligated with T4 ligase in 4 µl reaction system. Maximal 40 ng DNA with molar ratio of insert to vector from 1:1 to 3:1 was incubated with 0.4 µl of 10 × T4 ligase buffer at 16 °C for 16 h and enzyme was inactivated by 65 °C for 10 min.

2.2.1.6 Polymerase chain reaction (PCR)

PCR is a molecular technique, which is used for amplification of specific regions of a DNA strand (DNA template), which could be a plasmid, a part of gene, or a non-coding sequence. In this thesis, *Taq* and other two kinds of developed high fidelity polymerase, *Pfu*, phusion, were usually utilized for DNA fragments amplification. Taking *Taq*-polymerase as an example, the cycling starts with an initial denaturation step, followed by 20-35 cycles of denaturation, annealing and elongation steps. The annealing temperature mostly relies on the primer sequences. The reaction time is determined by the length of the template DNA. The elongation rate of *Taq*-Polymerase is about 100 bp/s, *Pfu*-Polymerase 8-16 bp/s and Phusion-Polymerase 33-66 bp/s. The reaction conditions are variable when using different DNA template and primers. The PCR product was analyzed with agarose gel electrophoresis.

PCR program in the case of *Taq*-Polymerase:

initial denaturation	94°C	5 min
denaturation	94°C	50 sec
annealing	50-68°C	1 min
elongation	72°C	1 min (back to step 2 until 35th cycle)
final elongation	72°C	6 min

PCR program in the case of Phusion-Polymerase:

initial denaturation	98°C	30 sec
denaturation	98°C	10 sec
annealing	50-72°C	10 sec
elongation	72°C	10 sec (back to step 2 until 35th cycle)
final elongation	72°C	5 min

The amplified DNA fragments were purified by agarose gel and recovered by SV Gel and PCR clean-up system kit.

Colony PCR

The aim of colony PCR is for screening of bacterial, virus or yeast clones which contain the inserts in correct size. Selected colonies were picked with sterile toothpicks from an agar plate. Then the toothpicks with bacterial were put into individual 1.5 ml tubes containing 10 µl of sterile water respectively. The bacterial were eluted to water after several seconds of rinse. 1 µl of each bacterial sample was taken out and used as template for PCR amplification which was then conducted to determine if the colony contained the DNA fragment of interest.

For the phage colony PCR, single phage plaque was picked and infected 200 µl of BLT 5403 cells (OD_{600nm}=0.5-1), shaking until cell lysis. The phage lysate was obtained by centrifugation 8,000 × g for 10 min. 2 µl of phage lysate was added to 10 mM EDTA, pH 8.0, briefly vortexed and heated at 65 °C for 10 min. After cooling down, the sample

was centrifuged at top speed for 3 min. 1 µl of soluble sample containing phage genome was used as DNA template in the PCR. The PCR products were evaluated by agarose gel electrophoresis.

2.2.1.7 Plasmid DNA sequencing

The plasmid DNA sequencing was performed by QIAGEN GmbH (Hilden).

2.2.2 T7 phage display

Among the various selection systems to isolate binding variants against specific target molecule, phage display and ribosome display are the most commonly utilized techniques. During these *in vitro* selection processes, genotype and phenotype of each variant are connected. In contrast to filamentous phage, the character of T7 phage assembly in the cytoplasm of *E. coli* cells makes it highly suitable for displaying scaffolds, without complicated transportation pathway to the periplasm. The DNA library was inserted into self-prepared phage vector and phage library was constructed using T7Select® System kits. In the biopanning process, after incubation with target molecule, unbound phages were removed and specifically bound phages were eluted by proteolytic reaction. The output phages were amplified and entered the next cycle of selection. They were also analyzed for detection of possible binding candidates.

2.2.2.1 T7 phage DNA preparation

Mid-copy vector T7Select 10-3b extraction

50 ml of fresh T7 phage lysate was prepared by infection of T7 phage in BLT5403 cells at OD_{600nm}=0.5. After centrifugation at 8,000 ×g for 10 min to remove cell debris, the phages were filtrated with 0.45 µm filtrate membrane. 12.5 ml PEG/NaCl (30%/2.5 M) was added and incubated at 4 °C for overnight. Phage particles were pelleted by centrifugation at 11,000 × g for 10 min and then resuspended with 5 ml of 20 mM

EDTA, pH 8.0. 12.5 µl of protease K (20 µg/µl) was added to an end concentration of 50 ug/ml. Then 125 ul of 20% SDS-solution was added to end concentration 0.5% and mixed several times. The dissolved phages were heated at 56 °C for 1 h and cooled down to RT. 5 ml phenol was added and mixed several times, followed by centrifugation at 3,000g for 5 min. 4 ml of upper solution was taken out and transfered to a new tube. Then 4 ml chloroform was added, mixed and centrifuged at 3,000 × g for 5 min. 3 ml of upper solution was taken out. 300 µl of 3 M sodium acetate, pH 7.0 and 7.5 ml EtOH was added and stored at 4 °C for 1 h to precipitate the phage DNA, followed by washing twice with 30 ml 70% EtOH and centrifuged at 7,000 × g for 2 min. The DNA pellet was dried in air until all EtOH was evaporated and then dissolved in 200 µl TE buffer. The DNA concentration was determined by absorption at 260 nm.

Phage vector arms preparation

For library construction, phage vector arms were prepared in large scale.

T7 phage vector DNA (3085.1 µg/ml)	435 µl
10×Tango buffer	120 µl
EcoRI	15 µl
HindIII	30 µl
total	600 µl

The reaction mixture was distributed to 12 PCR tubes, 50 µl per tube and incubated at 37°C for 2 h, followed by inactivation of enzymes at 80°C for 20 min. 0.3 µl of 1 unit/µl calf intestine alkaline phosphatase (CIAP) per tube was added and incubated at 37°C for 20 min, followed by inactivation of enzymes at 85°C for 15 min. The digested vector was loaded on 0.5% LE GP gel and recovered using Promega kit.

Ligation of hγBC DNA library with T7 phage vector arms

The human γB crystallin was chosen as the scaffold for library construction. Eight solvent-accessible sites on the first β-sheet of N-terminal domain were randomized

(Ebersbach *et al.*, 2007). All the eight randomization positions were induced by 19-trinucleotide mixer (free of condons for cysteine) in primers. To facilitate efficient phage elution by TEV protease in following selection and subsequent detection in phage ELISA, an N-terminal mycut tag and a C-terminal hexa-histidine tag were introduced (constructed by Dr. Li Yuan, Innoprofile, Martin-Luther university of Halle-Witternberg). The DNA library was amplified by PCR using primers carrying EcoRI and HindIII enzyme cleavage sites respectively. After digestion and recovery by agarose gel, the DNA library was inserted into T7 phage vector by T4 ligase.

hγBC DNA library (21.5 ng/µl)	15 µl
T7 phage vector arms (1000 ng/µl)	10 µl
T4 ligase buffer (NEB)	10 µl
T4 ligase (NEB)	10 µl
H_2O	55 µl
total	100 µl

The reaction proceeded at 16°C for 16 h, followed by inactivation of enzymes at 65°C for 10 min.

2.2.2.2 Construction of phage library

90 µl fresh DNA ligation product was mixed with 450 µl phage extract (provided by 3 kits) and incubated at RT for 4 h. The phage packaging was stopped by addition of 4.86 ml of LB media. 10 µl of fresh assembled phage sample was transferred to a new tube for phage titer and calculation of library diversity. The rest part inoculated 1.6 ml of BLT5403 cells at OD_{600nm} 0.6 and distributed for 100 µl per well in 96-deep well plate, shaking at 37°C. The cells were lysed after 2.5 h and further inoculate 40 ml of BLT5403 cells at OD_{600nm} 0.6, shaking for 1 h at 37°C. The cell debris was removed by centrifugation at 8,000 × g for 10 min. 5 ml of 80% glycerol was added to the phage library and stored at -80°C. 48 stochastic variants from phage library were sent to Qiagen (Hilden, Germany) for sequencing in order to analyze the functionality of the library.

2.2.3 Selection of binding variant against nPTH1R

Prior to selection, 1 ml of amplified phage library containing 1.8×10^{10} phage clones was incubated with 200 µl of M280 streptavidin Dynabeads (Invitrogen), which was previously blocked by sterile phosphate-buffered saline (PBS) containing 0.1% Tween-20 (v/v) and 2% BSA (v/v), in two low-binding 1.5 ml tubes (Eppendorf) for 1 h at RT. Unbound T7 phages were then transferred to new tubes containing biotinylated N-terminal PTH1R, further incubation at RT with continuously rolling. After 1.5 h, the phage-protein complex solution was added into 200 µl of new blocked M280 streptavidin Dynabeads and mix for 1 h. Unspecifically bound phages were removed from beads by washing step with PBST (0.1% Tween-20, v/v), followed by PBS. Bound phages were eluted by Tev protease cleavage in 300 µl reaction system (15 µl of 20 × Tev buffer, 3 µl of 0.1 M DTT, 272 µl H_2O, 10 µl Tev protease) for 2 h at RT. 2 µl of eluted phage sample was used for tittering. The rest immediately infected 100 µl BLT 5615 cells at OD_{600} 0.8 with additional 200 µl M9TB media in a 96-deep well plate. In addition, the uncleaved bound phages were collected directly by adding 100 µl BLT 5615 cells to M280 streptavidin Dynabeads. Cells were lyzed after 2.5 h and released phages were mixed and infected 20 ml of BLT 5615 cells for further amplification. The output phages were collected by centrifugation at 8,000 × g for 10 min, filtrated with 0.45 µm membrane, followed by precipitation with ¼ volume of PEG/NaCl (30%/2.5 M) solution on ice for overnight and centrifugation at 11,000 × g for 10 min. The precipitated T7 phages were dissolved in 1 ml of LB media containing 8% glycerol and stored at -80 °C for the next selection. In this study, all 4 rounds of selection were carried out with stepwise harsher washing condition and reduced concentration of target molecule, from 400 nM to 25 nM (shown in Tab. 2.6). The blocking buffer was also changed from PBST (0.1% Tween-20, v/v)-2% BSA (v/v) in the first two rounds to the casein blocking buffer (Sigma, Steinheim) in the last two rounds, to increase the stringency.

Tab. 2.6: Overview of selection conditions

Panning round	Target protein amount	Blocking buffer	Wash condition
1	8.4 µg biotinylated nPTH1R (400 nM)	PBST(0.1%)BSA(2%)	8x PBST (0.1%) 2x PBS
2	4.2 µg biotinylated nPTH1R (200 nM)	PBST(0.1%)BSA(2%)	12x PBST(0.1%) 2x PBS
3	2.1 µg biotinylated nPTH1R (100 nM)	casein blocking buffer	15x PBST (0.1%) 3x PBS
4	0.5 µg biotinylated nPTH1R (25 nM)	casein blocking buffer	18x PBST (0.1%) 3x PBS

2.2.4 Cultivation of *E. coli* cells

2.2.4.1 Transformation of *E. coli* cells with plasmid DNA

Both chemical transformation and electroporation were utilized for plasmid transformation into *E. coli* cells. For the chemical transformation, 2 µl of ligation product or purified plasmid DNA was added into 100 µl of chemical competent cells and incubated at 4°C for 30 min followed by hot-shock at 42°C for 90 sec. Then 1 ml of LB media was added to each sample immediately. The culture was incubated at 37°C for 1 h with shaking at 140 rpm. 100-1000 µl of the total culture was spread onto a LB-Agar plate containing corresponding antibiotic for colony titration.

For the electroporation, 20-40 ng of plasmids were added into 100 µl of electrocompetent BL21 cells, with gently mixing, the cells were incubated on ice for 30 min and then transferred into a pre-chilled electroporation cuvette (1 mm gap). The electroporator was adjusted to the following parameters:

Voltage: 1800 V

Resistance: 200 Ω

Capacity: 25 µF

After the electroporation, 1 ml of LB media was immediately added into the cuvette.

The cultures were incubated at 37°C for 1 h with shaking at 140 rpm. 100-1000 µl of the total culture was spread onto a LB-Agar plate containing corresponding antibiotic for colony titration.

2.2.4.2 Culturing of *E.coli* cells and recombinant protein production

Test expression in 2 ml culture scale

2 ml of autoinduction media containing antibiotic was inoculated with expression *E. coli* cells and incubated for 16-20 h at 37°C with shaking at 220 rpm. OD_{600nm} was measured and the cell culture (volume = of $1/OD_{600nm}$ ml) was centrifuged at 4,500 × g for 10 min. The cell pellet was dissolved in 100 µl of PBS buffer containing 20 µg of lysozyme and incubated in the thermomixer with 600 rpm at RT for 20 min. The cells were then frozen completely in liquid nitrogen and thawed subsequently by incubating in the waterbath. This process was repeated for 5 times. Then 0.3 µl of benzonase (25 U/µl) and 0.2 µl of 1 M $MgSO_4$ was added and incubated at RT for 30 min. 6 µl of disrupted cells were transferred to a new tube as total cell lysate sample. The rest 94 µl was centrifuged at the top speed for 30 min. The supernatant containing soluble proteins was transferred to a new tube as soluble fraction. The insoluble pellet was washed by 150 µl of PBS by pipetting gently and centrifuged at top speed for 30 min. The insoluble fraction was resuspended in 94 µl of 8 M urea, 100 mM Tris pH 8.0, 1 mM EDTA and incubated in the thermomixer with 1,000 rpm at RT for 10 min. 6 µl of each sample was mixex with 3 µl of 5 × SDS sample buffer and incubated at 95 °C for 10 min for SDS-PAGE analysis.

Preparative expression of hγBC variant

The gene of the human γB crystallin variant was isolated from T7 genome by PCR and inserted into pET23d expression vector with modified kanamycin resistant (Dr. Sven Pfeifer, Martin-Luther university of Halle-Witternberg) by NcoI and XhoI restriction sites (Fig. 2.1). The expression plasmid was then transformed into BL21(DE3) cells.

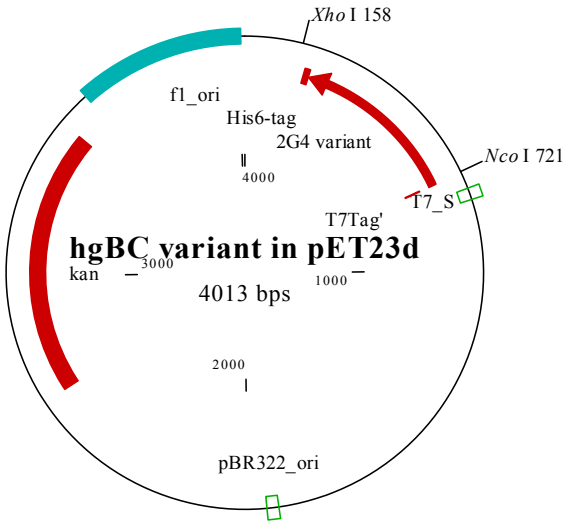

Fig. 2.1: Expression plasmid map for hγBC variant 2G4. The gene of hγBC variant 2G4 was inserted into expression vector pET23d with modified kanamycin resistant by *Nco* I and *Xho* I restriction sites. T7 promoter controls the expression of hγBC variant 2G4 with C-terminal hexahistidine tag. T7_S points out the starting site of T7 transcription and pBR322_ori represents the replication origin.

For large scale production, hγBC variant was expressed in shaking flasks with 20% volume of culture amout. The autoinduction culture started shaking with OD_{600nm} around 0.02 by inoculation with fresh prepared cell culture with OD_{600nm} between 0.5-1. After 20 h incubation at 37°C with shaking at 220 rpm, the cell pellet was harvested by centrifugation at 4,500 × g for 10 min.

For isotope labeled 2G4 protein production, 5 ml of dYT media was inoculated with cell glycerol stock and incubated for 8 h at 37°C, 220 rpm. Then 1.5 ml of dYT culture was used to inoculate 100 ml of M9 media and incubated for o/n. 2 l of M9 media was inoculated with 100 ml of M9 culture and OD_{600nm} started around 0.2. Cells grow until OD_{600nm} reaches 1 and induced by IPTG at the end concentration 1 mM. After 6 h growth, cell pellet was harvested by centrifugation at 7,000 rpm for 10 min.

Cell pellet from 100 ml of culture was resuspended in 10 ml of lysis buffer (50 mM NaH_2PO_4, 500 mM NaCl, 10 mM imidazole, 2.5 mM $MgSO_4$) with 1.5 mg lysozyme per gram of wet cell pellet. Ultrasonication was used to disrupt cells for 5-time pulses of 30 sec, with 30 sec pause in between. Then 2 µl of benzonase and 50 µl of 0.1 M PMSF was added and incubated for 30 min at RT. The soluble protein fraction was obtained by

centrifugation at 50,000 × g for 20 min.

Preparative expression of nPTH1R

For insoluble protein nPTH1R prepration, inclusion bodies were extracted from *E. coli* cells. 1 g of cell pellet was dissolved in 4 ml of 0.1 M tris/HCl pH 7.0 buffer, 1 mM EDTA. 2 mg lysozyme per gram cell pellet was added and incubated at RT for 30-40 min. Then end concentration of 3 mM $MgCl_2$ and 10 µg/ml DNase I was added and further incubated for 30-40 min at 4°C. The cells were disrupted by high-pressure dispersion at 600 bar. ½ volume of buffer 1.5 M NaCl, 60 mM EDTA, 6%Triton X-100 was added and incubated for 30 min at 4°C. The inclusion bodies were harvested by centrifugation at 10,000 rpm for 30 min and 3-time wash with 0.1 M tris/HCl pH 7.0 buffer, 20 mM EDTA.

1 g of inclusion bodies was then resuspended in 10 ml of 0.1 M Tris/HCl pH 8.0 buffer, 0.1 M DTT, 6 M guanidine hydrochloride for 2 h at RT and centrifuged at 20,000 rpm for 10 min to remove the aggregates. Acetate was added into the soluble fraction until pH value reached 2-3 and the protein sample was filtrated with filter membrane 0.45 µm befor applied to ÄKTA system.

2.2.5 Protein chemical methods

2.2.5.1 Sodium dodecyl sulfate polyacrylamide gel electrophoresis (SDS-PAGE)

NuPAGE 4 - 12% Bis-Tris Gels with 12 or 17 wells were utilized. The NuPAGE gels don’t contain SDS. Up to 20 µl of protein sample was mixed with 5 × SDS sample buffer and heated at 95°C for 10 min. For reduced samples, β-mercaptoethanol was added to the protein sample with a final concentration of 2% (v/v). The electrophoresis lasted 45 min at 200 V. The running buffer was NuPAGE MES buffer. The gels were stained in coomassie solution with shaking for at least 1 h.

2.2.5.2 Western blot

The WesternBreeze Chomogenic Immunodetection Kit (Invitrogen) was used to detect proteins immobilized on polyvinylidene difluoride (PVDF) membranes. 5 µl of prestained protein standard (Invitrogen) was loaded in the NuPAGE 4 - 12% Bis-Tris Gels. After electrophoresis, proteins were transferred onto a PVDF membrane using NuPAGE Transfer Buffer. 10 ml of primary antibody solution (diluted with blocking buffer) was used to detect the bound protein. The secondary antibody and the chomogenic substrate were respectively provided by the kit: anti-mouse IgG alkaline phosphatase conjugated, BCIP/NBT substrate for alkaline phosphatase.

2.2.5.3 Protein purification

Immobilized metal ion affinity chromatography (IMAC)

IMAC is used for the purification of fusion proteins containing shorter or longer polyhistidine tags, such as $(His)_6$ or $(His)_{10}$. The column, when charged with Ni^{2+} ions, selectively retains proteins if complexforming amino acid residues, in particular histidine, are exposed on the protein surface. The metal Ni^{2+} is held by chelation with nitrilotriacetic acid (NTA) covalently attached to a solid support. $(His)_6$ fusion proteins can be easily eluted with buffers containing imidazole.

Size exclusion chromatography (SEC)

SEC separates molecules according to differences in size as they pass though a gelfiltration medium packed in a column. The medium is a porous matrix in the form of spherical particles. The smaller molecules can diffuse into the pores and stay longer in the medium, while molecules larger than pores directly pass through the column. Gelfiltration can be used in separating small molecules, such as excess salts or free labels from large molecules and it is also a simple solution for buffer exchange.

Hydrophobic interaction chromatography (HIC)

HIC is based upon van der Waals attraction forces between solvent-accessible non-polar groups (hydrophobic patches) on the surface of biomolecules and the hydrophobic ligands (alkyl or aryl groups) covalently attached to the gel matrix. HIC is sensitive to discriminate non-polar groups normally buried in the tertiary structure of proteins with exposed when the polypeptide chain is incorrectly folded or damaged. Therefore, it can be used for separating the pure native protein from other forms or detecting protein conformational changes. Protein binding to HIC adsorbents is promoted by moderately high concentrations of salts, which can also stabilize the protein structure. Elution is accomplished by a linear or stepwise decrease in the concentration of salt.

Purification of hγBC variant

After cell disruption, the soluble fraction was loaded onto 5 ml Histrap column in ÄKTAexplorer system. Unbound proteins were washed away by 20 column volume (CV) of NPI-20 buffer and further 5 CV of NPI-35 buffer. The bound His-tagged protein was eluted with 5 CV of NPI-500 buffer and the protein fraction from the biggest peak was collected in a 5-ml loop automatically with parameters of level and slope (starting collection at 20 mAU and 10 mAU/min, and ending at 20 mAU and 20 mAU/min respectively).

The collected protein was further loaded onto HiLoad 16/60 Superdex 75 *prep grade* column and eluted with 1.3 CV of 1×PBS, 1 mM EDTA. The purity of the protein was monitored by SDS-PAGE gel.

Purification of nPTH1R

The solubilized inclusion bodies of nPTH1R was loaded onto HiPrep 26/10 Desalting column and eluted with 0.1 M tris/acetate pH 4.0, 1 mM EDTA, 4 M guanidine hydrochloride. The collected protein fractions were adjusted with NaOH to pH 8.0, filtrated and applied onto Histrap HP 5 ml column. Unbound protein was washed away with 2 CV of 0.1 M tris/HCl pH 8.0, 4 M guanidine hydrochloride and further with

5 CV of 0.1 M tris/acetate pH 6.3, 4 M guanidine hydrochloride. The bound protein was eluted with 3 CV of 0.1 M tris/acetate pH 4.5, 4 M guanidine hydrochloride.

The purified inclusion bodies were collected and diluted rapidly into refolding buffer 50 mM tris/HCl pH 8.0, 1 M L-Arginine, 1 mM EDTA, 5 mM GSH, 1 mM GSSG. All 4 pulses were performed with 6 h pause in between and the protein end concentration shouldn't exceed 0.2 mg/ml, while guanidine hydrochloride concentration in the final refolding buffer was less than 0.1 M. The refolded protein sample was concentrated with vivaflow 200 to about 100 ml. Unfolded or misfolded protein was precipitated slowly in 4 portions with ammonium sulfate to end concentration 1 M. The aggregates were removed by centrifugation at 30,000 g for 30 min and filtration with 0.45 μm filter membrane.

Then the protein sample was loaded onto HiTrap phenyl FF 1 ml column with binding buffer A 50 mM tris/HCl pH 8.0, 0.8 M L-Arginine, 1 M ammonium sulfate and eluted with buffer B 50 mM tris/HCl pH 8.0, 0.8 M L-Arginine in 3 segment: 10 CV of step elution with 60% buffer B, 20 CV of gradient elution from 60% to 100% buffer B, and further 15 CV of 100% buffer B. The protein fractions were pooled and finally polished by HiLoad 16/60 Superdex 75 *prep grade* column and eluted with 1.5 CV of 50 mM tris/HCl pH 8.0 buffer, 300 mM ammonium sulfate. The purity of the protein was analyzed by SDS-PAGE gel.

2.2.5.4 Biotinylation of nPTH1R

For conveniently immobilization, nPTH1R was chemically biotinylated by EZ-Link® Sulfo-NHS-LC-Biotin. In PBS pH 7.4, N-terminus of the protein or several primary amines in the side chain of lysine residues are available for labeling with NHS-activated biotin reagents. In the reaction, 100 μl of protein sample in PBS was incubated with Sulfo-NHS-LC-Biotin at 4°C for 2 h, with molar ratio 1:20. The free Sulfo-NHS-LC-Biotin was removed by dialysis overnight at 4°C. This product was used

in selection of hγBC variant. In PBS pH 6.5, only N-terminus of the protein can be biotinylated and the molar ratio of protein to biotin reagent was 1:2 in the reaction. The mono-biotinylated product was used in the SPR measurement.

2.2.5.5 Protein dialysis and concentration

For buffer change, the protein solution was dialyzed in 3,500 MWCO Slide-A-Lyzer Dialysis Cassette (0.1-3 ml) or 1,000 MWCO dialysis membrane for larger volume. The protein dialysis proceeded for 24 h at 4°C with 3-time buffer exchanges. For concentration of protein solution, Vivaspin 4, 20, 500 (Sartorius Stedim) were utilized for 4 ml, 20 ml and 500 µl of protein sample, respectively.

2.2.5.6 Protein concentration measurement

The pure protein concentration was measured by DU 730 UV/Vis Spectrophotometer. The extinction coefficient was calculated by program Protparam (http://expasy.org/tools/protparam.html). The spectrum ranged from 220 nm to 330 nm. The protein concentration was calculated by the optical absorption value at 280 nm (Equation 1).

$$A_{280} = \epsilon_{280} \cdot c \cdot d \qquad \text{(Eq. 1)}$$

A_{280} Absorption at 280 nm

ϵ_{280} Extinction coefficient of protein at 280 nm in $M^{-1}cm^{-1}$

c protein concentration in M

d path length

The protein concentration in mg/ml was calculated by multiplying molecular weight of protein in g/mol, which was also from program Protparam.

2.2.6 Enzyme-Linked Immuno Sorbent Assay (ELISA)

ELISA was used to detect interaction of two binding molecules. 30-500 ng ligand molecule in 100 µl was immobilized in a 96-well microtiter plate at 4°C for overnight, in parallel with BSA or lysozyme as negative control. Unbound ligand was washed away by PBST (0.1% Tween) for 3 times. Then unspecific binding sites were blocked by 1 × casein blocking buffer (Sigma) with incubation at RT for 1 h. After 3-time wash with PBST (0.1% Tween), binding protein or phage lysate in series of dilution was added for 100 µl per well. In competition ELISA, binding protein was mixed with free ligand as competitor at RT for 1 h before added into microtiter plate. After 1 h incubation at RT, the plate was washed again by PBST (0.1% Tween) for 3 times and the binding protein was recognized by antibody with peroxidase conjugated, 100 µl per well, at RT for 1 h. After 3-time wash with PBST (0.1% Tween), peroxidase substrate (50 µl TMB or TMBxtra per well) was added and the reaction was stopped by 50 µl per well of 0.5 M H_2SO_4. The Absorption at 450 nm was measured by microtiter plate reader (Beckman Coulter).

For concentration-dependent ELISA, the raw data were fitted in nonlinear regression function (Equation 2) and for competition ELISA, one-site competition equation (Equation 3) was used for affinity determination. In the pH-screening experiment, the raw data were fitted in sigmoid equation (Equation 4) and pKa value was hence addressed.

$$y = B_{max} \times x/(K_D + x) \qquad \text{(Eq. 2)}$$

y	binding signal measured in ELISA
B_{max}	calculated maximum binding signal
x	protein concentration
K_D	calculated apparent dissociation constant

$$y = A_2 + (A_1-A_2)/(1 + 10^{(x-\log x_0)}) \quad \text{(Eq. 3)}$$

y	binding signal measured in ELISA
A_1	calculated maximum binding signal
A_2	calculated minimum binding signal
$\log x_0$	calculated concentraion at the transition midpoint
x	log concentration of competitor protein

$$y = y_0+a/(1+\exp(-(x-x_0)/b)) \quad \text{(Eq. 4)}$$

y	binding signal measured in ELISA
y_0	calculated minimum binding signal
x	pH
x_0	pKa
a	calculated maximum binding signal - calculated minimum binding signal
b	the slope of the curve within pKa.

2.2.7 Mass spectrometry

The chemical modified protein was identified by mass spectrometry. Ionized components of the protein sample are separated in the electromagnetic fields by their mass to charge ratio. There are two primary methods for ionization of proteins, electrospray ionization (ESI) and matrix-assisted laser desorption/ionization (MALDI). The protein sample was firstly desalted by Ziptip (Millipore) before measurement. In this work, ESI was used by Dr. Schierhorn in Biochemistry institute at the Martin-Luther university of Halle-Witternberg.

2.2.8 Surface plasmon resonance spectroscopy (SPR)

Surface plasmon resonance (SPR) is used to study interaction between molecules, one of which is immobilized on the sensor surface and the other passes over the surface in the running buffer. The detected response is proportional to the molecular mass on the surface. The analysis consists of three steps: immobilizing target molecule on the sensor chip, followed by monitoring injected binding partner interacting with target and finally removing bound partner from target. In this thesis, Sensor Chip SA with covalently attached streptavidin was used for capturing biotinylated target protein nPTH1R. The functionality of immobilized nPTH1R was verified by interaction with ligand PTH1-84. Running buffer was 1 × PBS, 1 mM EDTA, pH 7.8. The binding measurement proceeded at 22°C, with flow rate 30 µl/min. Different concentration of binding variant PTH ligand was injected and associated with target nPTH1R for 120 sec. Then the injection stopped and the sensor chip was washed with running buffer for 300 sec. To remove the binding partner completely, it was further washed with the regeneration solution 10 mM glycine/HCl pH 2. The activity of immobilized nPTH1R was not impaired. The binding responses were analyzed by software BIAevaluation (GE Healthcare Life Sciences).

2.2.9 Isothermal titration calorimetry (ITC)

Isothermal titration calorimetry (ITC) is the only technique that can directly measure the binding energetics of biological interaction. The Gibbs energy, enthalpy, entropy, and heat capacity changes associated with binding can be accurately determined by ITC. The binding analysis of nPTH1R to ligand PTH1-84 or hγBC variant 2G4 was performed in VP-ITC Isothermal Titration Calorimeter (Microcal LLC, Northampton, USA). All protein samples were dialyzed against 1 × PBS, 1 mM EDTA, pH 7.8 and filtrated before measurement. The data was analyzed by Origin 7.0 (MicroCal Northampton, USA).

PTH1-84 binding to nPTH1R

At 20°C, 300.2 µM ligand PTH1-84 was titrated into 28.0 µM nPTH1R in 29 injections with 2 µl for the first injection and 10 µl for the other 28 injections. As reference, the identical ligand PTH1-84 sample was titrated into1 × PBS, 1 mM EDTA pH 7.8 for correction of enthalpy simply caused by peptide dilution.

hγBC variant 2G4 binding to nPTH1R

211 µM hγBC variant 2G4 was titrated into 19.7 µM nPTH1R using the same program as above described in 29 injections at 20°C, in parallel with the reference of the identical hγBC variant 2G4 sample titrated into buffer.

PTH1-84 binding to hγBC variant 2G4 - nPTH1R complex

158.4 µM hγBC variant 2G4 was incubated with 15.8 µM nPTH1R for 1 h at RT. Then, 171.8 µM PTH1-84 was titrated to the mixed complex as above described in 29 injections at 20°C, in parallel with the reference of the identical PTH sample titrated into 158.4 µM hγBC variant 2G4.

2.2.10 Differential Scanning Fluorimetry (DSF)

Differential scanning fluorimetry is a rapid and inexpensive method to evaluate protein themal stability, owing to the small amounts and low concentrations of protein required. The protein unfolding process is monitored by an increase in the fluorescence of a dye with affinity for hydrophobic parts of the protein, which are exposed as the protein unfolds. DSF experiments are typically performed by using a real-time PCR instrument, in this particular thesis, LightCycler 480 II. The fluorescent dyes for DSF are highly fluorescent in non-polar environment, like the hydrophobic sites on unfolded proteins, while the fluorescence is quenched in aqueous solution. 10 µg protein was diluted in 50 µl PBS containing 2× sypro orange dye. Thermal unfolding followed between 20-90°C with shift of approximately ΔT=1°C/min. The fluorescence intensity is plotted as a function of temperature which forms a sigmoidal curve that can be described by a

two-state transition. The inflection point of the transition curve (Tm) is calculated using Boltzmann equation as above described (Equation 4, Chapter 2.2.6) with following parameters (Schneider, 2009).

y fluorescence intensity

y_0 minimum intensitiy

x temperature

x_0 T_m

a calculated maximum binding intensity - calculated minimum binding intensity

b the slope of the curve within T_m.

2.2.11 Circular Dichroism (CD) spectroscopy

Circular Dichroism (CD) spectroscopy technique is widely used for the evaluation of the conformation and stability of proteins. Circular dichroism refers to the differential absorption of left and right circularly polarized light by optically active chiral molecules. The secondary structure of proteins can be analyzed by CD because the peptide bond is asymmetric and the amide chromophore of the peptide bond dominates the CD spectra of proteins at far-UV region. Aromatic residues (tryptophan, tyrosine and phenylalanine) and cysteine (or disulfide bonds) can exhibit circular dichroism in the near-UV region to provide information on the tertiary structure. In this thesis, the secondary structures of single proteins and thermal stability were analyzed by Jasco J-815 CD-Spectropolarimeter (Jasco, Groß-Umstadt).

The secondary structure of isolated hγBC variant was analyzed by far-UV CD spectrum. 10 µM protein sample in cuvette of 0.1 cm pathlength was measured from 200-260 nm with bandwidth of 1 nm at 20 °C. The signal/noise ratio was improved by 10 spectra accumulation. The protein sample was prepared in 5 mM NaH_2PO_4, 15 mM NaCl, pH 7.8. All the spectra data were corrected by buffer signal and normalized to the the mean residue molar ellipticity by the Equation 5.

$$[\theta]_{mrw} = \theta \times 100 \times M / C \times l \times n \qquad \text{(Eq. 5)}$$

$[\theta]_{mrw}$	mean residue molar ellipticity (deg cm^2 $dmol^{-1}$)
θ	measured ellipticity (deg)
l	optical path (cm)
C	concentration (mg/ml)
M	molecular mass of the protein (Da)
n	number of residues in the protein

Temperature induced protein unfolding was monitored by the wavelength 217 nm. 10 µM protein sample in cuvette of 0.1 cm pathlength was measured in the range of 20-82°C, with speed of 1°C/min. The data point at each increment of 0.2°C was recorded and fit in Boltzmann equation (Equation 2).

2.2.12 NMR spectroscopy

Nuclear magnetic resonance (NMR) spectroscopy is based on research of the magnetic properties of certain atomic nuclei, such as ^{1}H, ^{13}C, ^{15}N, to reveal their chemical environments. From the past few decades, it became an important technique to study the structure and dynamics of protein. In this thesis, the interaction of hγBC binding variant during the titration of target molecule nPTH1R was analyzed using ^{1}H-^{15}N 2D heteronuclear single quantum correlation (HSQC, Vuister and Bax, 1992; Mori *et al.*, 1995) and 3D NMR experiments. The experiments were nicely performed by Mohanraj Gopalswamy from institute of Physics/Biophysics, Martin-Luther university of Halle-Witternberg. Sequence-specific resonance assignments of ^{15}N-^{13}C-labeled hγBC variant were aquired from the 2D HSQC and TROSY (Transverse relaxation optimized spectroscopy) (Pervushin *et al.*, 1997) based 3D experiments (Kay *et al.*, 1990; Clore and Gronenborn, 1991; Grzesiek and Bax, 1992; Salzmann *et al.*, 1998) at protein concentration 780 µM. The specific amino acids involved in the binding interaction were identified by NMR titration experiment. This experiment was carried out using

443 μM nPTH1R titrated into 340 μM ^{15}N-labeled hγBC variant 2G4 and pertubration was monitored by ^{15}N-FHSQC (Mori *et al.*, 1995) or ^{15}N-TROSY-HSQC (Pervushin *et al.*, 1997). Following the nPTH1R-2G4 complex formation, 1.1 mM PTH ligand was further titrated to the NMR sample for competition assay. All NMR data were recorded by Bruker Avance III-Spectrometer 800 MHz at 25°C. The spectra were processed by NMRPipe (Delaglio *et al.*, 1995) and analyzed using NMRView software (Johnson and Blevins, 1994). All protein samples were prepared in 50 mM sodium phosphate, 200 mM NaCl, 0.02 % NaN_3, 10% D_2O and pH 7.8.

3 Results

3.1 Preparation of target molecule nPTH1R

The N-terminal extracellular domain of parathyroid hormone 1 receptor (nPTH1R) from the class B G-protein-coupled receptors was chosen as a target protein for selection of human γB crystallin (hγBC) based binding variants. The preparation of nPTH1R was based on the established protocol (Grauschopf *et al.*, 2000) and optimized as described in methods Chapter 2.2.4.2. The functionality of purified nPTH1R was monitored by ITC with ligand PTH1-84.

3.1.1 Production and purification of target molecule nPTH1R

The gene of nPTH1R was cloned into the vector pET15b and transformed into *E. coli* BL21(DE3) strain (Nils Drechsler, Institute of Biochemistry and Biotechnology, Martin-Luther university of Halle-Witternberg). The cells were grown in minimal salt media through the process of fermentation. The cultivation temperature was 37 °C. 13 h after feeding with glucose solution, OD_{600nm} of the cell culture reached 87.2 and the expression of protein was induced by IPTG at a final concentration of 1 mM for 4 h until OD_{600nm} reached 100.8. The cells were harvested by centrifugation at 4,500 × g for 10 min. The total wet biomass was 1,240 g. After cell lysis, 31.4 g of inclusion bodies were extracted from 300 g cell pellet and dissolved in buffer containing 6 M guanidine hydrochloride and 100 mM DTT. nPTH1R was purified from solubilized inclusion bodies by IMAC. 2.5 mg/ml eluted protein (17 ml) was refolded by pulse renaturation in 2 l of buffer with redox shuffling system (50 mM Tris/HCl pH 8.0, 1 M L-Arginine, 1 mM EDTA, 5 mM GSH, 1 mM GSSG). The correctly folded protein was separated from unfolded and misfolded protein by ammonium sulfate precipitation and subsequent hydrophobic interaction chromatography (HIC). In the last step, gel filtration was utilized to polish the protein. The purity of prepared nPTH1R was

monitored by SDS-PAGE (Fig. 3.1A). In the analytical size exclusion chromatography, a single sharp peak of monomer nPTH1R was obtained, and no dimer or aggregates were found (Fig. 3.1B). Electrospray ionization (ESI) mass spectroscopy confirmed the molecular mass of 21,496 Da for the prepared nPTH1R (data not shown). The yield was 60 µg protein/g wet cell biomass.

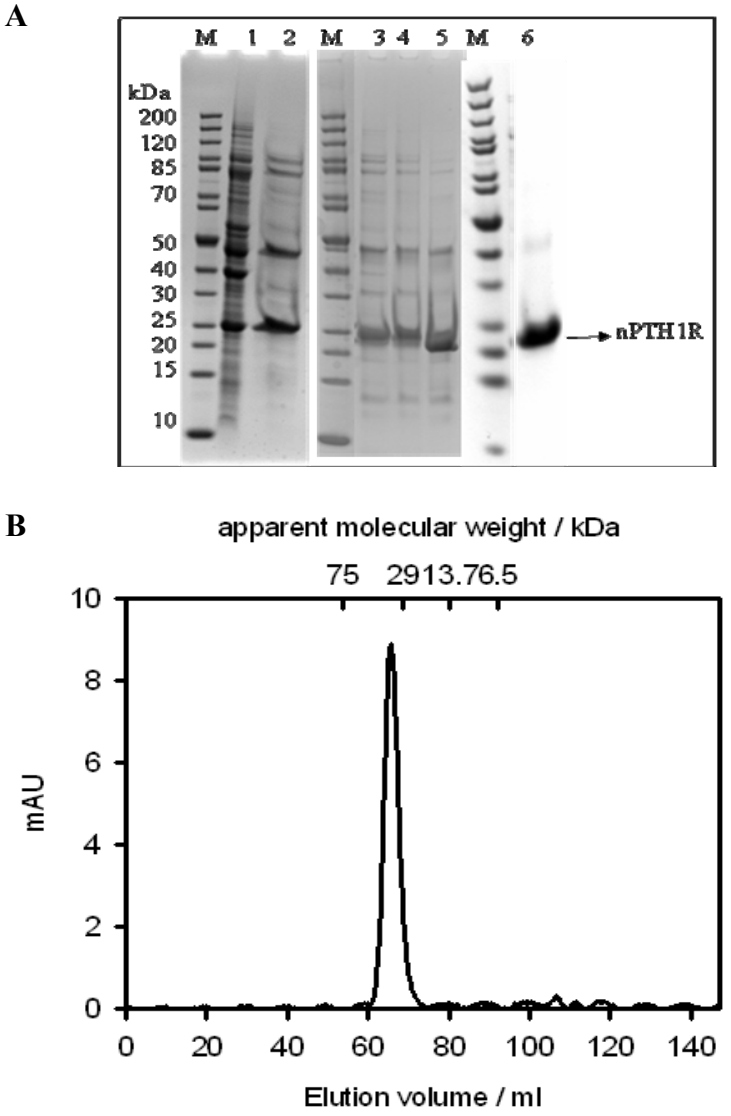

Fig 3.1: A. SDS-PAGE analysis of purified nPTH1R. Protein samples from each purification step were analyzed by 4-12% gradient gel and subsequently stained by coomassie blue. M stands for fermentas unstained protein ladder. In the 1st lane, solubilized inclusion bodies of nPTH1R are loaded. The 2nd lane shows the protein purified by IMAC. Lane 3 contains the protein after pulse-renatuaration and concentration. nPTH1R purified by ammonium sulfate precipitation is shown in lane 4. Lane 5 and 6 represent the protein purified by HIC and subsequent gelfiltration, respectively. **B. Analytical size exclusion chromatogram of nPTH1R.** 500 µl of 10 µM nPTH1R was loaded onto gel filtration HiLoad16/60 Superdex 75 prep grade column in running buffer PBS, 1 mM EDTA.

3.1.2 Functionality test of nPTH1R and biotinylated nPTH1R

The functionality of nPTH1R was analyzed by demonstrating its binding to the ligand PTH1-84 monitored by ITC. Figure 3.2 shows a typical titration experiment and evaluated data. The data showed that the binding interaction was exothermal. The dissociation constant was calculated to be 8.4 μM. The free binding enthalpy ΔG_{ITC}, the apparent binding enthalpy ΔH_{ITC}, the apparent binding entropy ΔS_{ITC} and the number of binding site N are listed in Table 3.1.

Tab. 3.1: Thermodynamic parameters of nPTH1R binding to PTH1-84

ΔG_{ITC}	-6.85 ± 0.16 kcal/mol
ΔH_{ITC}	-10.79 ± 0.16 kcal/mol
ΔS_{ITC}	-13.60 cal/mol·K
N	1.16 ± 0.01
K_D	8.40 ± 0.39 μM

The apparent binding enthalpy ΔH_{ITC} for -10.8 kcal/mol revealed that the binding reaction is an enthalpy-driven process. The negative change of the apparent binding entropy ΔS_{ITC} indicated that, during the complex formation, the structural conformation of one or both binding partners has been restricted or water molecules have been involved in the complex (Grauschopf *et al.*, 2000). The functional part of PTH ligand is the N-terminal fragment 1-34, which consists of two continuous helices. The amphipathic α-helix 15-34 docks into an extended hydrophobic groove formed by nPTH1R during the binding interaction (Pioszak and Xu, 2008). This structural fixation during binding interaction is assumed to contribute greatly to the negative entropy change. The number of binding site N not only suggested the 1:1 stoichiometry of binding partners nPTH1R and ligand PTH1-84, but also comfirmed the functionality of the refolded nPTH1R, which contained almost no inactive population.

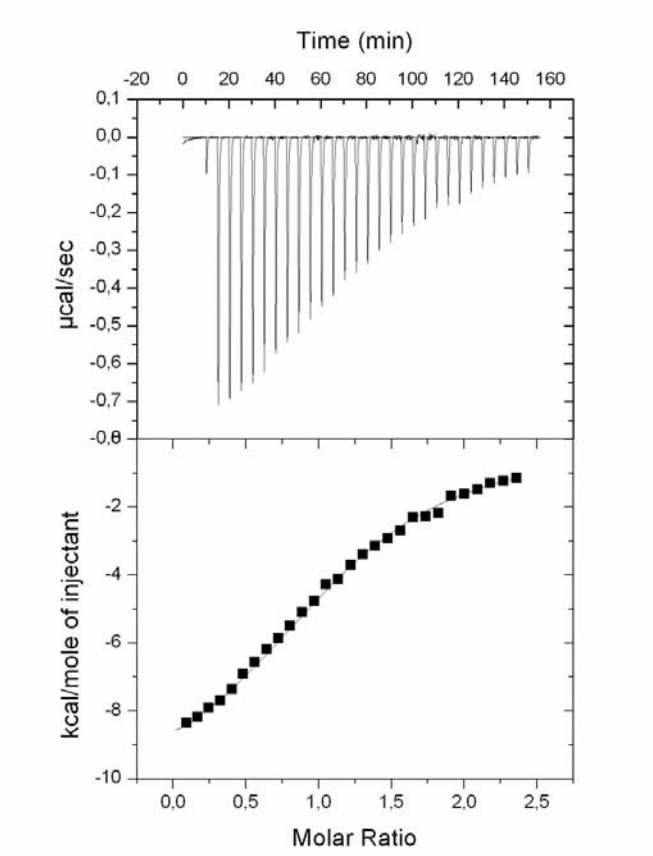

Fig 3.2: isothermal titration calorimetry analysis of binding interaction between nPTH1R and PTH1-84. At 20°C, 300.2 µM ligand PTH1-84 was titrated into 28.0 µM nPTH1R in 29 injections with 2 µl for the first injection and 10 µl for the other 28 injections. Protein and ligand were both prepared in PBS, 1 mM EDTA, pH 7.8. Top: baseline subtracted raw data of heat energy. Bottom: peak-integrated and concentration-normalized enthalpy change plotted against nPTH1R/PTH1-84 ratio. The experimental data were fit to a 1:1 binding model in the solid line.

For convenient immobilization in the subsequent selection process, the target molecule nPTH1R was chemically biotinylated. The functionality of biotinylated nPTH1R was further confirmed by ELISA and surface plasmon resonance (SPR). In streptavidin coated 96-well plate, biotinylated nPTH1R could be recognized by anti-nPTH1R-antibody in a concentration-dependent manner (data not shown). In the SPR measurement (Fig. 3.3), biotinylated nPTH1R was immobilized on the streptavidin (SA) chip and 0-20 µM PTH1-84 was injected. The real-time sensorgram demonstrated that PTH1-84 could bind biotinylated nPTH1R on the chip in a fast association, as well as fast dissociation process. The interaction occured in a concentration-dependent manner. The dissociation constant was determined to be 6.8 µM, in agreement with the

result of the ITC measurement (Fig. 3.2). Therefore, it can be concluded that biotinylated nPTH1R is still functional.

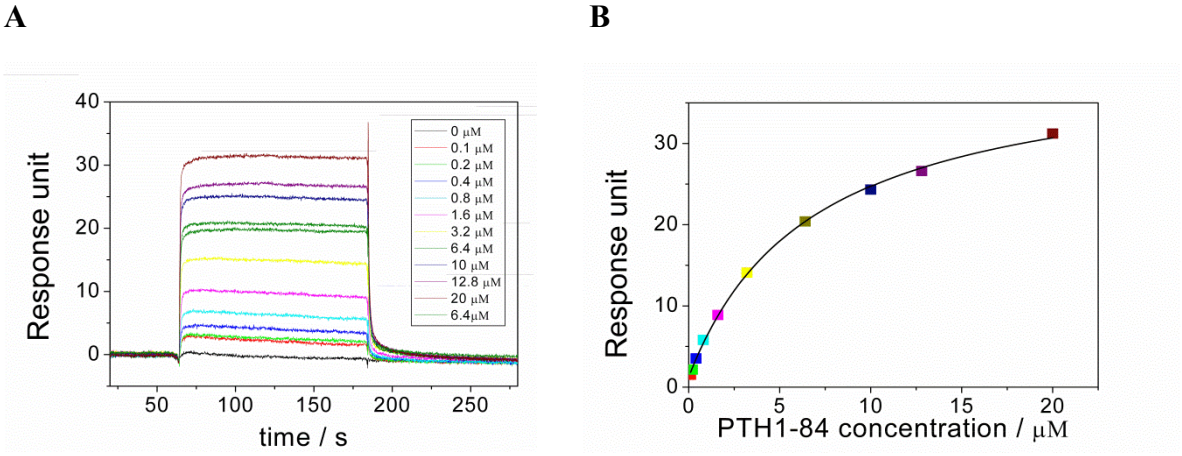

Fig. 3.3: Binding of biotinylated nPTH1R to PTH1-84 monitored by surface plasmon resonance (SPR) measurement. 105.7 response unit (RU) of biotinylated nPTH1R was immobilized on the streptavidin chip and 0-20 µM of PTH ligand 1-84 was injected at a flow-rate of 30 µl/min. The protein sample was prepared in running buffer PBS, 1 mM EDTA, pH 7.8. The real-time response signals are shown in Figure A. The response units at the steady-state are plotted against PTH1-84 concentration and fitted to 1:1 binding curve in Figure B. The K_D was calculated to be 6.77 ± 0.5 µM.

3.2 Phage library construction and selection against nPTH1R

To select binding proteins against target molecule nPTH1R, a cDNA library containing hγBC variants with eight randomization sites on the surface-exposed β-sheet of the N-terminal domain was constructed by a trinucleotide-based strategy (Fig. 1.3, described in detail in Chapter 1.3, Dr. Li Yuan, Innoprofile, Martin-Luther university of Halle-Witternberg). For the selection process the T7 phage display technique was chosen from variety of selection methods. During T7 phage assembly, fast folding scaffold variants don't need to be transported across the cell membrane into the periplasm for packaging as it would be the case of M13 phage display. They can be directly and efficiently displayed on the phage surface upon cytosolic phage assembly.

3.2.1 T7 phage library construction

322.5 ng of hγBC cDNA library, which contained thereotically 32 copies of each DNA variant, was inserted into 10 μg of self prepared mid-copy T7 phage vector. Using T7 phage extract provided from three T7Select® System kits, a phage library containing total quantity of 1.6 x 10^8 packaged primary phage clones was obtained, a library diversity similar to that previously described for T7 phage system (Dai *et al.*, 2008). To determine the functional portion of the library encoding the human γB crystallin variants, DNA sequences of 48 primary phage clones were analyzed. The sequencing result showed that 54% of total hγBC variants were correct in sequence and probably displayed on the T7 phage surface. Another T7 phage library displaying hγBC variants with identical randomization sites constructed by traditional NNK strategy demonstrated only 46% functionality (Dr. Li Yuan, Innoprofile, Martin-Luther university of Halle-Witternberg). From this result, it is clear that the library functionality depends more on the quality of synthesized oligonucleotides in the PCR reaction than the type of randomization strategy. Commercial oligonucleotides with randomization positions contain a heterogenous mixture of variable molecules with single nucleotide insertion or deletion, which can not be completely removed after synthesis. Several such oligonucleotides used for library construction lead to great influence on the final functionality. Under this condition, the trinucleotide-based library still surpasses the NNK-based library. Since *E. coli* BLT5403 used for T7 phage amplification does not suppress termination by the amber codon, the present trinucleotide-based strategy introducing no stop codon can enhance the functionality of the phage library. Besides, amino acid residues could be more equally distributed in the trinucleotide-based strategy and unwanted cysteine was successfully excluded.

The original phage library was amplified in fresh BLT5403 cells and reached 2.6× 10^{10} plaque forming units (pfu) per ml. About 100 copies of each phage variant were present in 1 ml of phage library lysate that was used as input phages during the selection.

3.2.2 hγBC binder selection against biotinylated nPTH1R

In order to select hγBC variants that bind specifically to nPTH1R the hγBC library was subjected to four rounds of selection by mixing the phage library and biotinylated nPTH1R. The binding complexes were captured by M280 streptavidin Dynabeads. This selection-in-solution method ensures that all the epitopes on target molecule nPTH1R are accessible for binding variants.

Tab 3.2: Overview of the panning procedure in the selection process

Panning round	Target protein biotinylated nPTH1R	Wash condition	Input phage	Output phage	Ratio output : input
1	8.4 µg (400 nM)	8 x PBST (0.1%) 2 x PBS	$1.8x\ 10^{10}$	$6.3x\ 10^{5}$	$3.5x10^{-5}$
2	4.2 µg (200 nM)	12xPBST(0.1%) 2 x PBS	$2.2x\ 10^{10}$	$5.7x10^{5}$	$2.6x10^{-5}$
3	2.1 µg (100 nM)	15x PBST (0.1%) 3 x PBS	$1.6x\ 10^{10}$	$2.1x10^{3}$	$1.3x10^{-7}$
4	0.5 µg (25 nM)	18x PBST (0.1%) 3 x PBS	$1.1x\ 10^{10}$	$3x10^{4}$	$2.7x10^{-6}$

To obtain highly specific binders with great affinity, the selection stringency was enhanced by reducing target molecule concentration and increasing washing steps from round to round. The amount of input and output phage during each round of the selection are listed in Table 3.2. Comparing the ratio of output and input phages from the first to the last round, no obvious enrichment was detected, probably due to the greatly reduced target protein concentration in the last two rounds and even harsher washing conditions.

A

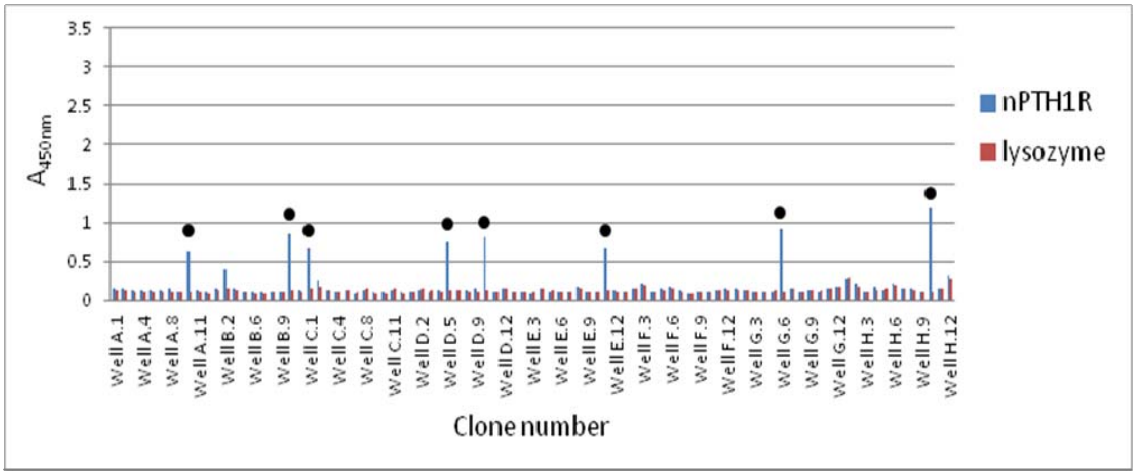

B

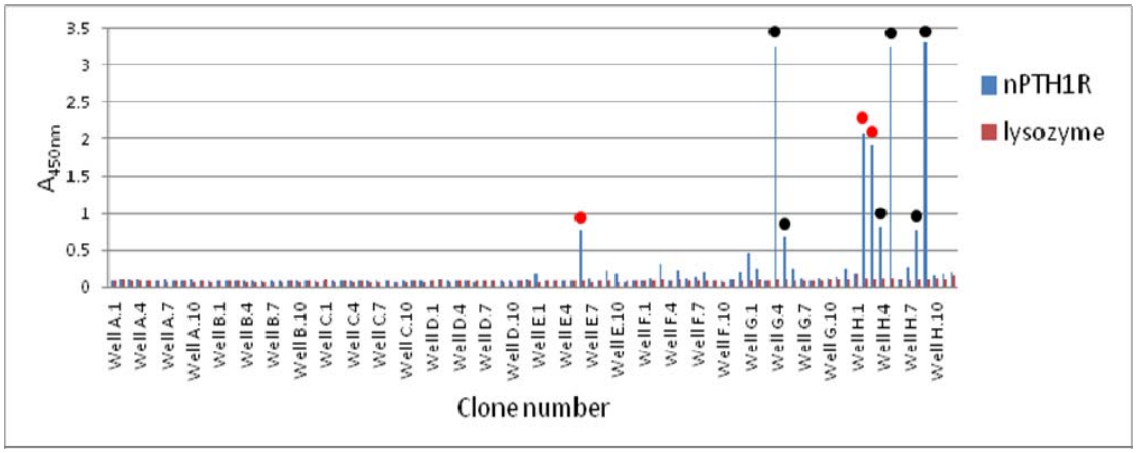

Fig. 3.4: phage ELISA with 48 output phage clones randomly picked from 1st and 2nd round of selection (A), 3rd and 4th round (B). 300 ng nPTH1R or lysozyme per well was immobilized in 96-well MediSorp plate (Nunc). 250 µl of freshly prepared phage clone lysate per well were added with end concentration 0.1% of tween-20. The unbound phages were removed by 3-time wash with PBST(0.1%) and bound phages were detected by an anti-γB crystallin antibody with horseradish peroxidase conjugated. The dark red bars correspond to the binding signal of phage clone to lysozyme and blue bars to target molecule nPTH1R. The phage clones displaying functional hγBC variants with correct sequences are marked with "●" and the variants with frameshift in DNA sequences marked with "●".

Subsequently, 48 phage clones obtained from each round were screened against the target molecule nPTH1R by ELISA, with lysozyme as a negative control (Fig. 3.4). The variants, whose binding signals to nPTH1R were higher than 0.5, were chosen to be analyzed further by phage clone PCR and sequencing. The results showed that three variant sequences contained frameshift, marked with light red point and all the other variant sequences were correct, marked with black point. Three variants 2G4, 2H5, 2H9

with highst binding level from the 4th round of the selection (Fig. 3.4B) shared the identical sequence (Fig. 3.5, K2F, T4K, Y6H, E17F, T19V, R36E, E38A). All the other positive variant sequences are shown in the section appendix Fig 7.2.

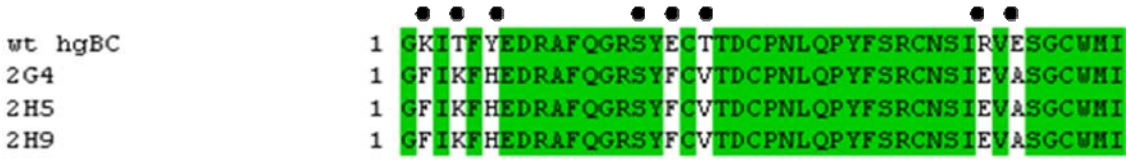

Fig. 3.5: The sequence comparison of selected hγBC variant repeatedly obtained in the 4th round with wt hγBC. The randomization sites are marked with "●".

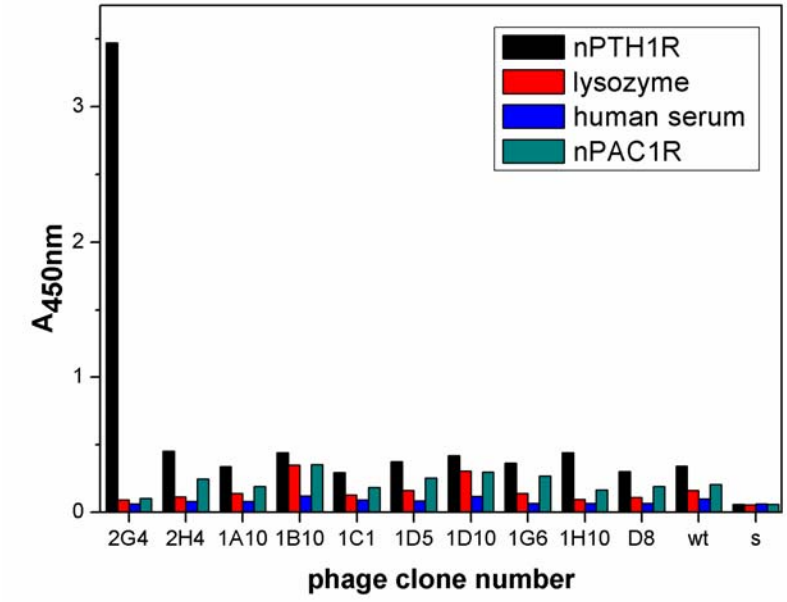

Fig. 3.6: Specificity ELISA with selected T7 phage clones displaying functional hγBC variants. Negative target controls were lysozyme, human serum and the N-terminal domain of the pituitary adenylate cyclase-activating polypeptide receptor (nPAC1R) - another class B GPCR ectodomain. S and wt stand for phages displaying S-tag peptide and wild type human γB crystallin, respectively, which were used as negative phage controls. The ELISA process was the same as described above.

All these positive variants were analyzed in the second round of screening with other negative control target molecules: human serum and the N-terminal domain of the pituitary adenylate cyclase-activating polypeptide receptor (nPAC1R) - another class B GPCR ectodomain (Fig. 3.6). In this specificity ELISA, the hγBC variant 2G4 stands out, showing obvious strong binding signal to target nPTH1R, while exhibiting very low levels of unspecific interaction with the other negative control proteins. In another set of

controls, T7 phages displaying S-tag peptide or wild type human γB crystallin showed no detectable binding to all the targets, as expected (Fig. 3.6). This promising candidate 2G4 (Fig. 3.7) was therefore chosen for purification and further characterization.

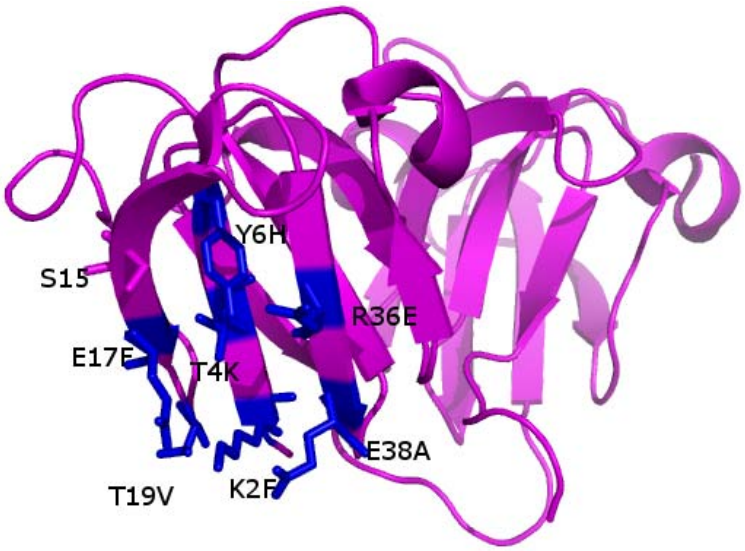

Fig. 3.7: Mutation sites of three selected identical hγBC variants. Seven mutation sites on the surface-exposed β-sheet of human γB crystalline are shown in blue, K2F, T4K, Y6H, E17F, T19V, R36E, E38A. The side chains of these seven wild type amino acids were highlighted in sticks (PDB entry 2jdf).

3.3 Expression and purification of the selected binding variant 2G4

After subcloning the gene into pET23d vector, non-labeled hγBC variant 2G4 protein was produced recombinantly in *E. coli* BL21(DE3) cells in 2 l scale of auto-induction media in shaking flask at 37°C. After 20 h, OD_{600nm} of cell culture reached 10-14 and the wet cell biomass 7-12 g/l culture. Isotope labeled 2G4 variant was produced in 2 l scale of M9 media. Protein expression was induced by IPTG at a final concentration of 1 mM when OD_{600nm} reached 0.8-1. After 6 h, the cells for single labeled ^{13}C-2G4 protein were harvested at OD_{600nm} 10-14 and double labeled ^{13}C, ^{15}N-2G4 protein at OD_{600nm} 2-3. hγBC variant 2G4 was approximately 30% soluble expressed, as shown in Fig. 3.8B. Following cell disruption, hγBC variant 2G4 was purified by immobilized metal-affinity chromatography (IMAC), followed by subsequent gel filtration (Fig. 3.8A). The chromatogram demonstrated a single sharp peak under the detection of

280 nm wavelength. No aggregates or oligomeres were found during the purification. The hγBC variant 2G4 was eluted at approximately 86 ml, in agreement with monomer wild type hγBC. According to different cell media, approximately 17-40 mg of 2G4 protein per liter culture was obtained, with more than 95% purity, as monitored by SDS-PAGE (Fig. 3.8B).

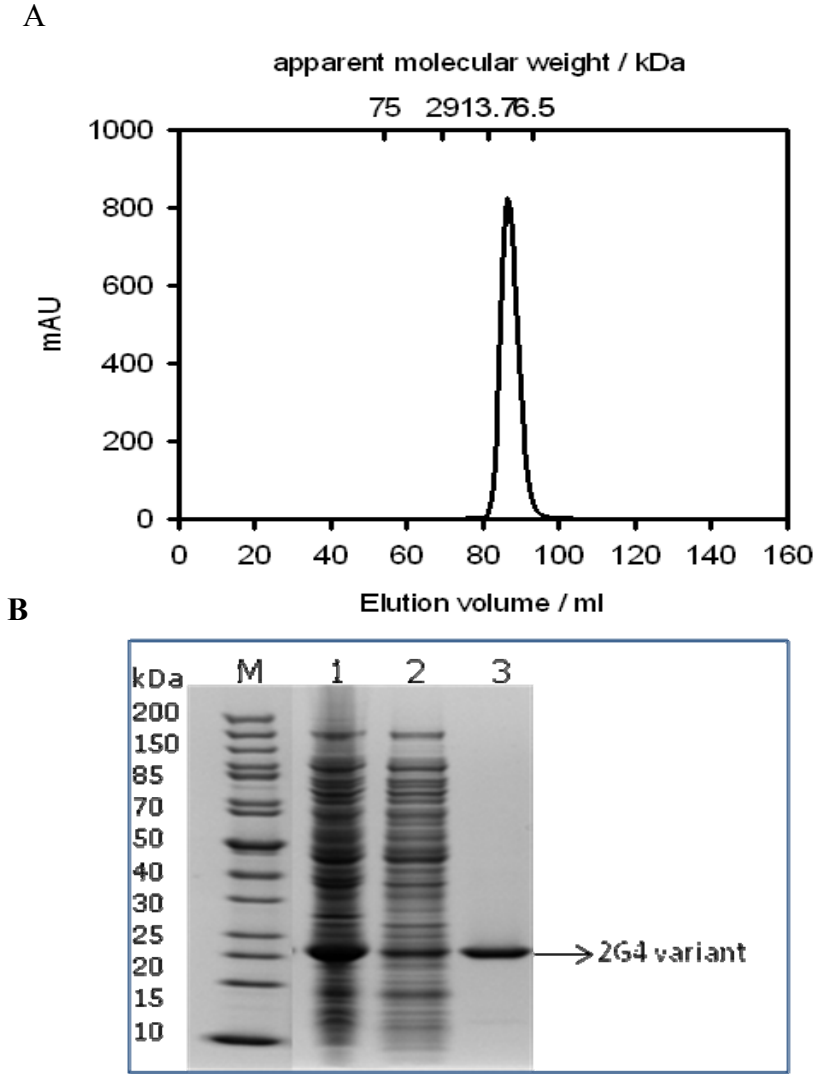

Fig. 3.8: A. Size exclusion chromatogram of hγBC variant 2G4. After purification by IMAC, hγBC variant 2G4 was loaded onto gel filtration HiLoad16/60 Superdex 75 prep grade column in running buffer PBS, 1 mM EDTA. **B. SDS-PAGE analysis of purified hγBC variant 2G4.** Protein samples from each purification step were analyzed by 4-12% gradient gel and subsequently stained by coomassie blue. M stands for fermentas unstained protein ladder. In the 1st lane, total cell lysate was loaded. The 2nd lane shows the soluble protein fraction after cell disruption. Lane 3 contains hγBC variant 2G4 purified by IMAC and gel filtration.

3.4 *In vitro* characteristics of 2G4

3.4.1 Biophysical characterization

A scaffold protein is required to be highly stable to accommodate amino acid mutations in the randomization sites. Due to the substitution of seven residues on the surface-exposed β-sheet of the scaffold molecule hγBC, the overall structure and stability of isolated variant 2G4 as well as wild type hγBC was investigated by far-UV CD spectroscopy (Fig. 3.9). Both proteins showed a negative minimum at 217 nm and a shoulder at 205 nm, the amplitude of the signal of variant 2G4, however, was approximately 20% less compared to that of wild type hγBC. This result suggested that 2G4 variant may be slightly less structured, in comparison with wild type hγBC. However, the spectra difference in this wavelength region could also be induced by changes of aromatic amino acids or their microenvironments.

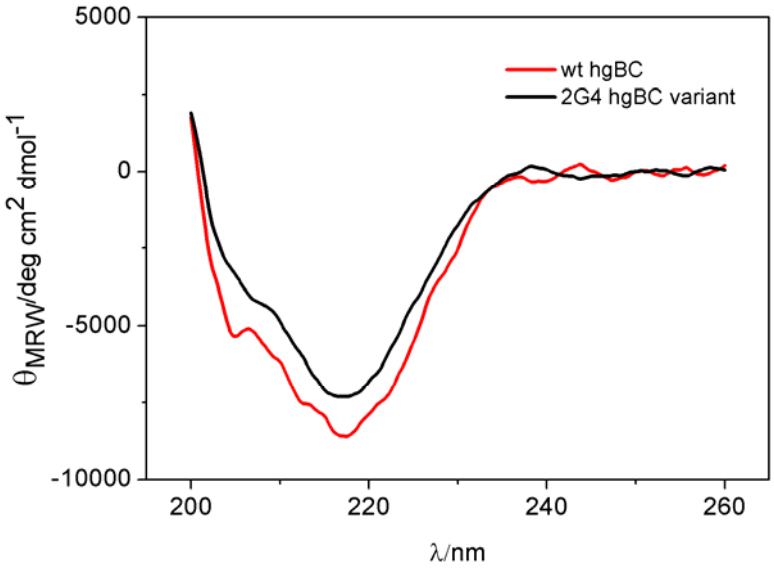

Fig. 3.9: Secondary structure analysis of hγBC variants. Far-UV CD spectra of wild type hγBC (red line) and 2G4 hγBC variant (black line) were recorded from 260 nm to 200 nm. The protein samples were prepared in 5 mM NaH_2PO_4, 15 mM NaCl pH 7.8.

3.4.2 Thermal stability

To estimate whether the seven amino acid substitutions affect the structured stability of the protein, thermal induced denaturation of 2G4 as well as wild type hγBC was analyzed by two different methods, differential scanning fluorimetry (DSF) and CD spectroscopy. In the DSF measurements, the transition midpoint was calculated to be 61.93 ± 0.07 °C for the variant 2G4 and 70.92 ± 0.19 °C for wild type hγBC, respectively (Fig. 3.10A). This result was further verified by CD spectroscopy revealing T_m = 59.95 ± 0.06 °C for 2G4 and 72.79 ± 0.08 °C for wild type hγBC (Fig. 3.10B). The temperature induced unfolding was not reversible and aggregation was observed for both wild type and 2G4 hγBC at high temperature.

A **B**

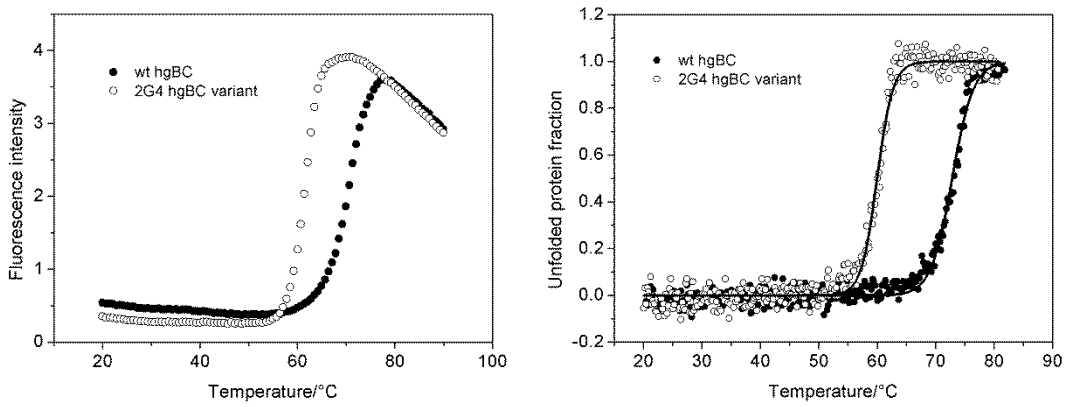

Fig. 3.10: Thermal stability of 2G4 hγBC variant and wild type hγBC analyzed by DSF (A) and CD spectroscopy (B). A. In the DSF measurements, 9.5 µM protein was prepared in 50 µl PBS containing 2× sypro red dye (diluted from 5000× commercial stock solution). Thermal induced unfolding was followed from 20 to 90°C with a heating rate of approximately ΔT=1°C/min. All data were corrected by the buffer signal. **B.** 10 µM protein in 5 mM NaH_2PO_4, 15 mM NaCl, pH 7.8 was used for CD spectroscopy experiments. Thermal induced unfolding was monitored from 20 to 82°C at 217 nm with a heating rate of ΔT=1°C/min.

3.4.3 Binding ability of 2G4 to full length PTH1R

Concentration-dependent ELISA was also performed to evaluate the binding ability of hγBC variant 2G4 to full length PTH1R (Fig. 3.11). In this particular ELISA, 0-2 µg per well of full length PTH1R freshly reconstituted in proteoliposome were immobilized in

a 96-well plate. 5 µM hγBC variant 2G4 and wild type hγBC were applied for recognition, separately. It is obvious, that variant 2G4 could bind full length PTH1R in a concentration-dependent manner. Compared to wild type human γB crystallin, apparently 2G4 showed unspecific binding to the plate, causing a relative high background signal. Due to the limited preparation of PTH1R, binding saturation could not be achieved for accurate affinity determination.

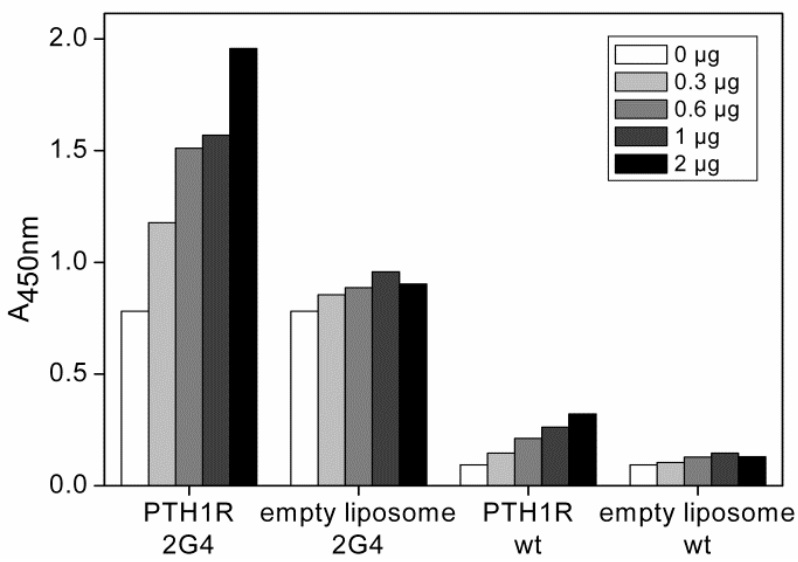

Fig. 3.11: Binding ability test of hγBC variant to full length PTH1R. 0-2 µg of PTH1R, freshly reconsitituted in proteoliposome, were immobilized on a micro titer plate, using identical quantity of pure empty proteoliposome as negative control. 5 µM of hγBC variant 2G4 and wild type human γB crystallin were added, respectively. Bound molecules were detected by anti-hγBC-Ab with POD conjugated.

3.4.4 Characterization of the interaction of 2G4 and nPTH1R - binding affinity

The affinity of variant 2G4 to the target protein nPTH1R was analyzed by concentration-dependent ELISA (Fig. 3.12A) and competition ELISA (Fig. 3.12B). In concentration-dependent ELISA, the raw data were fitted nonlinearly to a 1:1 binding mode (Equation 2) revealing an apparent dissociation constant (K_D) of 0.69 µM. This result was further verified by the competition ELISA, in which the data were fitted to a one-site competition equation (Equation 3) and K_D was calculated to be 1.35 µM. With these two methods, a low micromolar binding affinity was determined for hγBC variant 2G4 to nPTH1R.

Isothermal titration calorimetry (ITC) was also utilized to evaluate the binding affinity of isolated hγBC variant 2G4 to nPTH1R (Fig. 3.13). The data showed that the binding interaction was exothermal and the dissociation constant was calculated to be 20.9 µM. The free binding enthalpy ΔG_{ITC}, the apparent binding enthalpy ΔH_{ITC}, the apparent binding entropy ΔS_{ITC} and the number of binding site N are listed in Table 3.3.

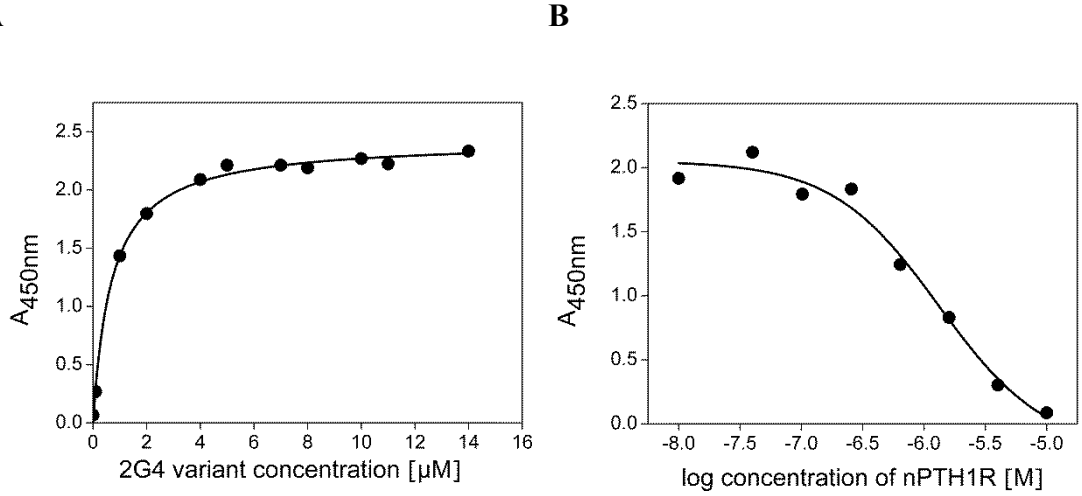

Fig. 3.12: Binding affinity of hγBC variant 2G4 to nPTH1R determined by A) concentration-dependent ELISA and B) competitive ELISA. A. 0-14 µM of purified variant 2G4 were added to 30 ng/well target protein nPTH1R coated on ELISA plate wells. The amount of bound hγBC variant was detected by an anti-hγBC-Ab with POD conjugated. Fitting the raw data to a one-binding-site model, the K_D value was calculated to be 0.69 ± 0.05 µM. **B.** 100 nM of purified variant 2G4 was incubated with 0-10 µM of competitor nPTH1R for 1 h at RT and then added to 100 ng/well of nPTH1R coated wells. The amount of hγBC variant was detected by anti-hγBC-Ab with POD conjugated. Fitting the raw data to a one-competition-site model, the K_D value was calculated to be 1.35 ± 0.33 µM.

The apparent binding enthalpy ΔH_{ITC} of -4.3 kcal/mol and the apparent binding entropy ΔS_{ITC} of 6.8 cal/mol·K revealed that the binding reaction between hγBC variant 2G4 and nPTH1R is driven by both enthalpy and entropy changing process. The number of binding site N revealed the 1:1 stoichiometry of binding partners nPTH1R and hγBC variant 2G4.

Tab. 3.3: Thermodynamic parameters of nPTH1R binding to hγBC variant 2G4

ΔG_{ITC}	-6.28 ± 0.50 kcal/mol
ΔH_{ITC}	-4.28 ± 0.50 kcal/mol
ΔS_{ITC}	6.83 cal/mol·K
N	1.01± 0.08
K_D	20.92 ± 2.48 µM

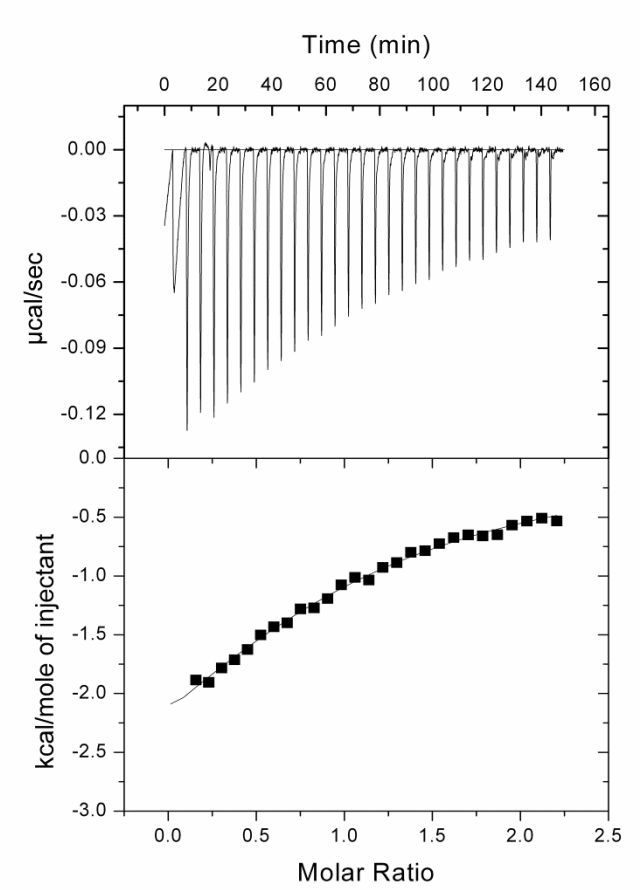

Fig 3.13: Binding interaction of hγBC variant 2G4 to nPTH1R analyzed by isothermal titration calorimetry (ITC). At 20°C, 211 µM hγBC variant 2G4 was titrated into 19.7 µM nPTH1R in 29 injections with 2 µl for the first injection and 10 µl for the other 28 injections. nPTH1R and hγBC variant 2G4 were prepared in PBS, 1 mM EDTA pH 7.8. Top: baseline subtracted raw data of heat energy. Bottom: peak-integrated and concentration-normalized enthalpy change plotted against nPTH1R/2G4 ratio. The experimental data were fit to a 1:1 binding model in the solid line.

3.4.5 Characterization of the interaction of 2G4 and nPTH1R – competition with PTH

The natural ligand of PTH1R is PTH. Binding of PTH to its receptor controls the Ca^{2+} homeostasis in the organism. Artificial binding protein interacting with PTHR, such as 2G4, might be of therapeutic interest if it influences the interaction of PTH1R with its ligand, thus conveying an agonistic or antagonistic activity. Whether or not 2G4 interferes with the binding of PTH to PTH1R was analyzed by isothermal titration calorimetry. Three experiments were conducted: (i) ligand PTH 1-84 titrated to nPTH1R (shown above in Fig. 3.2); (ii) ligand PTH 1-84 titrated to the complex of nPTH1R and

hγBC variant 2G4 (molar ratio 1:10, Fig 3.14, over 99% of nPTH1R was occupied by hγBC variant 2G4); (iii) hγBC variant 2G4 titrated to nPTH1R (shown above in Fig 3.13). All three results demonstrated typical titration data. It is clear that all three binding reactions were exothermal. The dissociation constant, the free binding enthalpy ΔG_{ITC}, the apparent binding enthalpy ΔH_{ITC}, the apparent binding entropy ΔS_{ITC} and the number of binding site N are listed in Table 3.4.

Tab. 3.4: Summary of thermodynamic parameters of ITC experiments

	PTH1-84 binding nPTH1R (i)	PTH1-84 binding nPTH1R-2G4 hγBC complex (ii)	2G4 binding nPTH1R (iii)
ΔG_{ITC}	-6.85 ± 0.16 kcal/mol	-7.65 ± 0.20 kcal/mol	-6.28 ± 0.50 kcal/mol
ΔH_{ITC}	-10.79 ± 0.16 kcal/mol	-18.52 ± 0.20 kcal/mol	-4.28 ± 0.50 kcal/mol
ΔS_{ITC}	-13.60 cal/mol·K	-31.7 cal/mol·K	6.83 cal/mol·K
N	1.16 ± 0.01	1.12 ± 0.01	1.01± 0.08
K_D	8.40 ± 0.39 μM	2.07 ± 0.1 μM	20.92 ± 2.48 μM

Comparing the ΔH_{ITC} value between PTH1-84 binding to the single protein nPTH1R (-10.79 kcal/mol) and the complex of nPTH1R-2G4 (-18.52 kcal/mol), no increase was found. Supposing that PTH1-84 binds nPTH1R on the identical site as variant 2G4, variant 2G4 would need to dissociate from nPTH1R before PTH1-84 could bind. The dissociation enthalpy for 2G4 variant was 4.3 kcal/mol, and association enthalpy for PTH1-84 was -10.8 kcal/mol (Tab. 3.4). The total enthalpy for this two-step reaction should be -6.5 kcal/mol, which was obviously in great disagreement with the result from the respective titration experiment (-18.5 kcal/mol). Binding of PTH to nPTH1R in the absence and presence of 2G4 led to a very similar free binding enthalpy ΔG_{ITC} (Tab. 3.4). Hence, there is no competition binding of 2G4 and PTH to nPTH1R via identical or overlapping binding sites, nor does 2G4 binding induces a conformational switch in nPTH1R that would interfere either positively or negatively with PTH binding.

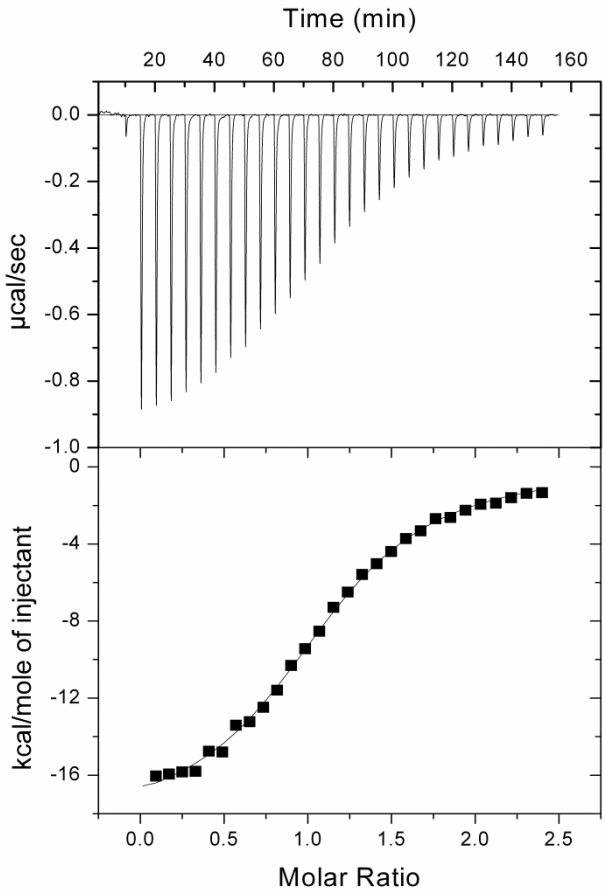

Fig. 3.14: Competition binding analysis of PTH1-84 and 2G4 hγBC variant to nPTH1R by isothermal titration calorimetry. 15.8 µM nPTH1R and 158.4 µM 2G4 hγBC variant were mixed at RT for 1 h. At 20°C, 171.8 µM ligand PTH1-84 was titrated into nPTH1R-2G4 hγBC variant complex in 29 injections with 2 µl for the first injection and 10 µl for the other 28 injections. All three proteins were prepared in PBS, 1 mM EDTA. In the reference titration experiment, same amount of PTH1-84 was titrated into 158.4 µM 2G4 hγBC variant. No binding interaction was detected (data not shown). Top: baseline subtracted raw data of heat energy. Bottom: peak-integrated, and concentration-normalized enthalpy change plotted against nPTH1R/PTH1-84 ratio. The experimental data were fit to a 1:1 binding model in the solid line.

3.4.6 Characterization of the interaction of 2G4 and nPTH1R – pH dependent

The binding of 2G4 to nPTH1R was found to be pH-dependent strongly as shown in Figure 3.15. The interaction was not detectable at pH below 6.8 and it increased in affinity at pH above 6.8. Fitting the data to sigmoid equation (Chapter 2.2.6, Equation 4), the p*K*a value was calculated to be 7.11. At the 6th amino acid position of hγBC variant 2G4, the original tyrosine residue in wild type hγBC was substituted by

histidine in 2G4. The imidazole side chain of histidine has a p*K*a approximately 6.0. This value could differ in a certain range due to the protein microenvironment (Grimsley *et al.*, 2009). To evaluate whether this particular histidine plays an important role during the 2G4-nPTH1R interaction, another hγBC variant based on 2G4, only with histidine mutated back to original tyrosine, termed as H6Y variant, was prepared. The protein was expressed in the same pET23dK^{R} vector and BL21 (DE3) cells, subsequently purified by IMAC and gelfiltration. In the pH screening experiment, H6Y variant behaved almost identically as 2G4 variant, revealing the p*K*a of 7.14. This result clearly showed that this particular histidine at the randomization position of hγBC variant was not responsible for the gain in affinity at pH above 6.8. There are also no other histidines surrounding the designed binding site. Hence, it is assumed that the cause for the pH-dependent manner probably lies on the histidines from the epitope of nPTH1R.

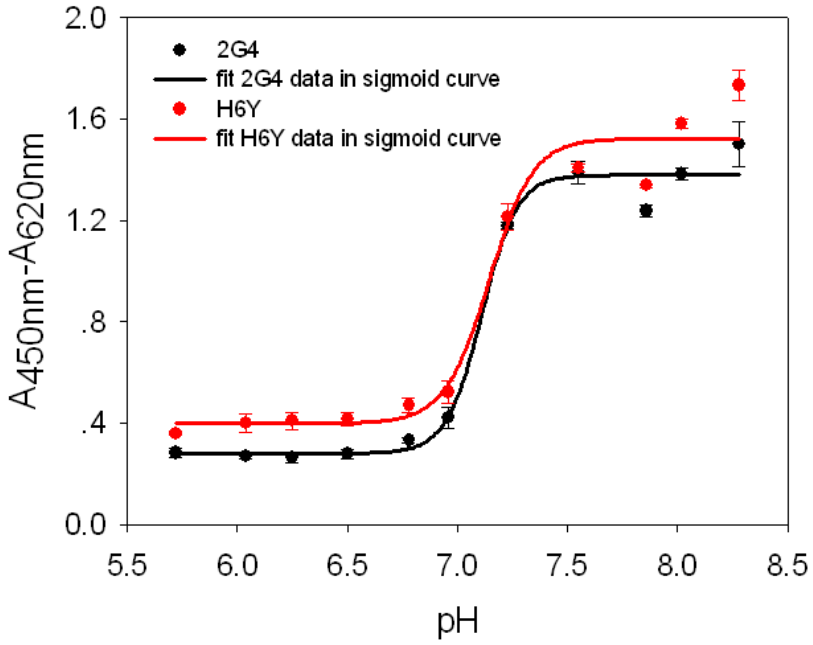

Fig. 3.15: pH-dependent binding of hγBC variants to nPTH1R. Binding ability of variant 2G4 and H6Y to nPTH1R was tested in a pH range from 5.72 to 8.28. 1 µM of hγBC variant was applied. Bound molecules were detected by ELISA using α-hγBC antibody POD conjugated.

3.5 Structural characterization of 2G4 binding to nPTH1R

3.5.1 Alanine scanning of 2G4

The back mutation of histidine at the 6th position of 2G4 to the original tyrosine of the wild type sequence did not lead to a change in binding of 2G4 to its target nPTH1R. This probably indicates that H6 of 2G4 is not involved in the binding site that interacts with nPTH1R, even though it is part of the randomized surface of the protein. To find out which specific amino acid was involved in the binding of hγBC variant 2G4 to nPTH1R, each residue on the designed randomization site was mutated to alanine, generating variants F2A, K4A, H6A, S15A, F17A, V19A, E36A, A38G, respectively. The cloning, expression and purification process was the same as above described for variant H6Y (Chapter 3.4.6). The binding ability of these variants to nPTH1R was tested in ELISA (Fig. 3.16). The result showed that, compared to 2G4, variant F2A and F17A lost approximately 90% of binding function. Therefore, it is clear that both residues F2 and F17 on the hγBC variant 2G4 play the most important role on the interaction with nPTH1R (Fig. 3.17).

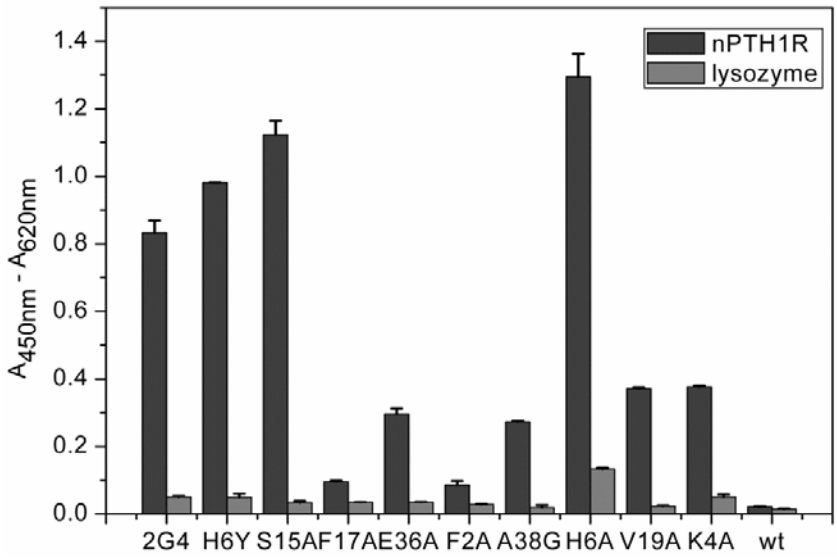

Fig. 3.16: ELISA analysis of variants based on 2G4 in the alanine scanning experiment. 1 μM of purified hγBC variants were separately added to 100 ng/well target protein nPTH1R coated wells, lysozyme as negative target control and wild type hγBC as negative binder control. The amount of bound hγBC variants was detected by an anti-hγBC-Ab with POD conjugated.

Besides that, variants E36A, A38G, V19A and K4A also presented only around 40% of binding intensity of 2G4 to nPTH1R, suggesting these four residues E36, A38, V19 and K4 surrounding F2 and F17 also contribute to the interaction of 2G4 and nPTH1R. The K_D values of these four variants were estimated by concentration-dependent ELISA, ranging from 5.84 µM to 55.91 µM, listed in Table 3.5. Variants H6A, H6Y, as well as S15A, exhibited high binding signals to nPTH1R with 0.12 to 0.29 µM affinity, indicating that H6 and S15 of 2G4 variant are not involved in the interaction.

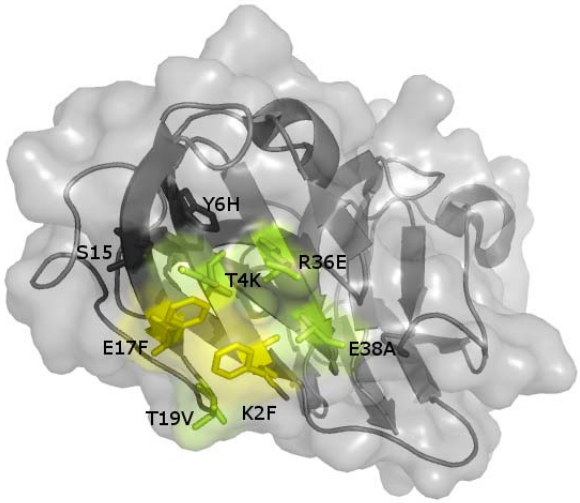

Fig. 3.17: Demonstrated model of isolated hγBC variant 2G4 constructed by Pymol software. Seven mutation sites of variant 2G4 were generated based on wild type hγBC structure by pymol. F2 and F17 residues, which play the most important roles in the binding interaction to nPTH1R, are colored in yellow. E36, A38, V19 and K4 residues, which also contribute to the interaction, are colored in green. S15 and H6 residues are not involved in the binding event and colored in black. The side chains of randomization residues on variant 2G4 were highlighted in sticks.

In order to ensure that the discovered changes in binding to nPTH1R are not caused by considerable structure changes of 2G4 induced by the alanine substitutions, the secondary structure of all these hγBC variants were analyzed by Far-UV CD spectroscopy (Fig. 3.18). All proteins showed a spectrum very similar to that of 2G4. This result suggested that hγBC variants based on variant 2G4, generated in alanine scanning, are correctly folded and demonstrate obvious β-sheet structure. The slight differences in signal intensities are probably due to the slight changes in structure or aromatic amino acids and their microenvironments.

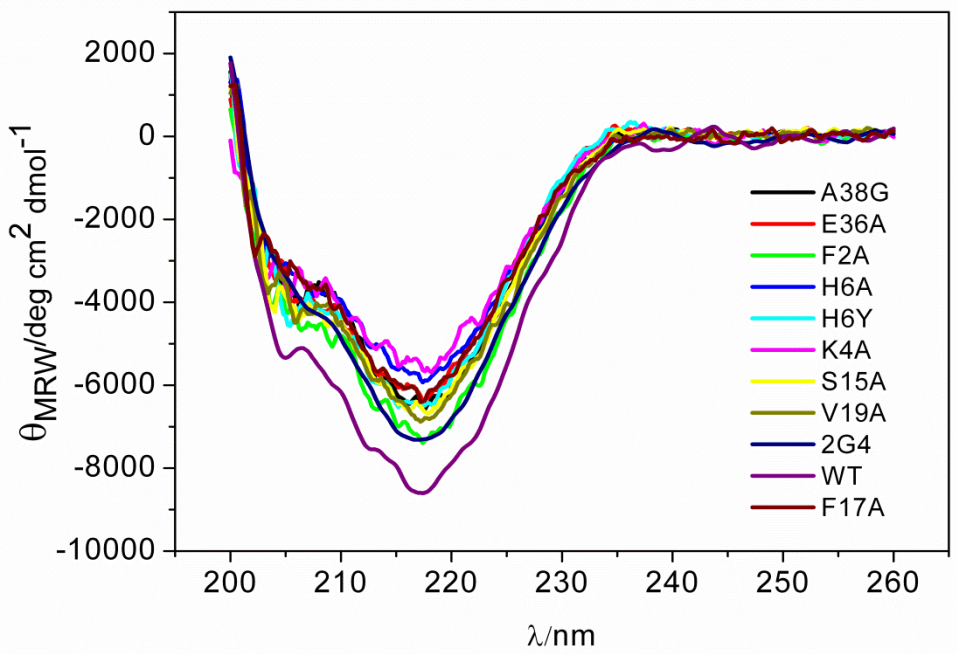

Fig. 3.18: Secondary structure analysis of hγBC variants. Far-UV CD spectra of hγBC variants were recorded from 260 nm to 200 nm. The protein samples were prepared in 5 mM NaH_2PO_4, 15 mM NaCl pH 7.8.

Tab. 3.5: Protein yield and dissociation constant of variants in alanine scanning

Variant	Protein yield per l culture	K_D
2G4	41.8 mg	0.69 µM
H6Y	31.6 mg	0.23 µM
H6A	3.9 mg	0.29 µM
S15A	35.2 mg	0.12 µM
E36A	37.6 mg	27.35 µM
A38G	24 mg	17.35 µM
V19A	47.2 mg	55.91 µM
K4A	7.9 mg	5.84 µM
F2A	44 mg	-
F11A	42.4 mg	-

The yield of expression of these hγBC variants of the alanine scanning experiment are listed in Table 3.5. All the variants can be produced in the same level as variant 2G4, in the range from 24 to 44 mg per liter auto-induction culture, except variant H6A and K4A with only 3.9 mg and 7.9 mg respectively. The solubility of these two variants was analyzed by SDS-PAGE (Fig. 3.19). Compared to other variants S15A, V19A and 2G4, which could be approximately 30-60% soluble expressed, H6A and K4A only contained around 10% soluble fraction. This result suggests that, although histidine and lysine on

the randomization sites don't contribute much to the binding of 2G4 to nPTH1R, their function in solubility of the protein ensures 2G4 to be repeatedly selected during the panning procedure. Summarizing these results, it is assumed that the binding area of variant 2G4 at least consists of six residues F2, F17, E36, A38, V19 and K4.

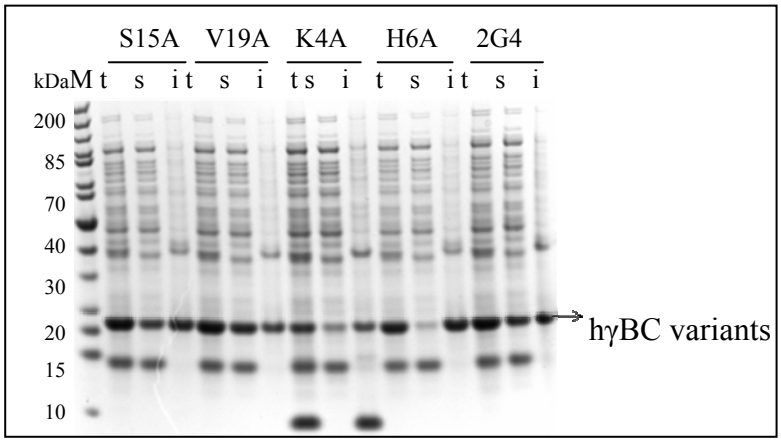

Fig. 3.19: SDS-PAGE analysis of hγBC variants solubility. t stands for total cell lysate, s for soluble fraction and i for insoluble fraction.

3.5.2 NMR studies

The structural information on the nature of the physical interaction of 2G4 and nPTH1R was analyzed by NMR experiments. The backbone resonances of a ^{15}N-HSQC spectrum of hγBC variant 2G4 were assigned by using standard 2D and 3D NMR experiements (Fig. 3.20). In a NMR titration experiment, 443 µM unlabeled nPTH1R was titrated into 340 µM ^{15}N-labeled hγBC variant 2G4 to reach finally a 1.4-fold molar access. The interaction was monitored in PBS, 1 mM EDTA, pH 7.8. Perturbation of the back bone chemical shift or the intensity change upon complex formation was monitored by ^{15}N-FHSQC or ^{15}N-TROSY-HSQC spectra, shown in Fig. 3.21. Binding of 2G4 to the large molecule nPTH1R led to line-broadening of many amide resonances which at the end of the titration disappeared. This phenomenon was probably caused by reaching the intermediate exchange regime in the complex state, or/and conformation change of the molecule. Dilution of labeled protein concentration during titration could also lead to reduced intensity up to a certain level.

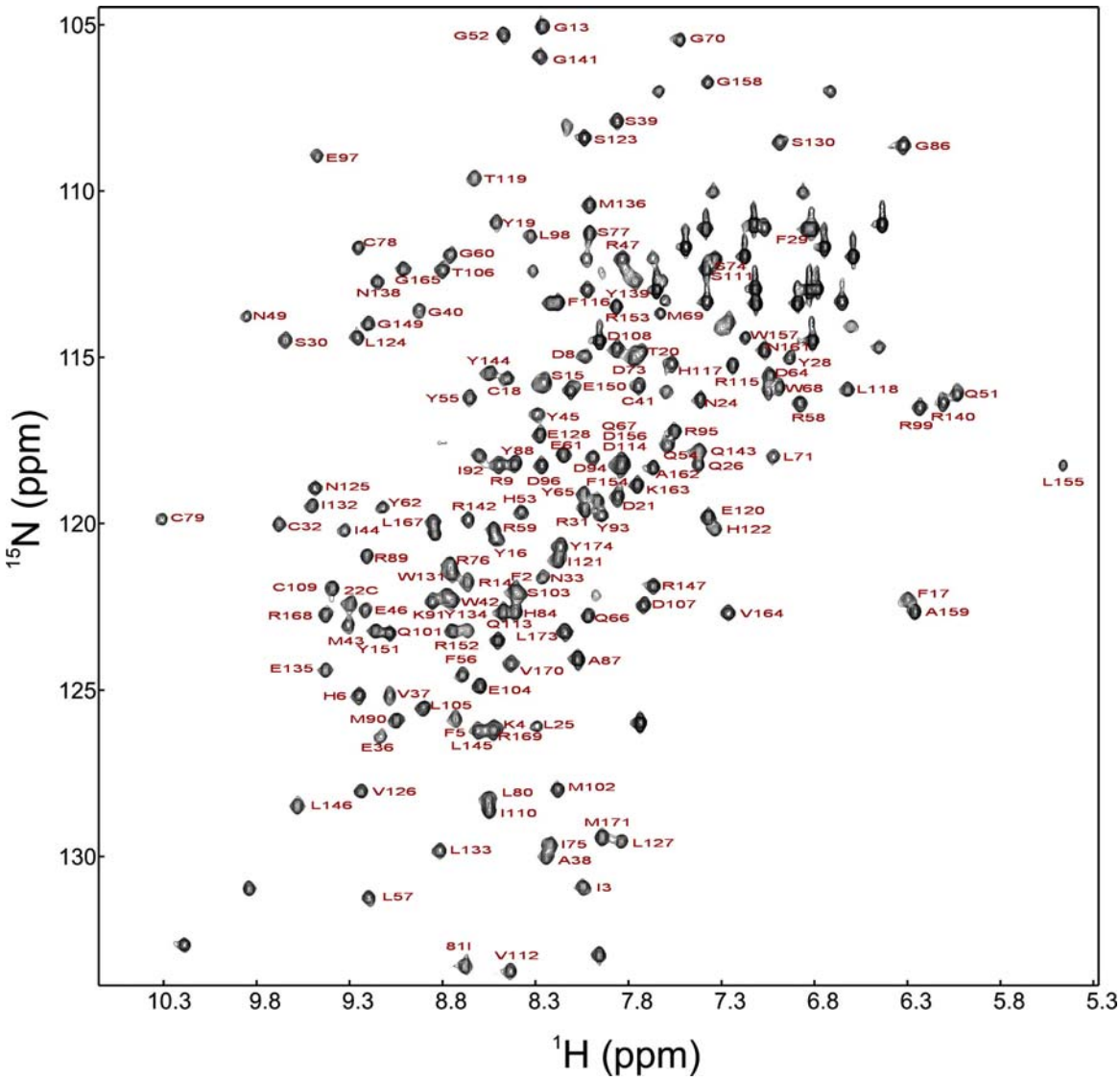

Fig. 3.20. The assigned 2D ^{15}N-HSQC spectrum of hγBC variant 2G4. Spectrum was measured at 25 °C in 50 mM sodium phosphate, 200 mM NaCl, 0.02 % NaN_3, 10% D_2O and pH 7.8. Cross-peaks are labeled with residue numbers.

The plot of normalized NMR intensities of the cross-peaks was used to localize the residues of 2G4 that are affected upon binding to nPTH1R. Amino acids F2, I3, F17, C18, E36, A38, G40, E61, Y62, which lost more than 76% signal intensity (plot signal lower than 0.24, Fig. 3.22A), were identified to be highly involved in the binding interaction, mapped in Fig. 3.22B. The calculated area of these residues on the surface of 2G4 is approximately 434 Å^2, while the originally designed binding area by eight randomization sites was 560 Å^2. According to Houk's paper describing that binding

affinity can be predicted by surface area buried upon binding, 90 Å^2 per lgKa unit (Houk *et al.*, 2003), here 434 Å^2 binding area of 2G4 to nPTH1R corresponds to a K_D of 15 µM, which is in the similar range as the result from ITC (Tab. 3.3). Among the residues in the binding region, F2, F17, E36, A38 are the randomized positions, whose interaction to nPTH1R has also been confirmed by alanine scanning experiment (Fig. 3.17). Two other randomized residues, H6 and S15, did not show any changes in their backbone NMR signal, proving that these residues are not involved in binding which is in perfect agreement with the data of the alanine scanning experiment.

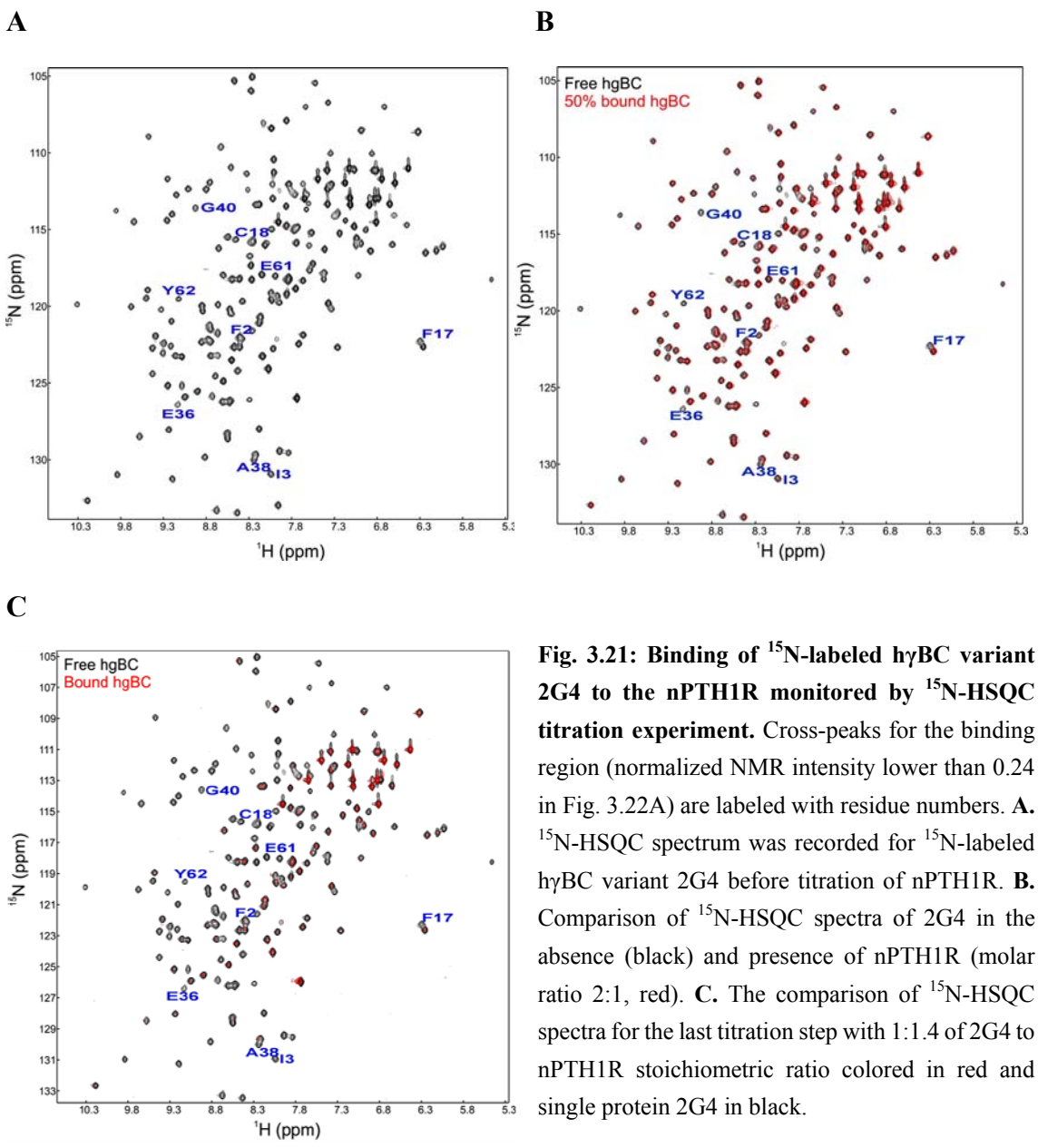

Fig. 3.21: Binding of ^{15}N-labeled hγBC variant 2G4 to the nPTH1R monitored by ^{15}N-HSQC titration experiment. Cross-peaks for the binding region (normalized NMR intensity lower than 0.24 in Fig. 3.22A) are labeled with residue numbers. **A.** ^{15}N-HSQC spectrum was recorded for ^{15}N-labeled hγBC variant 2G4 before titration of nPTH1R. **B.** Comparison of ^{15}N-HSQC spectra of 2G4 in the absence (black) and presence of nPTH1R (molar ratio 2:1, red). **C.** The comparison of ^{15}N-HSQC spectra for the last titration step with 1:1.4 of 2G4 to nPTH1R stoichiometric ratio colored in red and single protein 2G4 in black.

The residues I3, C18, G40, E61 and Y62, whose NMR signals decreased in intensity, are located in the neighborhood of randomization sites and assumed to help fix the binding interaction. Simply by this NMR intensity plot, the contribution of individual residues involved in the interaction could not be differentiated. Labeled variants in alanine scanning experiment and identical titration experiments are further needed for estimation of each mutated residues. Fitting the intensity data to 1:1 binding model for each amino acid involved in the interaction (Fig. 3.23), an average K_D of 23.2 µM was obtained.

A

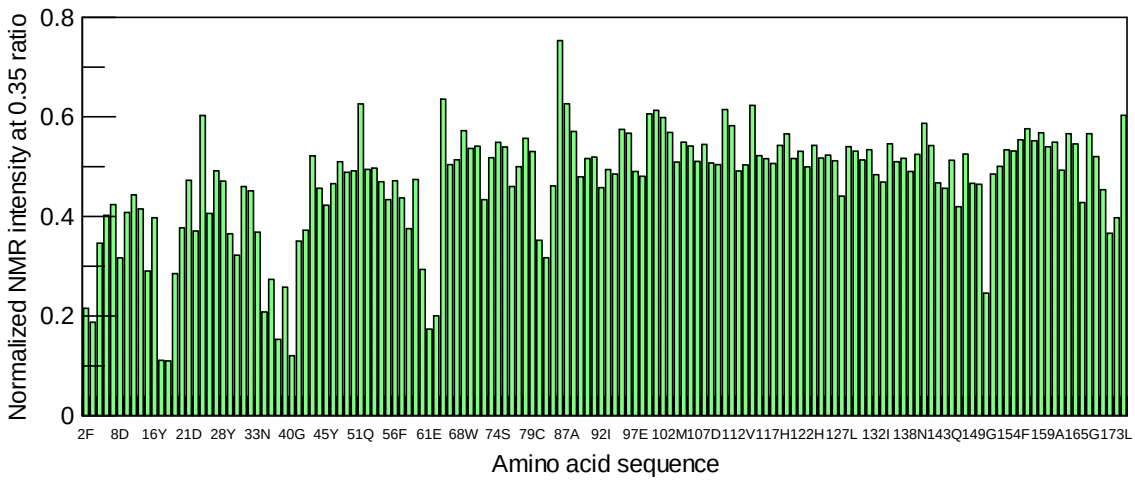

B

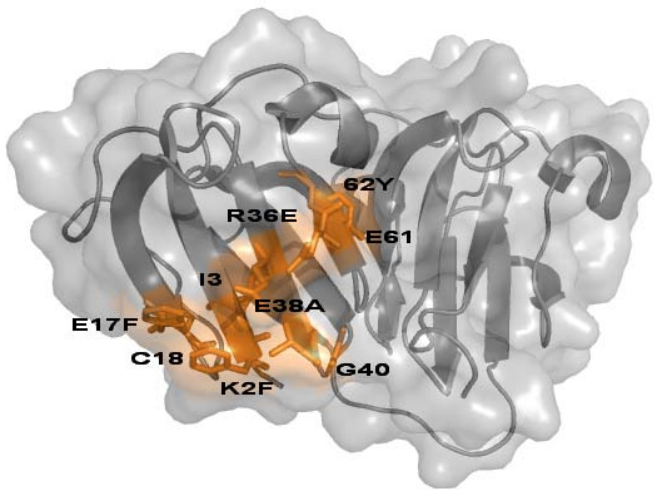

Fig. 3.22: Binding surface of hγBC variant 2G4 to nPTH1R identified by NMR intensity changes. A. NMR intensity plot of ^{15}N-2G4 binding to nPTH1R. Intensities were picked form 0.35:1 (nPTH1R:2G4) complex spectrum of ^{15}N-HSQC titration experiments and normalized against spectrum of free ^{15}N-2G4. **B.** Binding region (normalized NMR intensity lower than 0.24 in Fig. 3.22A) mapped in model structure of hγBC variant 2G4 by Pymol software.

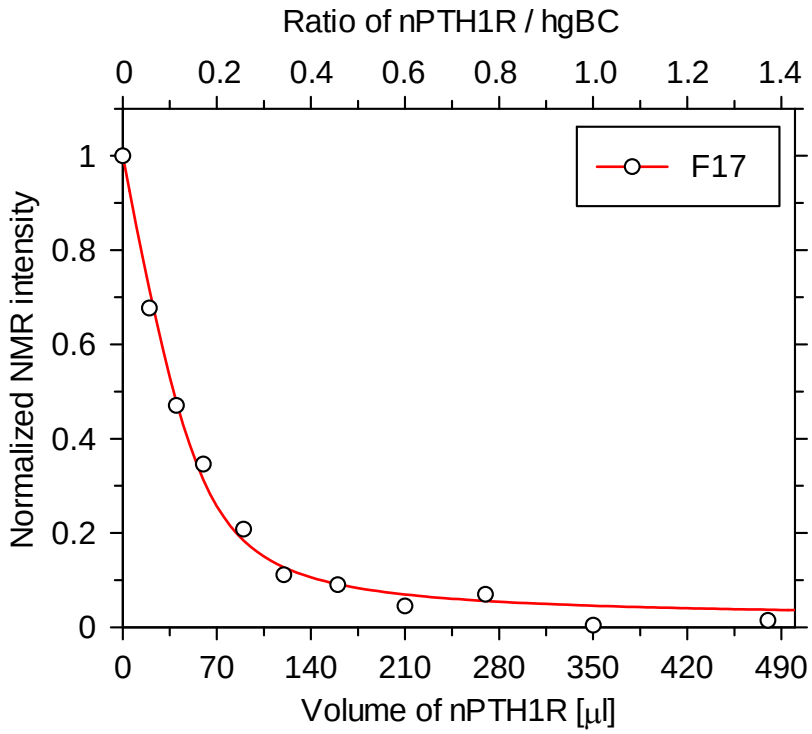

Fig. 3.23: Analysis of K_D for binding of hγBC variant 2G4 to the nPTH1R by NMR intensity plot. Upon NMR titration the intensity of the free ^{15}N-2G4 decreases due to complex formation. The normalized NMR Intensity of the F17 amide cross-peak was plotted against volume of nPTH1R/fraction of nPTH1R to 2G4. All the other residues involved in the interaction were applied in this model and approximately same K_D values were obtained, resulting in the average K_D of 23.2 ± 6.3 µM.

Following the titration of non-labeled nPTH1R to ^{15}N-labeled hγBC variant 2G4, 1.1 mM ligand PTH was titrated into the formed ^{15}N-labeled hγBC variant 2G4-nPTH1R complex in 4 steps and reached an end concentration of 233 µM PTH, while the final concentration of nPTH1R was 180 µM and ^{15}N-labeled hγBC variant 2G4 129 µM. The K_D of 2G4 to nPTH1R is approximately 1 µM according to the ELISA result and PTH to nPTH1R 8 µM, both with 1:1 binding stochiometry. Hence, in this high protein concentration solution, the occupancy of nPTH1R by both hγBC variant 2G4 and PTH is over 96%. Supposed that competition occurs between PTH and hγBC 2G4 binding to nPTH1R, addition of ligand PTH to the complex of ^{15}N-labeled hγBC variant 2G4 should at least partly recover the spectrum of 2G4. However, continued decrease in intensity was observed.

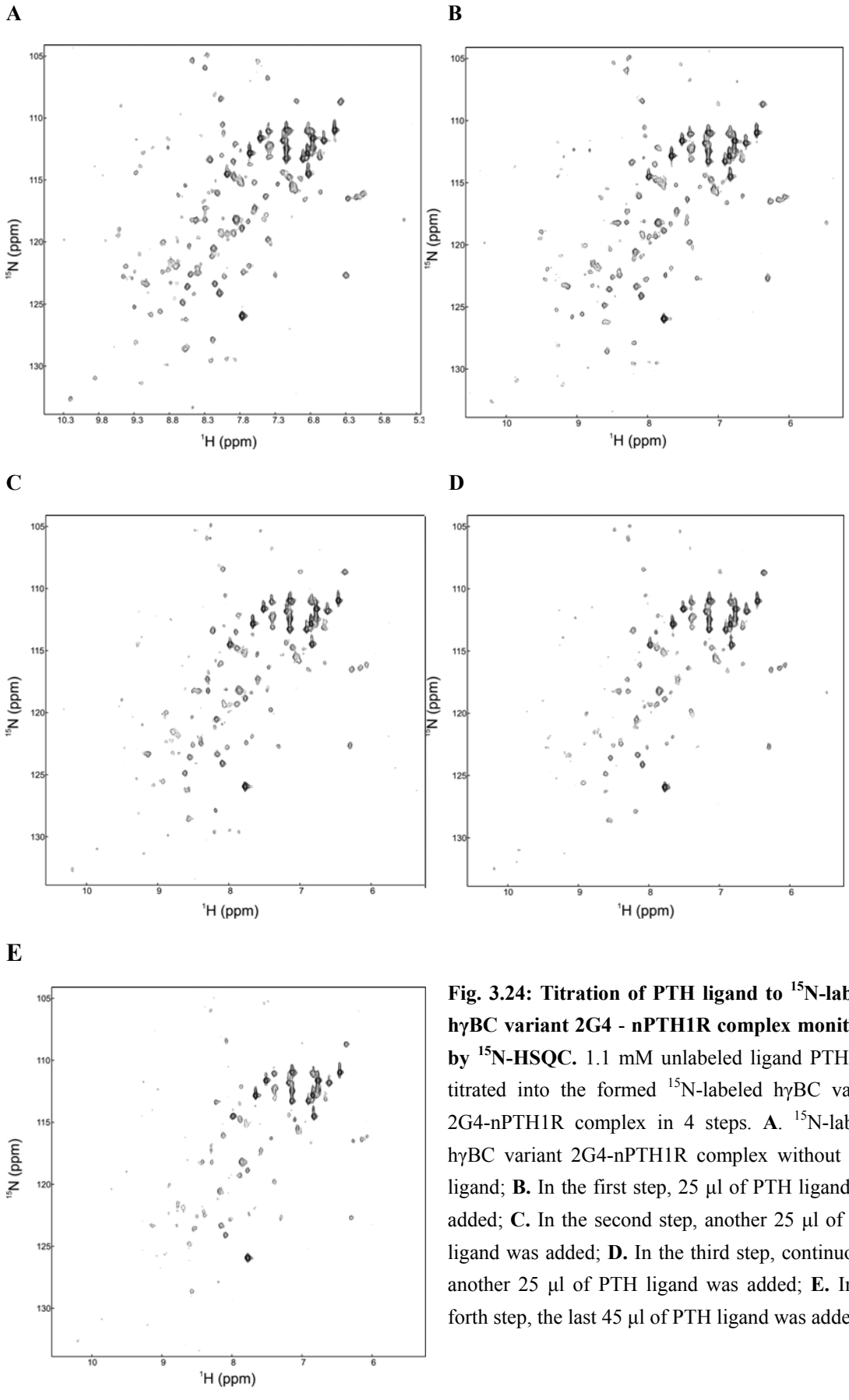

Fig. 3.24: Titration of PTH ligand to ^{15}N-labeled hγBC variant 2G4 - nPTH1R complex monitored by ^{15}N-HSQC. 1.1 mM unlabeled ligand PTH was titrated into the formed ^{15}N-labeled hγBC variant 2G4-nPTH1R complex in 4 steps. **A**. ^{15}N-labeled hγBC variant 2G4-nPTH1R complex without PTH ligand; **B.** In the first step, 25 µl of PTH ligand was added; **C.** In the second step, another 25 µl of PTH ligand was added; **D.** In the third step, continuously another 25 µl of PTH ligand was added; **E.** In the forth step, the last 45 µl of PTH ligand was added.

In Fig. 3.24, from A to E, with titrating PTH ligand to the complex, the intensity of ^{15}N-labeled hγBC variant 2G4 became slightly weakened simply due to the dilution or formation of the even larger complex ^{15}N-labeled hγBC variant 2G4 – nPTH1R – PTH. Therefore, this result indicates that no competition exists between PTH and hγBC variant 2G4 in binding to nPTH1R. This result is highly consistent with the ITC measurements (Chapter 3.4.5).

4 Discussion

4.1 Preparation of recombinant nPTH1R in *E. coli* cells

3D structures of GPCRs are still extremely difficult to be determined. Further effort will be focused on developing strategies and tools to co-crystallize GPCRs with small and soluble proteins, which can sufficiently mediate crystal contacts. Crystal structures of full-length class A GPCRs have been well resolved (Palczewski *et al.*, 2000; Cherezov *et al.*, 2007; Warne *et al.*, 2008; Jaakola *et al.*, 2008) to facilitate the understanding of GPCR activation, whereas only structures of extracellular domains of class B GPCRs have been determined so far (Parthier *et al.*, 2009; Grace *et al.*, 2007; Sun *et al.*, 2007; Parthier *et al.*, 2007; Runge, *et al.*, 2008; Pioszak and Xu, 2008; Pioszak *et al.*, 2008). Compared with class A GPCRs, class B GPCRs contain a relative larger extracellular domain, which is stabilized by disulfide bonds. Besides fixation of transmembrane helices, extrinsic stabilization of the class B GPCR ectodomains is likewise required for crystallization and structure determination. Human parathyroid hormone 1 receptor, a class B GPCR, is involved in the metabolic disease osteoporosis, which leads to great pharmaceutical interest of the molecular structure of the receptor and its ligand-bound complex. However, until now only a little was known about its structure in atomic level, like for other family members of class B GPCRs.

N-terminal extracellular domain of PTH1R was chosen as target molecule for selection of binding proteins in this thesis. Therefore, sufficient amount of highly functional nPTH1R in homogeneous form is required in the selection process and subsequent binder characterization. Using fermentation technique with minimal salt media, nPTH1R was recombinantly produced in *E. coli* cells with high yield of biomass from 6 l culture. nPTH1R contains 3 disulfide bonds and forms inclusion bodies upon expression in *E. coli* cells. After cell lysis, inclusion bodies were isolated and purified by IMAC. The protein was then refolded by pulse renaturation (Grauschopf *et al.*, 2000)

with two important parameters to achieve high population of functional protein. The end concentration of refolded protein and guanidine hydrochloride must not exceed 0.2 mg/ml and 0.1 M, respectively. In the renaturation buffer, reduced and oxidized glutathione with 5:1 molar ratio as a redox shuffling system helps the formation of correct disulfide bonds. 1 M L-Arginine serves as a solubilizing agent to enhance protein folding. This function has already been observed in other refolding protocols, such as the human tissue-type plasminogen activator (Rudolph *et al.*, 1995), and antibody Fab fragments (Buchner and Rudolph, 1991).

Isothermal titration calorimetry confirmed the functionality of nPTH1R by its specific ligand binding properties. The dissociation constant was determined to be 8.4 μM, in the same range as previously published (Grauschopf *et al.*, 2000), and 1:1 binding stoichiometry was obtained. Compared to membrane-bound full-length PTH1R, which binds PTH with K_D in a range from 0.5 to 5 nM (Gardella *et al.*, 1993, Goldman *et al.*, 1988), decreased affinity was observed for N-terminal extracellular domain alone. It has already been proved previously, that the extracellular loops and the transmembrane regions of PTH1R also contribute to the binding interactions with PTH ligand. The bioactive portion of PTH ligand resides in the first 34 amino acids, which consists of an N-terminal and a C-terminal alpha-helix. The C-terminal alpha-helix from S17 to V31 forms a hydrophobic surface and binds to the pocket of N-terminal extracellular domain of the receptor (Pioszak and Xu, 2008). The N-terminal helix of PTH ligand binds weakly to the extracellular loops and the transmembrane regions of the receptor. It can induce the conformational changes involved in receptor activation (Dean *et al.*, 2006). With this explanation, no suspicion should be aroused on the functional state of refolded nPTH1R. Surface plasmon resonance measurement confirmed that chemically biotinylated nPTH1R could bind PTH1-84 with 6.8 μM affinity, in good agreement with the result from the ITC experiment. In summary, nPTH1R extracted from inclusion bodies of *E. coli* cells is capable to fold into a homogeneous functional conformation with correct disulfide bonds. The yield of protein is sufficient for subsequent selection process and further characterization of possible binding variants.

4.2 Isolation of human γB crystallin binder against nPTH1R

4.2.1 Construction of T7 phage library

An artificial binding protein against PTH1R, based on human γB crystallin, would be an interesting candidate for therapeutic or diagnostic applications as well as for basic research, especially structural analysis by co-crystallization, due to its potential high-yield production and superior biophysical properties. In order to creat an artificial binding site on the surface of γB crystalline, eight solvent exposed positions of a β-sheet of the N-terminal domain were randomized. The calculated potential binding surface is about 560 $Å^2$. The theoretical library diversity can reach 1.7×10^{10}. In the first generation of hγBC binders, different variants have been selected from a M13-phage display library with a size of 4.5×10^8 clones against targets, such as estradiol/testosterone, human IgG-Fc and human proNGF protein (Ebersbach *et al.*, 2007). The isolated human γB crystallin variants can be conveniently produced in *Escherichia coli*, yielding up to 100 mg of purified protein per liter culture by fermentation. These variants exhibit micro- to nanomolar binding affinity to their specific targets and high level of stability against high temperature, extreme pH condition and denaturing agent, e.g. guanidinium hydrochloride. The crystal structure of the IgG-Fc binding variant SPC-1-G3 reveals that the eight designed randomization positions can be substituted without great structural changes of the protein backbone structure.

In this context, the T7-based phage display method was utilized to select human γB crystallin variants, which specifically bind to the N-terminal extracellular domain of parathyroid hormone 1 receptor. Compared to traditional filamentous phages, T7 phages assemble and display the inserted protein variant in the cytoplasm of *E. coli* cells and are then released into the media by cell lysis. T7-based phage display technique has not as well established as filamentous phage display. However, diverse peptides or proteins

have been reported to be successfully displayed on T7 phages, such as Streptavidin-binding peptide (10 aa) (Schmidt and Skerra, 1993), RGD peptide (8 aa) from adenovirus penton protein (Bai *et al.*, 1993), T7 endonuclease (149 aa) (de Massy *et al.*, 1987) and *E. coli* β-galactosidase (1015 aa) (Rosenberg *et al.*, 1996). Compared to M13 libraries, peptide libraries displayed on T7 phages showed fewer amino acid biases, resulting in enhanced peptide diversity due to different processes of viral morphogenesis (Krumper *et al.*, 2006). The filamentous phage assembly requires an additional secretion process. The peptides and proteins, which are not compatible with a secretory machinary within the bacterial cell membrane, can not be displayed on the M13 phages. This phenomenon does not occur when using T7 phages.

Besides phage display techniques, ribosome display is also a well developed methodology for selection of highly specific binders. It has the advantage of less limitation on cDNA library diversity, in comparison with M13-phage display restricted by transformation efficiency and T7-phage display by phage extract amount. However, protein folding in the ribosome display can not be controlled and the stability of ternary complexes responsible for coupling phenotype and genotype is limited to certain environments, especially under harsh conditions regarding pH or temperature.

The experiment was started with testing whether human γB crystallin molecules can be functionally displayed on the T7 phage surface. First-generation human γB crystallin binder SPC-5 (Ebersbach *et al.*, 2007, provided by Scil proteins) was used to be displayed on T7 phage surface, in parallel using wild type crystallin as control. Western blot results proved the successful display of wild type human γB crystallin and binder SPC-5 on T7 phage surface. Phage ELISA results showed that binder SPC-5 on T7 phage can still efficiently recognize its specific target estradiol, in parallel with low level of cross reaction to control protein BSA. Wild type human γB crystallin on T7 phage demonstrated no binding activity to both estradiol and BSA (data not shown). The compatibility of T7 phage system and human γB crystallin protein was hence confirmed. With commercial T7Select Packaging kits, a phage library with a diversity of total

1.6 x 10^8 packaged primary phage clones was constructed *in vitro* from naïve cDNA library. This library size was in the same range as the first generation of human γB crystallin library displayed on filamentous phages (Ebersbach *et al.*, 2007).

4.2.2 Selection of human γB crystallin binder against nPTH1R

During the biopanning process, 1.8 × 10^{10} phage clones, representing approximately 100 copies of each individual hγBC variant, were utilized in the first round of selection against biotinylated nPTH1R. Alltogether four rounds of selection were proceeded in solution by means of incubation of phage library and multi-biotinylated nPTH1R, followed by capture of binding complex with streptavidin beads. Compared to traditional selection using N-terminal immobilized target protein on a microtiter plate or immunotube, this selection-in-solution method provided complete accessibility of all sites of nPTH1R for binding candidates and reduced the possible accumulation of variants which bind to the C-terminus of nPTH1R, which are obviously unwanted and meaningless for further use of these binders in contact of the full length PTH1R.

During the biopanning process, several strategies were carried out to improve the quality of potential binders. Firstly, before phage library interacting with target molecule, it was incubated with same amount of streptavidin beads as pre-panning. The phage clones, which can unspecifically bind the beads probably due to the truncated hγBC variant on the surface, stayed in the tube and the non-bound phages were then transferred to the target molecule for complex formation. This step could efficiently remove part of non-functional phage variants before selection. Secondly, after selection, the target-bound phages were recovered by both enzymatic proteolysis and *in situ* elution. Two combined elution methods ensure the complete recovery of bound phages. At last, from round to round, the concentration of target molecule was greatly decreased and washing condition became much harsher, in the aim to obtain binders with high affinity and specificity.

After four rounds of selection, 48 clones from each round output phages (total 192 clones) were analyzed by ELISA. 17 clones with obvious binding signal to nPTH1R were sequenced. 9 functional variants were subsequently tested with other negative control targets for specificity. Finally, one human γB crystallin variant 2G4 with seven mutation residues on the eight designed positions (K2F, T4K, Y6H, E17F, T19V, R36E, E38A) was isolated. The phage ELISA results revealed that 2G4 molecule displayed on T7 phages could strongly bind its target protein nPTH1R in a highly specific manner.

4.3 Charaterization of isolated human γB crystallin variants

4.3.1 Expression and purification of human γB crystallin variants

hγBC variant 2G4 was solubly expressed in *E. coli* cells and conveniently purified by IMAC and size exclusion chromatography, with more than 95% purity monitored by SDS-PAGE analysis. The yield was approximately 40 mg protein per liter culture in shake flask, which is in the range compared to first generation hγBC binders (Ebersbach *et al.*, 2007). This high-level yield guarantees its further potential applications in many fields, like biophysical characterization, NMR studies, and X-ray structure determination, affinity chromatography, or medical applications.

Variants of 2G4 generated by an alanine scanning of the randomized positions, were mostly well solubly expressed in *E. coli* cells, yielding from 24 mg to 47 mg protein per liter culture in shake flask, except variant H6A and K4A with only 3.9 and 7.9 mg, respectively. Structurally, the amino acid at the 6^{th} position of human γB crystallin is covered by the loop nearby and tolerates mainly tyrosine, histidine and tryptophan during the randomization (Schneider, 2010). Hence this histidine was enriched during the biopanning procedure, because of its contribution to the protein solubility and correctly folding, but not the direct binding reaction to nPTH1R. The charged residue lysine at the 4^{th} position of 2G4 on the solvent-exposed region could probably be

involved in an electrostatic interaction to promote the protein stability and solubility, and hereby selected. It also contributes slightly to the interaction to nPTH1R.

4.3.2 Secondary structure analysis and thermal stability test

A major advantage of scaffold proteins, compared with antibodies and their fragments, is their high level of thermodynamic stability. CD spectroscopy was utilized to analyze the secondary structure of isolated hγBC variant 2G4, as well as variants generated in alanine scanning experiments. Since hγBC molecule consists of four anti-parallel β-sheets and a small portion of α-helix, it shows a very distinguished CD spectrum. All crystallin variants showed a similar shape of the spectrum compared to that of the wild type but slightly differed in signal intensity. This revealed that all the hγBC variants were correctly folded and eight mutation sites didn't cause dramatic structural changes of the backbone. The result confirms our concept at the beginning, that the human γB crystallin with an extraordinary thermodynamic stability is an outstanding scaffold protein to accept substitutional changes on its surface due to generation of a binding site.

Two different methods, CD spectroscopy and differential scanning fluorimetry (DSF), were used to analyze the thermal stability of isolated variant 2G4 and both results showed the transition midpoint at approximately 60 °C, while the data for first-generation of hγBC binders ranged from 56 °C to 80 °C (Ebersbach *et al.*, 2007), and 40-60 °C for antibodies (Orr *et al.*, 2003), and about 72 °C for anticalins (Schlehuber and Skerra, 2002), 35 °C for affibodies (Wahlberger *et al.*, 2003), and 66-85 °C for ankyrin variants (Binz *et al.*, 2003).

4.3.3 Binding affinity determination of hγBC variant 2G4 to nPTH1R

The dissociation constant of hγBC variant 2G4 to nPTH1R was evaluated by ELISA, ITC and NMR titration. All these methods revealed a low micromolar binding affinity

between the two proteins. The data in the concentration-dependent ELISA and the competition ELISA were nicely fit to the corresponding equation, resulting in approximately 1 μM binding affinity. However, this K_D value is 20-fold lower than that measured by ITC and NMR titration. The ITC data revealed that binding reaction between hγBC variant 2G4 and nPTH1R was driven by both enthalpy and entropy changing processes. In the measurement, the heat change during the complex formation was very weak and the error deviation caused probably by protein concentration determination or data baseline adjustment was relatively large. For the NMR titration experiment, K_D value was determined by the signal intensity changes, which was caused by three possible reasons: firstly, the large 2G4-nPTH1R complex formation led to line-broadening of many amide resonances which at the end disappeared, especially occurring for the low micromolar affinity complex; secondly, the conformation of the molecule has changed during the binding interaction. Both explanations testified the interaction of hγBC variant 2G4 to nPTH1R. The third factor causing the reduced signal intensity is the dilution of labeled protein while titration of binding partner, which could be excluded simply by concentration correction. The difference of K_D values between ELISA and ITC, NMR results could also be due to the binding reaction status. In ELISA experiment, target protein nPTH1R was previously immobilized on the plate and this fixation probably benefited the accessibility for variant 2G4, while the reaction for these two binding partners in ITC and NMR experiments were totally in solution.

The association constant between two proteins could also be predicted by surface area buried upon binding, 90 $Å^2$ per lgKa unit (Houk *et al.*, 2003). 434 $Å^2$ binding area of 2G4 to nPTH1R has been identified by NMR studies, which corresponds to a K_D of 15 μM. This calculation method emphasizes the importance of the hydrophobic effect during binding interaction. The deviations from this simple relationship based on binding area could be caused by specific hydrogen bonds, electrostatic and van der Waals interactions. This calculated K_D value is in the similar range as the results obtained from other methods described above.

Considering this T7 phage library with a relative low diversity (1.6 x 10^8) and the primary screening without further maturation, the binding affinity of isolated variant in a low micromolar range is quite reasonable. The assumed binding area of variant 2G4, consisting of nine amino acids as above in NMR studies described, is calculated to be 434 $Å^2$ by Pymol software. Further strategies could be focused on generating a T7 phage library with larger repertoire by construction with more phage extract or addition of randomization sites on the hγBC scaffold to increase the binding surface for higher affinity and specificity. One successful example for the latter approach is the ubiquitin-based Affilin® scaffold. Monomeric ubiquitin-based scaffold possessing 7 or 8 randomization sites were selected against the N-terminal domain of the pituitary adenylate cyclase-activating polypeptide 1 receptor (nPAC1R). Binders with 28-247 μM affinity were obtained, while dimeric ubiquitin-based scaffold with combined 15 randomization sites could provide a contiguous binding patch larger than 800 $Å^2$ and binders against nPAC1R were isolated with obviously higher affinity, varying from 8.4 μM up to 35.5 nM (Song, 2012). This result clearly demonstrates the direct correlation between binding site area and binder affinity.

4.3.4 Binding interaction of hγBC variant 2G4 to target molecule nPTH1R

The binding nature of hγBC variant 2G4 to nPTH1R on the molecular level was investigated by alanine scanning experiment and NMR studies. Combined both results, two phenylalanine residues on the mutation sites 2 and 17 were found to contribute the most to the interaction with nPTH1R and the surrounding substitution positions, as well as residues in the neighbourhood also participated during the binding event. The eight mutation sites of the binding surface of variant 2G4 have been transferred to the other three β-sheets of human γB crystallin which are indeed structurally very similar to the β-sheet used in the first place. ELISA results showed that these variants could not bind to the target molecule nPTH1R (data not shown). This phenomenon fits quite well with our NMR studies. In NMR titration experiments, binding surface of 2G4 was identified, which was composed of not only randomization positions but also residues in the

neighbourhood. These residues also contributed to the binding interaction and their NMR intensities decreased greatly during the complex formation. Therefore, it could be concluded that the local structural conformation is also very critical for the binding event and slight changes could lead to the loss of the binding ability.

The binding of hγBC variant 2G4 to nPTH1R was also found to be pH-dependent and the binding event occurs only above pH 6.8. The pKa value of the histidine side chain imidazole is in this range and dependent on the surrounding microenvironment. Hence, histidine is very likely involved in the binding event. One histidine was found at the 6^{th} position of eight mutation sites of hγBC variant 2G4. When this residue was further mutated to alanine or tyrosine corresponding to the amino acid of wild type, the binding intensity still remained in the same level as variant 2G4. Therefore, this particular histidine was excluded from the hypothesis. Other histidines on the variant 2G4 are located far away from the generated binding surface. The histidine, which contributes greatly to the binding event, probably lies on the epitope of nPTH1R molecule. Five histidines of nPTH1R all reside on the surface-exposed positions, except H140 partially buried in the loop connecting two beta strands. All of them have the potential to play an essential role in the binding interaction to the hγBC variant 2G4. Alanine scanning could be further performed on nPTH1R to find out which one is the specific histidine involved in the interaction with variant 2G4.

Binding of PTH to nPTH1R is initiated greatly by hydrophobic interactions. Amino acid residues V21, W23, L24, L28, V31, and F34 form a hydrophobic surface on the helix of PTH ligand, which inserts into the hydrophobic groove formed by nPTH1R (Pioszak and Xu, 2008). The binding specificity of PTH to nPTH1R is enhanced by complementary shapematching between the two molecules and hydrogen bonds at both ends of the PTH helix. The fixation of unstructual PTH ligand leads to an obviously low apparent binding entropy (Table 3.1, Chapter 3.1.2), while hγBC variant 2G4 binds nPTH1R through surface to surface contact, and no secondary structure change of either 2G4 or nPTH1R is involved, confirmed by CD spectroscopy (Fig. 7.3, Appendix).

Combining the results from competition ITC and NMR studies, hγBC variant 2G4 binds nPTH1R at a totally different epitope from ligand PTH1-84. No competition between these two molecules occurs upon interaction with nPTH1R. 2G4 binding to nPTH1R also doesn't induce a conformational switch in nPTH1R that would interfere either positively or negatively with PTH binding. This particular binding property of 2G4 leads to its potential application in structural studies of PTH receptor, but not in therapeutical field.

5 Outlook

In this thesis, artificial binding proteins, based on human γB crystallin, were selected against a target molecule, N-terminal extracellular domain of parathyroid hormone 1 receptor, a class B GPCR. After four rounds of biopanning process, one hγBC binding variant, 2G4, was repeatedly isolated. It exhibits specific binding properties to nPTH1R as well as to the full length PTH1R. The binding with an affinity in a low micromolar range is not dependent on the presence or absence of the nature ligand PTH of the receptor. With these characteristics 2G4 might be used in affinity chromatography of PTH1R in its isolated as well as liganded form. Furthermore, 2G4 might be useful in Pull-Down experiments of PTH1R and in structural studies of the receptors specifically in co-crystallization experiments. By comparing the PTH1R structure in the absence and presence of ligand PTH, the conformational changes of PTH1R triggered by binding to the ligand PTH could be precisely interpreted, which has great meaning in new drug discovery.

2G4 does certainly not possess any therapeutic potential. For such an application the affinity is too low. In the next step, a library based on 2G4 could be generated by using error-prone PCR, for isolation of binders with higher affinity. One would not expect any agonistic or antagonistic function of 2G4 since it does not interfere with PTH binding to the receptor. In order to select a potentially therapeutically interesting binding variant against PTH1R from the given library, a selection process would be necessary in which the complex of the receptor (domain) and the ligand PTH is used as target and selection is performed in competition with receptor and ligand alone.

6 References

Abou-Samra, A. B., Jüppner, H., Force, T., Freeman, M. W., Kong, X. F., Schipani, E., Urena, P., Richards, J., Bonventre, J. V., Potts, J. T. Jr., *et al.* (1992). Expression cloning of a common receptor for parathyroid hormone and parathyroid hormone-related peptide from rat osteoblast-like cells: A single receptor stimulates intracellular accumulation of both cAMP and inositol trisphosphates and increases intracellular free calcium. Proc. Natl. Acad. Sci. USA Vol. 89: 2732-2736.

Aggarwal, S. (2009). What's fueling the biotech engine? Nature Biotechnol. 27: 987-993.

Attwood, T. K., and Findlay, J. B. (1994). "Fingerprinting G-protein-coupled receptors". Protein Eng 7 (2): 195-203.

Bai, M., Harfe, B., and Freimuth, P. (1993). Mutations that alter an Arg-Gly-Asp (RGD) sequence in the adenovirus type 2 penton base protein abolish its cell-rounding activity and delay virus reproduction in flat cells. J. Virol. 67: 5198-5205.

Barbas III C. F., Kang A. S., Lerner R. A., and Benkovic S. J. (1991). Assembly of combinatorial antibody libraries on phage surfaces: The gene III site. Proc. Natl. Acad. Sci. USA, 88(18): 7978-7982.

Beck, A., Wurch, T., and Corvaia, N. (2008). Editorial: therapeutic antibodies and derivatives: from the bench to the clinic. Curr. Pharm. Biotechnol. 9: 421-422.

Beck, A., Wurch, T., Bailly, C., and Corvaia N. (2010). Strategies and challenges for the next generation of therapeutic antibodies. Immunology volume 10: may 345-352.

Binz, H. K., Amstutz, P., Kohl, A., Stumpp, M. T., Briand, C., Forrer, P., Grutter, M. G. and Pluckthun, A. (2004). High-affinity binders selected from designed ankyrin repeat protein libraries. Nat Biotechnol 22: 575-582.

Binz, H. K., Stumpp, M. T., Forrer, P., Amstutz, P., and Pluckthun, A. (2003). Designing repeat proteins: wellexpressed, soluble and stable proteins from combinatorial libraries of consensus ankyrin repeat proteins. J. Mol. Biol. 332: 489-503.

Bloemendala, H., De Jonga,W., Jaenickeb, R., Lubsena, N. H., Slingsbyc, C., and Tardieu, A. (2004). Ageing and vision: structure, stability and function of lens crystallins. Progress in Biophysics & Molecular Biology 86: 407-485.

Buchner, J., and Rudolph, R. (1991). Renaturation, Purification and Characterization of Recombinant Fab-Fragments Produced in Escherichia coli. Biotechnology (N.Y.) *9*:

157-162.

Cherezov, V., Rosenbaum, D. M., Hanson, M. A., Rasmussen, S. G., Thian, F. S., Kobilka, T. S., Choi, H. J., Kuhn, P., Weis, W. I., Kobilka, B. K. and Stevens, R. C. (2007). High-resolution crystal structure of an engineered human b2-adrenergic G protein-coupled receptor. Science 318: 1258–1265

Clore, G. M. and Gronenborn, A. M. (1991). Structures of larger proteins in solution: three-and four-dimensional heteronuclear NMR spectroscopy. Science 252(5011): 1390-1399.

Dai, M., Temirov, J., Pesavento, E., Kiss, C., Velappan, N., Pavlik, P., Werner, J.H. and Bradbury, A. R. M. (2008). Using T7 phage display to select GFP-based binders Protein Engineering, Design & Selection vol. 21: 413–424.

Dean, T., Khatri, A., Potetinova, Z., Willick, G. E., Gardella, T. J. (2006). Role of amino acid side chains in region 17-31 of parathyroid hormone (PTH) in binding to the PTH receptor. J Biol Chem. 281(43):32485-95.

de Massy, B., Weisberg, R.A., and Studier, F.W. (1987). Gene 3 endonuclease of bacteriophage T7 resolves conformationally branched structures in double-stranded DNA. J. Mol. Biol. 193: 359-376.

Delaglio, F.,Grzesiek, S., Vuister, G. W., Zhu, G., Pfeifer, J., Bax, A. (1995). Nmrpipe - a Multidimensional Spectral Processing System Based on Unix Pipes. Journal of Biomolecular Nmr 6(3): 277-293.

Dutzler, R., Campbell, E. B. and MacKinnon, R. (2003). Gating the selectivity filter in ClC chloride channels. Science 300: 108-112.

Ebersbach, H., Fiedler, E., Scheuermann, T., Fiedler, M., Stubbs, M. T., Reimann, C., Proetzel, G., Rudolph, R., and Fiedler, U. (2007). Affilin–Novel Binding Molecules Based on Human γ-B-Crystallin, an All β-Sheet Protein. J. Mol. Biol. 372, 172-185.

Fiedler, M., Fiedler, U. and Rudolph, R. (2004). Generation of artificial binding proteins on the basis of ubiquitin proteins. International Patent Application WO/2004/106368.

Gardella, T. J., Wilson, A. K., Keutmann, H. T., Oberstein, R., Potts, J. T., Jr., Kronenberg, M., and Nussbaum, S. R. (1993). Analysis of parathyroid hormone's principal receptor-binding region by site-directed mutagenesis and analog design. Endocrinology 132: 2024-2030.

Gebauer, M. and Skerra, A. (2009). Engineered protein scaffolds as next-generation antibody. Therapeutics Current Opinion in Chemical Biology, 13:245-255.

Gensure, R. C., Gardella T. J., Jüppner, H. (2005). Parathyroid hormone and parathyroid hormone-related peptide, and their receptors Biochemical and Biophysical Research Communications, 328: 666–678.

Goldman, M. E., Chorev, M., Reagan, J. E., Nutt, R. F., Levy, J. J., and Rosenblatt, M. (1988). Evaluation of novel parathyroid hormone analogs using a bovine renal membrane receptor binding assay. Endocrinology 123: 1468-1475.

Grace, C. R., Perrin, M. H., Gulyas, J., Digruccio, M. R., Cantle, J. P., Rivier, J. E., Vale, W. W. and Riek, R. (2007). Structure of the N-terminal domain of a type B1 G protein-coupled receptor in complex with a peptide ligand. Proc. Natl. Acad. Sci. U. S. A. 104: 4858–4863.

Grauschopf, U., Lilie, H., Honold, K., Wozny, M., Reusch, D., Esswein, A., Schäfer, W., Rücknagel, K. P. and Rudolph, R. (2000) The N-Terminal Fragment of Human Parathyroid Hormone Receptor 1 Constitutes a Hormone Binding Domain and Reveals a Distinct Disulfide Pattern. Biochemistry 39: 8878-8887.

Grimsley, G. R., Scholtz, J. M., and Pace, C. N. (2009). A summary of the measured pK values of the ionizable groups in folded proteins. Protein science Vol. 18:247-251.

Grzesiek, S. and Bax A. (1992). Correlating Backbone Amide and Side-Chain Resonances in Larger Proteins by Multiple Relayed Triple Resonance Nmr. Journal of the American Chemical Society 114(16): 6291-6293.

Harrenga, A., and Michel, H. (1999). The cytochrome c oxidase from Paracoccus denitrificans does not change the metal center ligation upon reduction. J.Biol.Chem. 274: 33296.

He, M. Y. and Taussig, M. J. (2002). Ribosome display: Cell-free protein display technology. Briefings in functional genomics and proteomics vol 1 No. 2: 204-212.

Högbom, M., Eklund, M., Nygren, P.-Å. and Nordlund, P. (2003). Structural basis for recognition by an *in vitro* evolved affibody. Proc. Natl. Acad. Sci. USA 100: 3191-3196.

Hoffmann, A., Kovermann, M., Lilie, H., Fiedler M., Balbach, J., Rudolph, R. and Pfeifer, S. (2012). New Binding Mode to TNF-Alpha Revealed by Ubiquitin-Based Artificial Binding Protein. PLoS One. 7(2): e31298.

Holliger, P. and Hudson P. J. (2005). Engineered antibody fragments and the rise of

single domains. Nat Biotechnol vol. 23, 9: 1126-1136.

Houk, K. N., Leach, A. G., Kim, S. P. und Zhang, X. (2003). Binding affinities of host-guest, protein-ligand, and protein-transition-state complexes. Angew Chem Int Ed Engl 42: 4872-97.

Huber, T., Steiner, D., Röthlisberger, D., and Plückthun, A. (2007). In vitro selection and characterization of DARPins and Fab fragments for the co-crystallization of membrane proteins: The Na+-citrate symporter CitS as an example. J Struct Biol. 159(2):206-21

Hughes, B. (2010). 2009 FDA drug approvals. Nature Rev. Drug Discov. 9: 89-92.

Iwata, S., Ostermeier, C., Ludwig, B. and Michel, H. (1995). Structure at 2.8 Å resolution of cytochrome c oxidase from *Paracoccus denitrificans.* Nature 376: 660-669.

Jaakola, V. P., Griffith, M. T., Hanson, M. A., Cherezov, V., Chien, E. Y., Lane, J. R., Ijzerman, A. P. and Stevens, R. C. (2008). The 2.6 angstrom crystal structure of a human A2A adenosine receptor bound to an antagonist. Science 322: 1211–1217

Jaenicke, R. (1994). Eye-lens proteins: structure, superstructure, stability, genetics. Naturwissenschaften, 81: 423-429.

Jaenicke, R. and Slingsby, C. (2001). Lens Crystallins and Their Microbial Homologs: Structure, Stability, and Function. *Critical Reviews in Biochemistry and Molecular Biology,* 36(5):435-499.

Jimenez, R., Salazar, G., Baldridge, K. K. and Romesberg, F. E. (2003). Flexibility and molecular recognition in the immune system. Proc. Natl Acad. Sci. USA, 100: 92-97.

Johnson, B. A. and Blevins R. A. (1994). Nmr View - a Computer-Program for the Visualization and Analysis of Nmr Data. Journal of Biomolecular Nmr 4(5): 603-614.

Jones, P. T., Dear, P. H., Foote, J., Neuberger, M. S., and Winter, G. (1986). Replacing the complementarity-determining regions in a human antibody with those from a mouse.
Nature 321: 522-525.

Kay, L. E., Ikura, M., Tschudin, R., Bax, A. (1990). 3-Dimensional Triple-Resonance Nmr-Spectroscopy of Isotopically Enriched Proteins. Journal of Magnetic Resonance 89(3): 496-514.

Kenakin, T. (2001) Inverse, protean, and ligand-selective agonism: matters of receptor conformation. FASEB J. 2001 Mar, 15(3):598-611.

Kohl, A., Amstutz, P., Parizek, P., Binz, H. K., Briand, C., Capitani, G., Forrer, P., Plückthun, A., and Grütter, M. G. (2005). Allosteric inhibition of a kinase by a designed ankyrin repeat protein inhibitor. Structure 13: 1131-1141.

Koide, A., and Koide, S. (2007). Monobodies: antibody mimics based on the scaffold of the fibronectin type III domain. Methods Mol Biol 352:95-109.

Kondo, A., and Ueda, M. (2004). Yeast cell-surface display--applications of molecular display Appl Microbiol Biotechnol 64(1):28-40.

Krumpe, L.R., Atkinson, A.J., Smythers, G.W., Kandel, A., Schumacher, K.M., McMahon, J.B., Makowski, L. and Mori, T. (2006). T7 lytic phage-displayed peptide libraries exhibit less sequence bias than M13 filamentous phage-displayed peptide libraries.Proteomics 6: 4210-4222.

Kumaraswamy, V. S., Lindley, P. F., Slingsby, C. and Glover, I. D. (1996). An eye lens protein-water structure: 1.2 angstrom resolution structure of gamma B-crystallin at 150K. Acta Crystallog. sect. D, 52: 611-622.

Lee, S. Y., Choi, J. H., and Xu, Z. (2003). Microbial cell-surface display. Trends Biotechnol 21(1): 45-52.

Mannstadt, M., Jüppner, H., and Gardella, T. J. (1999). "Receptors for PTH and PTHrP: their biological importance and functional properties". Am. J. Physiol. 277 (5 Pt 2): F665-75.

Mayr, E. M., Jaenicke, R., and Glockshuber, R. (1997). The Domains in gB-crystallin: Identical Fold±Different Stabilities. J. Mol. Biol. 269, 260±269.

Millar, R. P. and Newton C. L. (2010). The Year In G Protein-Coupled Receptor Research. Mol Endocrinol 24(1): 261-74.

Mirecka, E. A., Hey, T., Fiedler, U., Rudolph, R., and Hatzfeld, M. (2009). Affilin Molecules Selected against the Human Papillomavirus E7 Protein Inhibit the Proliferation of Target Cells. J. Mol. Biol. 390, 710-721.

Moen, M. D. and Scott L. J. (2006) Recombinant Full-Length Parathyroid Hormone (1-84) Drugs; 66 (18): 2371-2381.

Mori, S., Abeygunawardana, C., Johnson, M. O., van Zijl P. C. (1995). Improved sensitivity of HSQC spectra of exchanging protons at short interscan delays using a new

fast HSQC (FHSQC) detection scheme that avoids water saturation. J Magn Reson B 108(1): 94-98.

Murer H., Forster I., and Biber J. (2004). The sodium phosphate cotransporter family SLC34, Pflugers Arch. 447 (5): 763-767.

Nussbaum, S. R., Rosenblatt, M., and Potts, J. T., Jr. (1980). Parathyroid hormone . renal receptor interactions. Demonstration of two receptor-binding domains. J. Biol. Chem. 255: 10183-10187.

Nygren P-A° (2008). Alternative binding proteins: Affibody binding proteins developed from a small three-helix bundle scaffold. FEBS J, 275:2668-2676.

Offermanns, S., Iida-Klein, A., Segre, G. V., and Simon, M. I. (1996). G alpha q family members couple parathyroid hormone (PTH)/PTH-related peptide and calcitonin receptors to phospholipase C in COS-7 cells, Mol. Endocrinol. 10(5): 566-574.

Oflazoglu, E. and Audoly, L. P. (2010). Evolution of anti-CD20 monoclonal antibody therapeutics in oncology. mAbs 2: 1-6.

Orr, B. A., Carr, L. M., Wittrup, K. D., Roy, E. J., and Kranz, D. M. (2003). Rapid method for measuring ScFv thermal stability by yeast surface display. Biotechnol. Prog. 19: 631-638.

Orwoll, E., Scheele, W., Paul, S., Adami, S., Syversen, U., Diez-Perez, A., Kaufman, J. M., Clancy, A., and Gaich, G. (2003). The effect of teriparatide [human parathyroid hormone (1-34)] therapy on bone density in men with osteoporosis. Journal of Bone and Mineral Research 18, 9-17.

Palczewski, K., Kumasaka, T., Hori, T., Behnke, C. A., Motoshima, H., Fox, B. A., Le Trong, I., Teller, D. C., Okada, T., Stenkamp, R. E., Yamamoto, M. and Miyano, M. (2000). Crystal structure of rhodopsin: a G proteincoupled receptor. Science 289: 739–745

Parthier, C., Kleinschmidt, M., Neumann, P., Rudolph, R., Manhart, S., Schlenzig, D., Fanghänel, J., Rahfeld, J. U., Demuth, H. U. and Stubbs, M. T. (2007). Crystal structure of the incretin-bound extracellular domain of a G protein-coupled receptor. Proc. Natl. Acad. Sci. U. S. A. 104: 13942–13947.

Parthier, C., Reedtz-Runge, S., Rudolph, R., and Stubbs, M. T. (2009). Passing the baton in class B GPCRs: peptide hormone activation via helix induction? Trends Biochem Sci. 2009 Jun;34(6):303-10.

Pervushin, K., Riek, R., Wider, G., Wüthrich, K. (1997). Attenuated T-2 relaxation by mutual cancellation of dipole-dipole coupling and chemical shift anisotropy indicates an avenue to NMR structures of very large biological macromolecules in solution. Proc. Natl Acad. Sci. USA, 94(23): 12366-12371.

Pfister, M. F., Ruf, I., Stange, G., Ziegler, U., Lederer, E., Biber, J., and Murer, H. (1998). Parathyroid hormone leads to the lysosomal degradation of the renal type II Na/Pi cotransporter, Proc. Natl. Acad. Sci. USA 95 (4): 1909-1914.

Pioszak, A. A., Harikumar, K. G., Parker, N. R., Mille, L. J. and Xu, H. E. (2010). Dimeric arrangement of the parathyroid hormone receptor and a structural mechanism for ligand-induced dissociation. J Biol Chem. 285(16):12435-44.

Pioszak, A. A., Parker, N. R., Suino-Powell, K. and Xu, H. E. (2008). Molecular recognition of corticotropinreleasing factor by its G-protein-coupled receptor CRFR1. J. Biol. Chem. 283: 32900–32912.

Pioszak, A. A. and Xu H. E. (2008). Molecular recognition of parathyroid hormone by its G protein-coupled receptor. Proc. Natl Acad. Sci. USA, 105(13):5034-5039

Potts, J. T., Kronenberg, H. M., and Rosenblatt, M. (1982). Advances in Protein Chemistry 35: 323-396.

Reichert, J. M. (2010). Antibodies to watch in 2010. mAbs 2: 1-16.

Robert, C., Gensurea,B., Thomas, J., Gardellaa, and Harald J. C. (2005). Parathyroid hormone and parathyroid hormone-related peptide and their receptors. Biochemical and Biophysical Research Communications 328: 666-678.

Rosenberg, A., Griffin, K., Studier F. W., McCormick M., Berg J., Novy R., and Mierendorf R. (1996). T7Select® Phage Display System: A powerful new protein display system based on bacteriophage T7. Newsletter of novagen No. 6.

Rudolph, R., Fischer, S., and Mattes. (1995). Process for the Activitation of T-PA or ING after Genetic Expression in Prokaryotes. U.S. Patent 5.453,363.

Runge, S., Thøgersen, H., Madsen, K., Lau, J. and Rudolph, R. (2008). Crystal structure of the ligand-bound glucagonlike peptide-1 receptor extracellular domain. J. Biol. Chem. 283: 11340–11347.

Russel, M. (1991). Filamentous phage assembly. *Mol. Microbiol.* 5, 1607-1613.

Salzmann, M., Pervushin, K., Wider, G., Senn, H. and Wüthrich, K. (1998). TROSY in triple-resonance experiments: New perspectives for sequential NMR assignment of large proteins. Proc. Natl Acad. Sci. USA 95(23): 13585-13590.

Schlehuber, S. and Skerra, A. (2002). Tuning ligand affinity, specificity, and folding stability of an engineered lipocalin variant- a so-called 'anticalin'- using a molecular random approach. Biophys. Chem. 96: 213-228.

Schmid, F.X. (1997). Optical spectroscopy to characterize protein conformation and conformational changes. In: Creighton TE, ed. Protein Structure: A practical approach. 2nd ed. Oxford, UK. Oxford University Press: 261–297.

Schmidt, T.G. and Skerra, A. (1993). The random peptide library-assisted engineering of a C-terminal affinity peptide, useful for the detection and purification of a functional Ig Fv fragment. Protein Eng. 6: 109-122.

Schneider, D. (2009). *Automatisierte Herstellung und Stabilitätscharakterisierung von γ-B-Kristallin-basierten, artifiziellen Bindeproteinen im Mikrotiterplattenformat. Diplomarbeit.* Institute of Biochemistry and Biotechnology at Martin Luther University Halle-Wittenberg

Schneider, M. (2010). *Die N-terminale Domäne des humanen γB-Kristallins als scaffold für artifizielle Bindeproteine. Diplomarbeit.* Institute of Biochemistry and Biotechnology at Martin Luther University Halle-Wittenberg

Segawa, H., Kaneko, I., Takahashi, A., Kuwahata, M., Ito, M., Ohkido, I., Tatsumi, S., and Miyamoto, K. (2002).Growth-related renal type II Na/Pi cotransporter, J. Biol. Chem. 277 (22) 19665-19672.

Skerra, A. (2007). Alternative non-antibody scaffolds for molecular recognition. Curr. Opin. Biotechnol. 18, 295-304.

Skerra, A. (2008). Alternative binding proteins: Anticalins-harnessing the structural plasticity of the lipocalin ligand pocket to engineer novel binding activities. FEBS J, 275(11): 2677-2683.

Smith, G. P. (1985). Filamentous fusion phage: novel expression vectors that display cloned antigens on the virion surface. Science 228 (4705): 1315-1317.

Song, B. (2012). Affilin® binding proteins selected against a class B GPCR ectodomain. urn:nbn:de:gbv:3:4-7322.

Son, M., Hayes, S. J., and Serwer, P. (1988). Concatemerization and packaging of bacteriophage T7 DNA in vitro: determination of the concatemers' length and

appearance kinetics by use of rotating gel electrophoresis. Virology 162: 38-46.

Steven, A. C., Serwer, P., Bisher, M. E. und Trus, B. L. (1983). Molecular architecture of bacteriophage T7 capsid. Virology 124: 109-20.

Storey, S. (2010). Respiratory syncytial virus market. Nature Rev. Drug Discov. 9: 15-16.

Strohl, W. R. (2009). Optimization of Fc-mediated effector functions of monoclonal antibodies. Curr. Opin. Biotechnol. 20: 685-691.

Studier, F.W. (2005). Protein production by auto-induction in high-density shaking cultures. Protein Expr. Purif. 41: 207–234.

Sun, C., Song, D., Davis-Taber, R. A., Barrett, L. W., Scott, V. E., Richardson, P. L., Pereda-Lopez, A., Uchic, M. E., Solomon, L. R., Lake, M. R., Walter, K. A., Hajduk, P. J. and Olejniczak, E. T. (2007). Solution structure and mutational analysis of pituitary adenylate cyclase-activating polypeptide binding to the extracellular domain of PAC1-RS. Proc. Natl. Acad. Sci. U. S. A. 104: 7875–7880.

Takakusagi, Y., Takakusagi, K., Sugawara, F., and Sakaguchi, K. (2010). Use of phage display technology for the determination of the targets for small-molecule therapeutics. Expert Opin. Drug Discov. 5: 361-389.

Tregear, G. W., Van Rietschoten, J., Greene, E., Keutmann, H. T., Niall, H. D., Reit, B., Parsons, J. A., and Potts, J. T., Jr. (1973). Bovine parathyroid hormone: minimum chain length of synthetic peptide required for biological activity. Endocrinology 93: 1349-1353.

Vilardaga, J. P., Lin I. and Nissenson, R. A. (2001). Analysis of parathyroid hormone (PTH)/secretin receptor chimeras differentiates the role of functional domains in the pth/ pth-related peptide (PTHrP) receptor on hormone binding and receptor activation. Mol Endocrinol. 15(7):1186-99.

Vuister, G. W. and Bax A. (1992). Resolution Enhancement and Spectral Editing of Uniformly C-13-Enriched Proteins by Homonuclear Broad-Band C-13 Decoupling. Journal of Magnetic Resonance 98(2): 428-435.

Warne, T., Serrano-Vega, M. J., Baker, J. G., Moukhametzianov, R., Edwards, P. C., Henderson, R., Leslie, A. G., Tate, C. G. and Schertler, G. F. (2008). Structure of a b1-adrenergic G-protein-coupled receptor. Nature 454: 486–491

Wahlberg, E., Lendel, C., Helgstrand, M., Allard, P., Dincbas-Renqvist, V., Hedqvist, A. *et al.* (2003). An affibody in complex with a target protein: structure and coupled folding. Proc. Natl Acad. Sci. USA, 100: 3185-9310.

Wörn, A. and Plückthun, A. (2001). Stability engineering of antibody single-chain Fv fragments. J. Mol. Biol. 305: 989-1010.

Xu, L., Aha, P., Gu, K., Kuimelis, R. G., Kurz, M., Lam, T., Lim, A. C., Liu, H., Lohse, P.
A. and Sun, L. (2002). Directed evolution of high-affinity antibody mimics using mRNA
display. Chem Biol 9: 933-942.

Zhou, Y., Morais-Cabral, J. H., Kaufman, A., and MacKinnon, R. (2001). Chemistry of ion coordination and hydration revealed by a K+ channel-Fab complex at 2.0 A resolution. Nature 414: 43-48.

Zuraw, B., Yasothan, U. and Kirkpatrick, P. (2010). Fresh from the pipeline: ecallantide. Nature Rev. Drug Discov. 9: 189-190.

7 Appendix

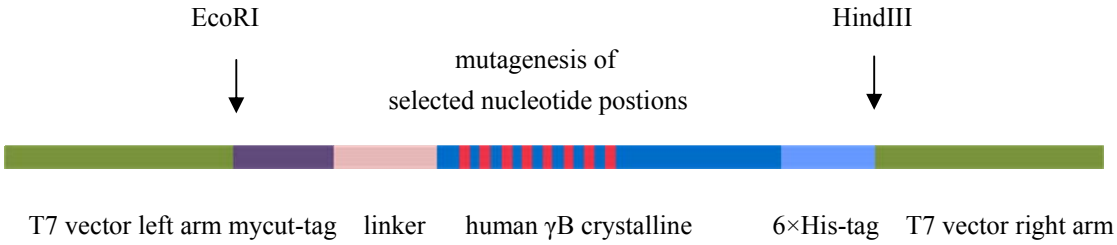

Fig. 7.1: Human γB crystallin library constructed in T7 vector. hγBC library with N-terminal mycut-tag and C-terminal his-tag was inserted into mid-copy T7 vector by EcoRI and HindIII enzyme cleavage sites.

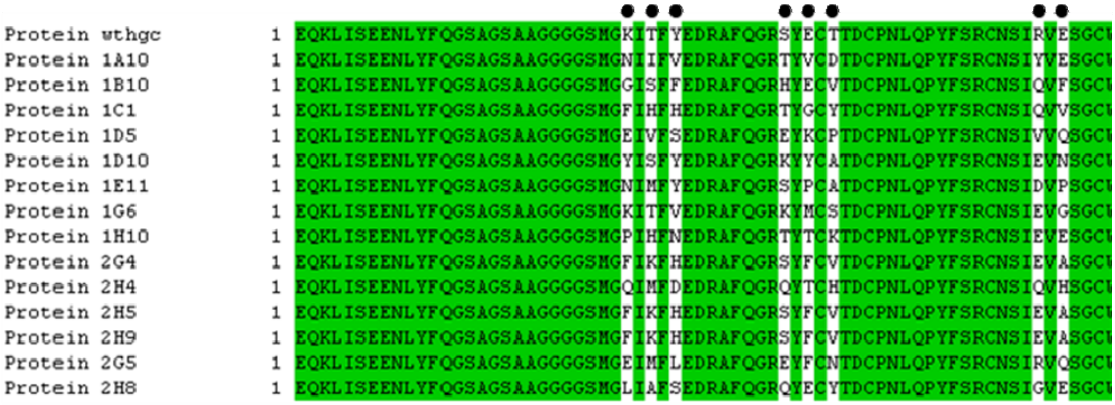

Fig. 7.2: The sequence comparison of selected positive hγBC variants. The randomization sites are marked with "●".

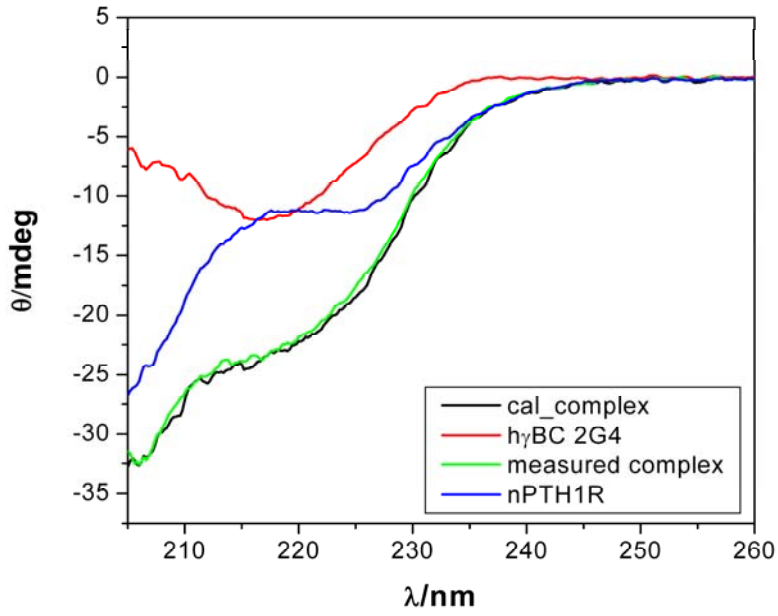

Fig. 7.3: Far-UV CD spectra of free hgBC variant 2G4, nPTHR1R and complex 2G4/nPTH1R.

10 µM of each single protein and complex (molar ratio 1:1, 1 h incubation at RT before measurement) were measured by far-UV CD spectroscopy. The measured complex spectrum fit well to a complex spectrum calculated by addition of two single protein spectra. This shows that during the binding interaction, no secondary structure changes of both proteins were involved.

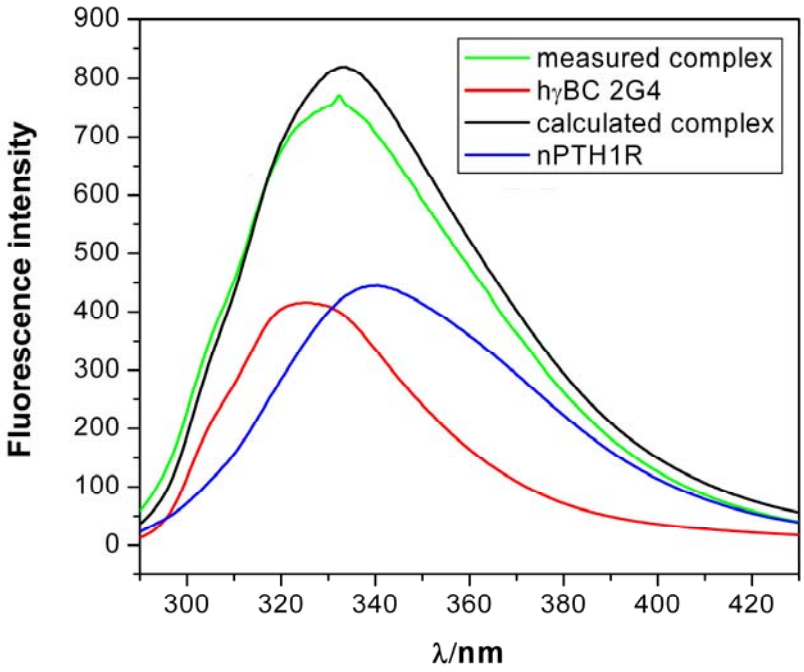

Fig. 7.4: Fluorescence emission spectra of free hgBC variant 2G4, nPTH1R and complex 2G4/nPTH1R. 1 µM of each single protein and complex (molar ratio 1:1, 1 h incubation at RT before measurement) were excited at 280 nm and fluorescence emission spectra from 290 nm to 430 nm recorded. The measured complex spectrum peak was blue shifted to 332.4 nm and the fluorescence intensity was quenched, compared to a complex spectrum calculated by addition of two single protein spectra (emission maximum at 333.8 nm). This indicates that the local environment of fluorophores from one or both binding partners has been changed during complex formation.

Acknowledgements

Here I would like to express my appreciation to Prof. Dr. Rainer Rudolph for providing me with the opportunity to work in junior research group "Artificial Binding Proteins" with a talented team of researchers.

I also thank Dr. Sven Pfeifer for generously sharing his time and knowledge throughout my study. His inspiring discussion, encouragement and supporting me to attend different kinds of conferences really enriched my study in depth and width. Also without Sven's effective management of the group, it's not possible to finish my work efficiently. I would like to acknowledge Dr. Hauke Lilie for providing me many great ideas, intensive discussion and his precious time on correcting my thesis. His observations and comments helped me to establish the overall direction of research.

I am grateful to Dr. Li Yuan for helping me start the project with establishment of T7 phage library. She has helped me greatly in theoretical knowledge and experiment skills. I wish to give my special thanks to Nils Drechsler and Dr. Peter Hanner for their help in preparation of nPTH1R. I greatly appreciate Dr. Andreas Hoffmann for giving me the idea of pH-screening experiment and many other wonderful ideas and discussions. I would like to express my sincere thanks to Patrick Studte for providing me lots of experienced molecular biological methods and always patient explaination. I greatly appreciate Dominik Schneider for DSF experiment and Dr. Sladjana Tomić and Dr. Bo Song for SPR measurement. I also want to thank Claudius Stordeur and Marian Schneider for their inspiring discussion.

I am indebted to Prof. Dr. Jochen Balbach and Mohanraj Gopalswamy for their time and effort on NMR studies, from labeled protein production to spectra analysis. Their generous contribution helped me to complete the analysis of binding interaction on molecular level.

I also would like to thank my bachelor student Anne Pospisil and deeply wish her a great career in the future. I greatly appreciate all the members in junior research group "Artificial Binding Proteins" and institute of biophysic for the nice working atmosphere and friendly help during the lab work and seminar discussions.

Last, but not least, I would like to dedicate this thesis to my parents for their love and understanding to support my study in Germany.

Publication and Posters

Publication in preparation:

- Selection of an artificial binding protein against the ectodomain of PTH1R

Posters:

- Protein society, Jul. 2011, Boston, title “Selection of an artificial binding protein against the ectodomain of PTH1 receptor”

- 2nd International Meeting GRK1026, Mar. 2011, Halle (Saale). “Artificial Binding Proteins for Crystallization of Membrane Proteins”

- *Biowissenschaftliches Netzwerk „Strukturen und Mechanismen der biologischen Informationsverarbeitung“*, Mar. 2010, Halle (Saale), title "Artificial binding proteins for crystallization of membrane proteins"

- PEGS Europe, Sep. 2009, Hannover, title "Purification of recombinant EPO produced in *E. coli*"

Curriculum Vitae

PERSONAL INFORMATION

Surname:	Zhang
Given Name:	Qi
Address:	Heinrich-Damerow-Str. 4, 06120 Halle (Saale), Germany
	Tel. No. 0049-345-5528520
E-mail:	mamaai6@hotmail.com
Date of Birth:	September, 21, 1983
Place of Birth:	Shaanxi, China
Nationality:	Chinese
	Present resident in Germany
Martial status:	Single

EDUCATION AND TRAINING

Apr. 2009-now:	Ph.D. work in Innoprofile Junior Research Group "Artificial Binding Proteins" at Martin-Luther university of Halle-Witternberg, supervised by Dr. Sven Pfeifer
Oct. 2005-Nov. 2008:	*Diplom* study of Biochemistry, in the institute of Biochemistry and Biotechnology at Martin Luther University Halle-Wittenberg *Diplom* thesis: Production and purification of *E. coli*-derived erythropoietin for panning against a phage display library supervised by Prof. Rainer Rudolph and Dr. Li Yuan Degree: *Diplom* of biochemistry
Sep. 2001-Jun. 2005:	Bachelor study of Pharmacy, in the institute of Pharmacy at Wuhan University, China Degree: Bachelor of Science
Sep. 1998-Jul. 2001:	High school student, at Xi'an Foreign Language Middle School, China

Eigenständigkeitserklärung

Hiermit erkläre ich, dass ich mich bisher weder mit dieser noch einer anderen Arbeit weder an der Martin-Luther-Universität Halle-Wittenberg noch einer anderen Einrichtung um die Erlangung eines akademischen Grades beworben habe. Ich versichere weiterhin, dass die vorliegende Arbeit selbstständig und nur unter Benutzung der angegebenen Quellen und Hilfsmittel erstellt wurde. Den benutzten Werken wörtlich oder inhaltlich entnommene Stellen sind als solche gekennzeichnet.

Halle, 2012-12-18 Zhang Qi